PERFORMANCE ANALYSIS AND TROUBLESHOOTING OF PROCESS CONTROL LOOPS

ROHIT RAMACHANDRAN

NATIONAL UNIVERSITY OF SINGAPORE

2005

PERFORMANCE ANALYSIS AND TROUBLESHOOTING OF PROCESS CONTROL LOOPS

ROHIT RAMACHANDRAN

(B.Eng.(Hons), NUS)

A THESIS SUBMITTED

FOR THE DEGREE OF MASTER OF ENGINEERING

DEPARTMENT OF CHEMICAL & BIOMOLECULAR ENGINEERING

NATIONAL UNIVERSITY OF SINGAPORE

2005

ACKNOWLEDGEMENTS

I would like to extend my gratitude to my main supervisor, Dr Lakshminarayanan Samavedham, affectionately known as Dr. Laksh, for many insightful conversations during the development of the ideas in this thesis and for helpful comments on the text. In addition to technical matters, I've also enjoyed our numerous discussions on music, politics, science and cricket. I am proud to say that my association with Dr Laksh also extends to the cricket field, where he and I are members of the same cricket club. I would also like to express my gratefulness to my co-supervisor Associate Professor Gade Pandu Rangaiah for agreeing to jointly supervise this project. His keen eye for detail and thorough supervision has significantly contributed to the quality of this thesis. Dr Laksh and Prof. Rangaiah are the sources of my inspiration in my wanting to pursue a career in pedagogy and they have shown me what it means to be a good researcher. For all this and more, I am indebted to them.

I am also indebted to the members of the Informatics and Process Control (IPC) group. Kyaw and Madhukar were vital in helping me overcome the initial inertia associated with my project. I thank Prabhat and Dharmesh for useful discussions on control loop performance assessment. Ramprasad (known as Rampa to his friends) and May Su were also wonderful colleagues to work with. Rampa in particular, whose knowledge of MATLAB is unrivalled, was of great assistance. I also wish to thank Mranal, with whom I've had many fruitful discussions on the subject of minimum variance control. My juniors, Raghu, Srini and Sundar have also been great company and I've relished our

numerous musings on research, life and love. Lastly, I'd like to sincerely thank my dearest colleague and friend, Balaji, who can always be counted on to lend a helping hand, be it helping me debug a MATLAB code or buying me coffee from Dily's. He has truly been a great confidante and for that I'm deeply grateful.

I would also like to express my deep appreciation to the various people who have helped me consolidate this thesis, in one way or another. I thank Dr. Keith Briggs, Prof. Sudeshna Sinha, Mr Gong Xiaofeng and Ms. Pavitra Padmanabhan for their efforts in explaining and simplifying the esoteric concept of chaos. I also thank Dr. Shoukat Choudhury, Ms. Zang Xiaoyun and Ms. Lakshmi Chaitanya for taking time off and facilitating discussions on higher order statistics, via email. I also gratefully acknowledge the MATLAB code provided by Prof. Sohrab Rohani and the relevant discussions I had on chaos in FCC units with Prof. Said Elnashaie. Mr P.N. Selvaguru and Mr Jaganathan Baskar have also been a great help to me by providing the industrial data used in this study. I also want to thank all the people I've met abroad at international conferences, with whom I've had interesting discussions pertaining to process control.

It is said that a man is known by the company he keeps. Throughout the course of my program, I have met and made many friends. I am indeed lucky to have gotten to know Senthil, Suresh, Karthiga, Anita, Murthy, Amrita, Mukta, Srinivas, Ye, Yew Seng, Huang Cheng, Yuva and Parthi. I would also like to thank my special group of friends who I have known for many years. I have tremendously enjoyed the company of Zahira, Magaesh, Sara, Dharini, Pam, Lavina, Pallavi, Laavi and Selva and will always remember

the good times we have had from watching movies to having late night drinks and dinner and philosophizing about life. Zahira in particular, has been a wonderful friend. She has seen me at my best and worst and yet always chooses to still be by my side. I thank her for her unwavering support and friendship throughout the many years I have known her. I would also like to acknowledge another special friend of mine, Kavitha. In the few months I have known her, she has struck me as an amazing person. From cooking me dinner, to helping me format my thesis, she has always answered my call for help and for that I thank her.

I would also like to acknowledge the financial support provided to me by the National University of Singapore, in the form of a research scholarship.

Last but not least, I want to express my deep gratitude to my sister Pooja and brother-in-law Nimesh, for allowing me to stay with them during the course of my masters program. They have gone out of their way to provide me with all the comforts and for that I am thankful. Finally I would like to thank my mum, dad and maternal grandparents (Thata and Ammama), without whose love and support, I would have never made it to this point. I dedicate this thesis to them with all my love and affection.

If I have seen this far,

it is because I have stood on the shoulders of giants

……. Isaac Newton

TABLE OF CONTENTS

SUMMARY

A typical chemical plant may employ several hundred to thousand control loops (feedback controllers) for the regulation of process variables. With the increased emphasis on production geared towards lower cost, higher profit and higher yield, chemical and related companies are relying more and more on their automatic control systems to ensure precise control of critical variables. Even when a loop performs well at the time of commissioning, its performance deteriorates over time due to changing operating conditions. In such a scenario, and especially with the easy availability of routine operating data, it makes sense to develop tools and procedures for measuring the performance of control loops and to determine the causes for loops exhibiting poor performance. Research work done in this thesis is motivated by the growing interest among the control research community towards performance monitoring and enhancement of control loops

For detecting poor control loop performance, many methods exist in the control literature. The minimum variance benchmark for control loop performance assessment (CLPA) that was first proposed by Harris (1989) is used in this study. With only the knowledge of time delay, this methodology can assess the performance measure of a loop. If a poorly performing control loop is identified, the basic remedy employed to improve performance is re-tuning the controller. However, this may have little or no effect in on the control loop performance index (CLPI) because the maximum achievable performance using the

feedback controller might have already been reached. This implies that there could be other reasons as to why the control loop is performing poorly.

Therefore, in this thesis, we propose a detailed framework that would systematically characterize the dynamics of a process variable to determine the cause(s) of its poor performance (if any). Various statistical and graphical techniques are coded to facilitate this analysis. This framework is implemented on an industrial fluid catalytic cracking (FCC) unit in which a temperature control loop is exhibiting less than satisfactory control loop performance. Our methodology is able to determine the cause(s) of the poor performance and to suggest suitable remedies to reduce the fluctuations and increase the CLPI of this temperature loop.

A novel framework that detects and diagnoses poor control loop performance is also proposed and tested on several realistic simulations and industrial case studies. Various mathematical models of valve nonlinearities are implemented to represent faults in the valves and a parameter estimation technique is incorporated to determine the type of valve nonlinearity. Subsequently, the framework is able to diagnose the cause of the poor CLPI and suggest the appropriate corrective action(s) by determining the effect of each control loop problem (i.e., poor controller tuning, valve nonlinearities and / or linear external oscillations) on control loop performance. Quantifying the individual effect of each of these control loop problems on CLPI, would enable the control engineer to make an informed decision in improving the performance of a control loop.

NOMENCLATURE

a: Hysteresis interval

b: Backlash interval

d: Stiction interval

F: First (θ-1) parameters of closed loop impulse response coefficients

G: Closed-loop servo process transfer function

N: Disturbance transfer function

Q: Controller transfer function

T: Process transfer Function

$\tilde{T}$: Delay free process transfer function

u_t: Process input

w_t: White noise signal

y_t: Process output

Greek Letters

β: Discriminating power

μ: Mean

σ: Standard deviation

τ: Lag

λ: Lyapunov exponent

θ: Time delay

η: Control loop performance index

LIST OF FIGURES

LIST OF TABLES

LIST OF PUBLICATIONS / PRESENTATIONS

R. Ramachandran, S. Lakshminarayanan and G.P. Rangaiah, "Process Identification using Open-Loop and Closed-Loop Step Responses", Journal of The Institution of Engineers, Singapore, 45 (6), 1-13, (2005).

R. Ramachandran, S. Lakshminarayanan and G.P. Rangaiah, "Investigating Chaos in an Industrial Fluid Catalytic Cracking Unit", Presented at the Graduate Student Association Symposium, Department of Chemical & Biomolecular Engineering, National University of Singapore, Singapore, September 2004.

R. Ramachandran, S. Lakshminarayanan and G.P. Rangaiah, "Detection of Nonlinearities and their Impact on Control Loop Performance", Presented at the National Conference on Control and Dynamical Systems, Mumbai, India, January 2005.

R. Ramachandran, S. Lakshminarayanan and G.P. Rangaiah, "Investigating Chaos in an Industrial Fluid Catalytic Cracking Unit", Presented at the American Control Conference, Portland, USA, June 2005.

CHAPTER 1

INTRODUCTION

This chapter contains sections on the definition and importance of process control followed by the motivation, objectives and organization of this thesis.

1.1 Prelusion

Process control is generically defined as an engineering discipline that deals with architectures, mechanisms and algorithms for maintaining the process output at specified values. In the recent years, the field of process control has seen much growth and has matured into one of the core areas of chemical engineering alongside thermodynamics, mass transfer, heat transfer, reactor kinetics and fluid dynamics (Luyben and Luyben, 1997). This quantum leap is reflected in the application of process control to many areas: (1) Agriculture, (2) Food and Beverage, (3) Life Sciences, (4) Pulp and Paper, (5) Pharmaceutical Industries, (6) Polymers and Plastics, (7) Refineries, (8) Chemical and Petrochemical plants and (9) Mineral Processing etc. However, regardless of the application, the purpose of process control is still the same and its objective is to ensure that the process is kept within certain specified boundaries, thus minimizing the variation in the process variables. Without an effective methodology to carry out this objective, the quality of the product and the safety of the plant personnel may be severely compromised. Therein lies the importance of process control.

For the purpose of this thesis, process control and its importance to chemical and related industries will be discussed. In the last decade, the performance criteria for chemical plants have become very stringent and exceedingly difficult to satisfy. Intense competition, tough environmental legislations, exigent safety regulations and rapidly changing socio-economic conditions have been the primary factors in the tightening of plant product quality specifications. This is further complicated given the fact that modern chemical plants are highly integrated and retrofitted. Such plants exhibit a high propensity to be upset as each individual unit is not an independent entity but rather dependent on other units due to the interconnected network. In view of the increased emphasis placed on safe and efficient plant operation to produce high quality products and given that good process control can help achieve this, process control has become an important research field.

1.2 Motivation

It is a well known fact that precise control of critical variables in a chemical plant, correlates directly with higher yield, better quality and lower cost thereby leading to increased profits. More often than not, chemical plants do not operate at their desired profit level and this is normally attributed to improper or inadequate process control. Hence, one may expect quick action to be carried out, the problem rectified and desired profit levels achieved. However, in reality, nothing could be further from the truth. Oftentimes, poor process control is attributed to the wrong cause thus suggesting the incorrect corrective action and resulting in no change or even worse conditions to the

current status. The responsibility of ensuring precise control of key variables lies with the control engineer who on average has to monitor 400 control loops (Desborough and Miller, 2001). This is a tough task and therefore it can be seen that the availability of a set of procedures that automatically estimate and diagnose the performance of a control loop will be much heralded in many chemical and related industries. The objectives of these tools would be to (1) detect poor performance, (2) diagnose the cause of poor performance and (3) implement the proper remedial action. These procedures must be non-invasive and use routine operating plant data. Whilst the first objective has been researched extensively in the literature (e.g., Desborough and Harris, 1992, 1993; Stanfelj et al., 1993; Horch, 1999; Huang, 1999; Xia and Howell, 2003), the remaining two objectives have not been thoroughly analyzed and remains an open area for research. A proper and focused study pertaining to these objectives would render succor to those concerned in various chemical plants. This is the motivation behind this thesis.

1.3 Problem Statement

In one of the local refineries, the riser temperature of the fluid catalytic cracking (FCC) unit was observed to have fluctuations of $\pm 5^0 C$ about the set-point which are higher than desired. These seemingly innocuous fluctuations, due to poor process control, affect the gasoline yield of the FCC unit which in turn has an adverse effect on the profit of the company. Hence, along with our industry contact we have attempted to ascertain the cause of these fluctuations and ameliorate the situation by implementing suitable corrective action(s).

1.4 Objectives

The final aim of this study is to reduce the riser temperature fluctuations to approximately $\pm 1^0 C$, as previous studies on other industrial FCC units have shown this to be possible (Grosdidier et al., 1993). However, it must be noted that different FCC units vary slightly in design and hence the same level of fluctuations in each unit may not be always possible. Given such a scenario, it is vital that in this study, we are able to pinpoint why in this particular industrial FCC unit, fluctuations within $\pm 1^0 C$ are not possible. Nevertheless, mitigating these fluctuations will be one of the focuses in this thesis. To accomplish the primary objective, there are various intermediate objectives that need to be addressed. Therefore the objectives of this study are summarized as follows.

- Implement a set of procedures that characterize the dynamics of routine operating plant data and use this to analyze the riser temperature data and other important controlled variables in the FCC unit. Chapters 3 and 4 cover these aspects of our study.
- Implement a dynamical model of the industrial FCC unit based on first principles to facilitate an in-depth study of certain key variables. The reader is referred to chapter 5 for more details on the dynamical model.
- Establish a control loop performance assessment (CLPA) framework to detect poor control loop performance of feedback loops. This framework should also ascertain the causes of this poor performance and then suggest suitable methods to improve the performance. The framework is discussed in detail in chapter 6.

1.5 Overview of the Thesis

This thesis is divided into seven chapters including this introductory chapter. Most of the chapters are inter-linked and it is advised that they be read in sequence. The contents of the chapters are as follows:

- Chapter 1 discusses the definition and important of process control and focuses on its impact on chemical and related industries. It then goes on to highlight the motivation, problem statement and objectives of this study.
- Chapter 2 provides a detailed description of the FCC unit. Dominant variables that influence the riser temperature and the current control strategy present in the existing unit are also included.
- Chapter 3 introduces a complete framework consisting of several mathematical and statistical techniques that can help to characterize the dynamics (i.e., linear or nonlinear, noise or chaos) of the process, using routine operating data. These techniques provide valuable insight into the nature of the data and therefore of the process.
- Chapter 4 analyzes the riser temperature data and other key variables using the techniques mentioned in chapter 3. From these analyses, specific knowledge of the process, which will assist in implementing suitable control strategies, is gathered.
- Chapter 5 describes the development and validation of a dynamical FCC model from first principles that realistically depicts the industrial FCC unit. It then goes

on to investigate the important variables in this model and propose a suitable control strategy or improve the one.

- Chapter 6 describes a consummate and novel approach to control loop performance assessment (CLPA) and enhancement. It aids the control engineer in detecting poorly performing control loops followed by establishing the causes (i.e., poor selection of tuning parameters, valve nonlinearity and / or linear external oscillations) of their poor performance. Thereafter, the effect of each of these causes is quantified (by determining the CLPI). By focusing on the more important causes of poor performance, appropriate rectification measures can be implemented to improve overall control loop performance.
- Chapter 7 concludes the thesis with a summary of its main contributions. It also provides recommendations for future work in this area.

CHAPTER 2

BACKGROUND ON THE FCC UNIT

This chapter contains sections on the overview of the industrial FCC unit, the dominant variables and the existing control strategy that is currently implemented in the unit.

2.1 Introduction

The FCC unit is one of the most important units and is known to contribute approximately 40% of the total revenue in a typical petroleum refinery (Wilson, 1997). It is the kernel of modern petroleum refining and its main function is to convert atmospheric residue (AR) from the crude distillation unit (CDU) into a multitude of value added products such as gasoline, middle distillates and light alkenes. The FCC unit is the most dominant conversion process in petroleum refineries and is also a major contributor of "value-added" products in the refining process. Fluid catalytic cracking is a process for splitting large molecules in the gas oil feedstock into smaller, more valuable gasoline molecules. The product yields from the FCC unit are dependent on the combination of feedstock and catalyst used. The FCC technology was initially developed in the 1930's and by 1942, the first commercial unit was ready.

The typical FCC unit consists of three major sections: the reactor-regenerator, the main fractionator and the light ends of gas concentration section. Today, the operation of the FCC unit has become advanced, encompassing the use of automatic process controllers to

control the key variables. This is because control of an FCC unit is an important and challenging problem. Precise control of the FCC unit is important because it affects product quality, yield and cost. It is a challenging problem due to the intricate and interacting nonlinear dynamics between the riser and the regenerator. This is further compounded by multiple steady states and input multiplicities (Arbel et al., 1995). Such complex dynamics may result in poor performance and reduced profits unless the unit is properly controlled.

2.2 Overview of the Industrial FCC unit

For the purpose of this study, the reactor-regenerator section of the FCC unit in a local refinery is analyzed. The simplified schematic of this section is shown in Figure 2.1. The main components of this section are the riser (labeled in Figure 2.1), the 1st and 2nd stage regenerator (labeled in Figure 2.1), the catalyst cooler and the withdrawal well (both not shown in Figure 2.1).

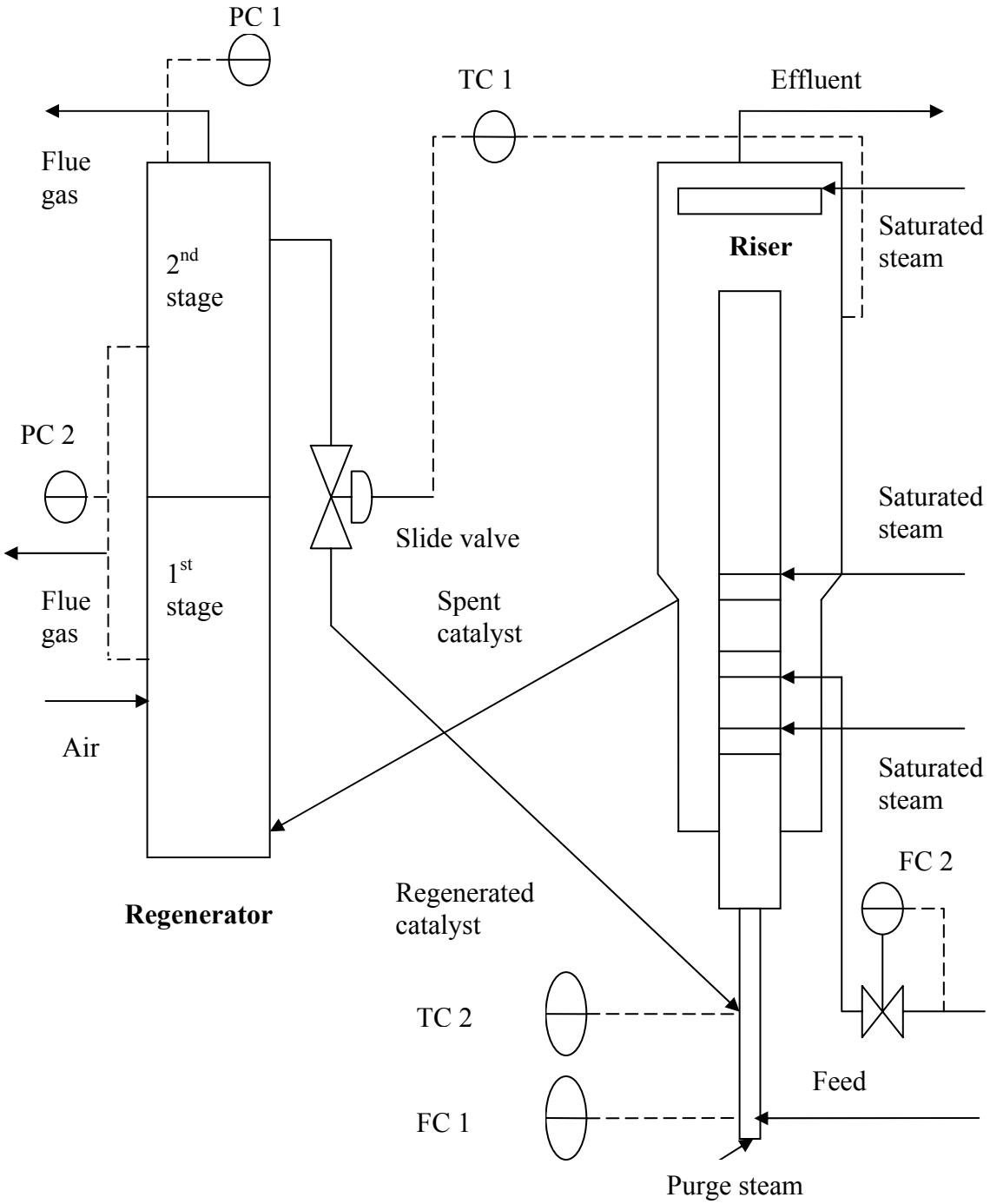

Figure 2.1: Simplified schematic of the FCC unit in the local refinery

The FCC unit in the local refinery is designed to crack AR from the CDU, which is fed into the feed surge drum (not shown in Figure 2.1) with other sources of feed such as heavy vacuum gasoil (HVGO) and light sulfur fuel oil (LSFO). The feed to the riser is preheated in a series of few heat exchangers (not shown in Figure 2.1) to the required temperature and then injected at the bottom of the riser, through the feed nozzles into the moving regenerated catalyst at high temperature. The cracking of the feed takes place in the riser. At the end of the riser the catalyst and hydrocarbon vapor disengage from each other. The catalyst flows down to the stripper where they are stripped free of the hydrocarbon by the saturated steam (labeled in Figure 2.1). The stripped catalyst is then sent to the regenerator for catalyst regeneration. The hydrocarbon vapors which are the effluent (labeled in Figure 2.1) pass through vertical pipes which discharge near the inlets of the four single stage cyclones (not shown in Figure 2.1) inside the upper section of the reactor. The entrained catalyst in the vapors is collected by the cyclones and flow down to the riser. The vapors leave the cyclones and flow into the main fractionator flash zone.

During the process of catalytic cracking in the riser, coke is deposited on the catalyst. The spent catalyst is sent to the two-stage regenerators. The catalyst is fluidized and the flows of the spent and regenerated catalysts (labeled in Figure 2.1) are controlled by the slide valves. The spent catalyst is partially regenerated by burning the coke with combustion air in the first stage regenerator (labeled in Figure 2.1). The partially regenerated catalyst flows upward to the second stage regenerator (labeled in Figure 2.1) via the lift line controlled by the plug valve. The catalyst cooler (not shown in Figure 2.1) helps to keep the temperature within a controlled range in the second stage regenerator especially

during the processing of higher percentage of carbon in the feed. It is expected that the cokes on the catalyst would have almost been burnt off in the second stage regenerator. The regenerated catalyst flows from the second stage regenerator and enters the riser where the hydrocarbon feed is injected at the bottom of the riser through fresh feed nozzles. A small amount of purge steam keeps the nozzles clear of any catalyst. As the fresh feed passes through the nozzles, it is finely atomized and dispersed in the steam injected in the feed nozzles.

2.3 Dominant Variables

Dominant variables are defined to be those that exert a strong influence on other variables. By controlling these dominant variables, fluctuations in other process variables will be mitigated. Therefore, it is imperative that the proper dominant variables are identified for the purpose of good control. The feed flowrate into the riser and temperature of the feed entering the riser have been identified as the two dominant variables of the FCC unit (Toh, 2002). Apart from these two dominant variables, three other variables although are not considered dominant, are identified as plausible causes for temperature variations in the riser. Therefore, the variations in all five variables are seen as a potential source of disturbance to the riser temperature. These variables along with their controller tags (labeled in Figure 2.1) are listed in Table 2.1.

Table 2.1: Description of disturbance variables

Controller tag	Process variable
FC 1	Feed flowrate into the riser
PC 1	Pressure of 2nd stage regenerator
PC 2	Pressure differential between 1st and 2nd stage regenerator
TC 2	Temperature of feed entering the riser
FC 2	Flow of saturated steam into the riser

2.4 Existing Control Strategy

As mentioned in chapter 1, the riser temperature (temperature control loop TC1) in the FCC unit is the focus of our current investigation. TC1 is a proportional-integral (PI) controller that operates in a feedback control configuration. TC1 controls the temperature of the riser by manipulating the opening of the slide valve (labeled in Figure 2.1) thereby adjusting the amount of regenerated catalyst fed back to the riser. The process variable is the riser temperature and the manipulated variable is the regenerated catalyst flow rate. When the temperature of the riser changes by more than 15% (due to poor control or other variables affecting the riser temperature), a supervisory controller will provide the set-point for TC1.

2.5 Summary

In this chapter, the industrial FCC unit was described, followed by dominant variables and the existing control strategy. In the next chapter, various statistical and mathematical methods used in this study will be presented.

CHAPTER 3

STATISTICAL TOOLS AND FRAMEWORK

This chapter contains sections on tests for stationarity, Gaussianity, nonlinearity and chaos followed by noise removal techniques.

3.1 Introduction

Traditionally, in the realm of process control, characteristics of data (such as nonlinearity) are detected by subjecting the process to an input excitation in either open-loop or closed-loop, followed by analyzing the process response. This approach albeit simple in implementation is not desirable. Given that any industrial process needs to operate under optimal conditions, data characterization under open-loop conditions would incur the risk of deviating from this optimum range, thus resulting in lower yield and loss of revenue. Even in closed-loop conditions, set-point changes that are implemented may bring forth the process to non-optimal conditions. Therefore, tools and procedures that do not require any excitation in the form of step changes or set-point changes are very much needed. The tools should use routine operating data which are perennially available due to major advances in sensor technology. Statistical procedures can uncover process characteristics in a manner that facilitates process understanding. Statistics, especially higher order statistics, although ubiquitous in the field of mathematics, is relatively new to process monitoring and the control literature. In the next few sections, an array of techniques that analyzes routine operating data will be presented.

3.2 Tests for Stationarity

A time series is said to be stationary if the distribution of a variable X_1, X_2,…, X_n is the same as the distribution of the variable shifted by some lag k, X_{1+k}, X_{2+k},…, X_{n+k}; i.e., the distribution of the variable does not depend on time t. Whenever one looks at the distribution for some segment, the dynamics remains the same. This implies that the observation is independent of time. In a nutshell, a stationary process has the property that the mean, variance and auto-correlation do not change over time. Qualitatively speaking, a flat looking time series, without trend, constant variance over time, constant auto-correlation structure over time and no periodic fluctuations would insinuate stationarity. A common assumption in many time series techniques is that the data are stationary. However, this is a fallacious assumption as in most cases the data are not stationary. One of the criteria to ensure that these statistical analyses provide accurate characterization of data is stationarity. Hence, two tests for stationarity are introduced to quantify stationarity mathematically.

A number of quantitative tests for stationarity exist but the two most common tests used in practice are the runs test and the reverse arrangements test. Of the two tests, the latter is more powerful in detecting non-stationarity (Padmanabhan, 2004). This section describes the details of these tests. These tests will be subsequently employed in chapter 4, to determine if process data are indeed stationary.

3.2.1 Runs Test

This widely used test for stationarity works by classifying data into two mutually exclusive categories identified simply by plus (+) and minus (-). For a given time series, we first find the mean (or median) and then go down the list of values, assigning a '+' if the value is greater than the mean and a '-' if it is less than the mean. The signs are then grouped into a series of runs, where a run is defined as a sequence of identical observations that is followed or preceded by a different observation or none at all. The total number of runs (r) is found. After this is done, a suitable level of significance (α) is selected. If r is such that

$$r_{N/2;1-\alpha/2} \leq r \leq r_{N/2;\alpha/2} \tag{3.1}$$

where N is the total number of samples, the signal is said to be stationary. For a 5% level of significance and 20 samples, r must lie between 6 and 15 and for a 5% level significance and 200 samples, r must lie between 86 and 115 (Bendat and Piersol, 1991). However, no confidence intervals for r are reported for more than 200 samples. While, a 5% level of significance is acceptable, a data length of 200 samples is too short, since we are dealing with data of around 4000 samples and more. Therefore, we need to find a way to circumvent this issue.

Hence, we have developed a code in MATLAB that divides the data into segments of 200 samples and calculates the total number of runs for each segment. Thereafter, the median value of the total number of runs is calculated (median is selected as opposed to the mean so as to mitigate the impact of outliers) and if it lies within the confidence interval, the data are deemed to be stationary.

3.2.2 Reverse Arrangements Test

This test is a more powerful test for stationarity than the runs test. It works as follows: if a random variable x is given by x_i where i = 1, 2,…., N, we count the number of times $x_i > x_j$ for i < j. Every such inequality is known as the reverse arrangement. In other words, let h_{ij} = 1, if $x_i > x_j$ and 0, otherwise. Then,

$$A = \sum_{i=1}^{N-1} A_i \text{ where } A_i = \sum_{j=i+1}^{N} h_{ij} \tag{3.2}$$

For instance, $A_1 = h_{12} + h_{13} + h_{14} + \ldots + h_{1N}$. Again, we choose a suitable significance level and if A is such that

$$A_{N;1-\alpha/2} \leq A \leq A_{N;\alpha/2} \tag{3.3}$$

where N is the total number of samples, the signal is stationary. With a significance level of 5% and 100 samples, the value of A must lie between 2145 and 2804 (Bendat and Piersol, 1991). Once again, the confidence interval is not available for larger data sets. Therefore, similar to the procedure in the runs test, a MATLAB code has been implemented to calculate A for each segment of 100 samples and then the median value of all the calculated A's is determined. If this value lies inside the confidence interval, the data are stationary.

3.2.3 Transformations to Achieve Stationarity

In the previous section, it was noted that several statistical techniques are applicable only to stationary data. Therefore, if the time series is not stationary, it can be transformed to achieve stationarity through the following techniques:

- The data can be differenced. That is, given the series Y_i, a new series $Z_i = Y_i - Y_{i-1}$ is created. The differenced data will contain one less sample compared to the original data. Although the data can be differenced more than once, often one difference is sufficient to achieve stationarity in process data.
- If the data contain a trend, we can fit a curve to the data and then model the residuals from that fit. Since the purpose of the fit is to simply remove long term trends, a simple fit, such as a straight line, is typically used.
- For non-constant variance, taking the logarithm or square root of the series may stabilize the variance. For negative data, a suitable constant can be added to make the entire data positive before applying the transformation. This constant can then be subtracted from the model to obtain predicted values and forecasts for future points.

3.3 Tests for Gaussianity

A time series is said to be Gaussian if it has a continuous symmetric distribution that follows the familiar bell shaped curve. Such a distribution is uniquely characterized by its mean and variance. Empirical evidence has shown that many measurement variables have distributions that are approximately Gaussian. Even when a distribution is non-Gaussian, the distribution of the mean of many independent observations becomes Gaussian as the number of observations becomes large (Schreiber and Schmitz, 2000). This gives credence to the evolution of many statistical tests that make the assumption that the data come from a Gaussian distribution. However, the presence of certain trends (such as

nonlinearities or chaos) can cause the time series to be non-Gaussian. Hence, the test for Gaussianity of a signal is a useful diagnostic tool. This is because, for a non-Gaussian signal there exist a special set of statistical tools that should be used as opposed to the more general statistical measures used for Gaussian signals. Refer to section 3.4 for a more elaborate discussion.

For this study, Kurtosis is used to determine if a time series is Gaussian. Kurtosis is the degree of peakedness of a distribution and is defined as the normalized form of the fourth central moment of a distribution. It is given by:

$$Kurtosis = \frac{\sum (x_i - \bar{x})^4 - 3}{N\sigma^4} \tag{3.4}$$

where x_i = data point, $\bar{x}$ = mean, N = number of samples and σ = standard deviation.
For a Gaussian distribution, the Kurtosis will be zero. In our study, we use the in-built Kurtosis function file in MATLAB to calculate Kurtosis.

3.4 Tests for Nonlinearity

In the previous section, it was mentioned that nonlinearities may render a time series non-Gaussian (Schreiber and Schmitz, 2000). Since many statistical procedures assume that the time series signal is Gaussian, it is imperative that the signal is investigated for nonlinearities. Previously, the statistical theory of linear stochastic processes had led to the development of a compendium of procedures and techniques for the numerical analysis of time series. These were tools that characterized the deterministic and

stochastic aspects of a time series. Currently, these tools have been extrapolated to nonlinear processes and some of these techniques will be discussed here.

There are two main reasons to use a nonlinear approach when analyzing time series data. Firstly, the plethora of linear methods has been exploited completely and yet cannot account for certain structures in the data. Secondly, there may be apriori knowledge that the system is nonlinear in nature and therefore it is unsatisfactory to use linear methods (Schreiber, 1999). While these may justify the usage of a nonlinear analysis, it is still important to mathematically establish nonlinearities in the data rather than relying on visual or intuitive judgement. In this section, we will discuss two formal statistical tests for nonlinearities.

3.4.1 Nonlinear Systems

Nonlinear systems are systems whose behaviour cannot be expressed as a linear function of its descriptors. In such a system, the principle of superposition is not valid and its equation cannot be split into the sum of its parts. This means that certain assumptions, approximations and mathematical approaches are not possible, implying that special techniques such as higher order statistics have to be implemented.

3.4.2 Higher Order Statistics

Higher order statistics (HOS) is a field of statistical signal processing that has become very popular in recent years (Nikias and Petropulu, 1993). It is a rapidly evolving signal analysis area with many applications in science and engineering. Applications of HOS are

abundant and include telecommunications, sonar, radar, geo-physics, image processing, speech processing, biomedicine, oceanography, plasma physics, econometrics and fluid mechanics.

The scope of HOS has recently been extended to chemical processes (Choudhury, 2004). HOS makes use of extra information on top of what is generally used in traditional signal processing. Therefore, HOS measures are extensions of second order measures (such as the auto-correlation function and the power spectrum). These second order measures work well if the time series signal has a Gaussian (normal) probability density function. However in practice, most processes deviate from Gaussianity especially when they exhibit nonlinear behavior. Such nonlinearities cause certain types of phase coupling which second order measures are unable to accurately identify as they contain no phase information (Nikias and Petropulu, 1993). Hence, HOS measures can be used to extract the correct phase information and detect nonlinearities.

3.4.3 Generating Functions

A generating function of a random variable is an expected value of a certain transformation of the variable. All generating functions have three important characteristics.

- Under mild conditions, the generating function completely determines the distribution of the random variable.
- The generating function of a sum of independent variables is the product of their generating functions.

- The moments of the random variable can be obtained from the derivatives of the generating functions.

Therefore, given any random variable x and a probability distribution function P(x), the moment generating function can be defined as the expectation of the transformation, e^{tx}, where $t \in R$, i.e.,

$$M_x(t) = E[e^{tx}] \tag{3.5}$$

Moments of the random variable are obtained from the coefficients of the Taylor's series expansion of the moment generating function about the origin.

$$M_x(t) = M_x(t)|_{t=0} + \frac{\partial M_x(t)}{\partial t}|_{t=0}\ (t-0) + \frac{1}{2!}\frac{\partial^2 M_x(t)}{\partial t^2}|_{t=0}\ (t-0)^2 + \frac{1}{3!}\frac{\partial^3 M_x(t)}{\partial t^3}|_{t=0}\ (t-0)^3 + ..$$

$$= M_x(t)|_{t=0} + \frac{\partial M_x(t)}{\partial t}|_{t=0}\ t + \frac{1}{2!}\frac{\partial^2 M_x(t)}{\partial t^2}|_{t=0}\ t^2 + \frac{1}{3!}\frac{\partial^3 M_x(t)}{\partial t^3}|_{t=0}\ t^3 + ... \tag{3.6}$$

From the right hand side of equation 3.6, the first derivative gives the first order moment:

$$m_1 = \frac{\partial M_x(t)}{\partial t}|_{t=0}$$

$$= \frac{\partial E[e^{tx}]}{\partial t}|_{t=0}$$

$$= E[xe^{tx}]|_{t=0}$$

$$= E[x] \tag{3.7}$$

The second derivative gives the second order moment:

$$m_2 = \frac{\partial^2 M_x(t)}{\partial t^2}|_{t=0} = \frac{\partial^2 E[e^{tx}]}{\partial t^2}|_{t=0} = E[x^2 e^{tx}]_{t=0} = E[x^2] \tag{3.8}$$

In a similar fashion, the third derivative leads to the third order moment:

$$m_3 = E[x^3] \tag{3.9}$$

Hence, we can write the moment generating function as

$$M_x(t) = E[e^{tx}]$$

$$= E[1 + tx + \frac{t^2}{2!}x^2 + \frac{t^3}{3!}x^3 + ...]$$

$$= 1 + tE[x] + \frac{t^2}{2!}E[x^2] + \frac{t^3}{3!}E[x^3] + ...$$

$$= 1 + tm_1 + \frac{t^2}{2!}m_2 + \frac{t^3}{3!}m_3 + ... \tag{3.10}$$

The first order moment is the mean (μ) of a data series. The second order moment is the variance (σ^2), the third order moment is the skewness and the fourth order moment is the Kurtosis.

3.4.4 Cumulants

Cumulants are an alternate set of statistical measures that can be used in place of moments due to their exceptional noise suppressing properties. A cumulant generating function is defined as the logarithm of the moment generating function. For a random variable x, the cumulant generating function is

$$C_x(t) \equiv \ln(M_x(t)) \tag{3.11}$$

Similar to moment generating functions, cumulants can also be derived from the Taylor's series expansion of the cumulant generating function.

$$C_x(t) = C_x(t)|_{t=0} + \frac{\partial C_x(t)}{\partial t}|_{t=0}\ (t-0) + \frac{1}{2!}\frac{\partial^2 C_x(t)}{\partial t^2}|_{t=0}\ (t-0)^2 + \frac{1}{3!}\frac{\partial^3 C_x(t)}{\partial t^3}|_{t=0}\ (t-0)^3 + ...$$

$$= C_x(t)\,|_{t=0} + \frac{\partial C_x(t)}{\partial t}\,|_{t=0}\; t + \frac{1}{2!}\frac{\partial^2 C_x(t)}{\partial t^2}\,|_{t=0}\; t^2 + \frac{1}{3!}\frac{\partial^3 C_x(t)}{\partial t^3}\,|_{t=0}\; t^3 + \ldots \tag{3.12}$$

Hence, the first order cumulant is given by:

$$c_1 = \frac{\partial C_x(t)}{\partial t}\,|_{t=0}$$

$$= \frac{\partial \ln[E[e^{tx}]]}{\partial t}\,|_{t=0}$$

$$= \frac{\partial \ln[1 + tm_1 + \frac{t^2}{2!}m_2 + \frac{t^3}{3!}m_3 + \ldots]}{\partial t}\,|_{t=0}$$

$$= \frac{1}{[1 + tm_1 + \frac{t^2}{2!}m_2 + \frac{t^3}{3!}m_3 + \ldots]}[m_1 + \frac{2t}{2!}m_2 + \frac{3t^2}{3!}m_3 + \ldots]\,|_{t=0}$$

$$= \mathrm{m}_1 \tag{3.13}$$

Similarly, the second, third and fourth order cumulants are:

$$c_2 = m_2 - m_1^2 \tag{3.14}$$

$$c_3 = m_3 - 3m_2m_1 + 2m_1^3 \tag{3.15}$$

$$c_4 = m_4 - 4m_3m_1 - 3m_2^2 + 12m_2m_1^2 + 6m_1^4 \tag{3.16}$$

3.4.5 Cumulant Spectra

Time series data are generally a good source of information. The statistical measures described so far have been developed to quantify signal characteristics. However, in the time domain analysis, not all the information of a signal can be captured. Therefore,

transforming the signal from time to frequency domain can expose the periodicities of the signal, detect inherent nonlinearities in the signal and help comprehend the dynamics of the signal generating process. The main tool for this kind of transformation is the Discrete Fourier Transform (DFT). The power spectrum, bispectrum and trispectrum are the special cases of the nth order cumulant spectrum that are a result of this transformation.

3.4.6 Power Spectrum

The power spectrum is the frequency domain counterpart of the second order cumulant (auto-correlation function) of a signal. For a given signal, the power spectrum gives a plot of the portion of a signal's power falling in a range of frequencies. Common ways of generating the power spectrum are by using the DFT or the maximum entropy method. In this study, the former is used and it has been coded in MATLAB. The power spectrum is given by:

$$P(f) = DFT[m_2(\tau)] \equiv \sum_{\tau=0}^{N-1} m_2(\tau) e^{-j2\pi f/N} \tag{3.17}$$

3.4.7 Bispectrum

The bispectrum is the frequency domain counterpart of the third order cumulant of a signal. The methodology used for estimating the power spectrum can also be extended to obtain the frequency domain counterparts of higher order spectra. The bispectrum is defined to be:

$$B(f_1, f_2) = DDFT[c_3(\tau_1, \tau_2)] \equiv E[X(f_1)X(f_2)X^*(f_1 + f_2)] \tag{3.18}$$

where DDFT stands for Double Discrete Fourier Transformation. Equation 3.18 shows that it is a complex quantity having both magnitude and phase. The bispectrum is plotted

against two independent frequency variables, f_1 and f_2 in a three dimensional plot. Any point in the plot represents the bispectral content of the signal at those particular frequencies and the bispectrum at any point measures the interaction between frequencies f_1 and f_2. This interaction between the two frequencies can be related to the nonlinearities present in the signal and herein lies its importance in the detection of nonlinearities.

In the same fashion, higher order spectra, known as polyspectra can be derived. However, in this thesis, higher order spectra of the fourth order and above are not discussed and the scope will be limited to power spectrum and bispectrum. This is because, bispectral analysis is sufficient as it is found to have the capability of detecting nonlinearities as the magnitude of the bispectrum will show nonzero peaks for a signal that is nonlinear. However, the variance across the bispectrum is not uniform and this may lead to spurious results. Therefore, a new quantity with an approximately flat variance can be normalized by dividing the bispectral estimate by this variance term. In literature, there are several normalization schemes for the bispectrum, each with its own advantages and disadvantages. Two of the popular schemes are:

- Bicoherence (Kim and Powers, 1979).
- Bicoherency Index (Nikias and Petropulu, 1993).

A useful feature of the first method is that it is bounded between 0 and 1. As for the second method, it is unbounded but it ensures a flatter variance which would ensure more

accurate quantification of nonlinearities. Hence, for this study, the second method is incorporated and is presented next.

3.4.8 Bicoherency Index (BI)

A normalized cumulant spectrum or the n[th] order coherency index is a function that combines two completely different entities which are the cumulant spectrum of order n, $C_n^x(\omega_1,...,\omega_{n-1})$ and the power spectrum of a process. Therefore, the bicoherency index which is also the third order coherency index is given by:

$$P_3^x(\omega_1,\omega_2) = \frac{C_3^x(\omega_1,\omega_2)}{[C_2^x(\omega_1).C_2^x(\omega_2).C_2^x(\omega_1+\omega_2)]^{\frac{1}{2}}} \tag{3.19}$$

The magnitude of this index is known as the bicoherency index (BI). There are practical situations where it is imperative to be able to distinguish between a linear Gaussian process, a linear non-Gaussian process and a nonlinear non-Gaussian process. A linear Gaussian process has zero n[th] order moments and this ensures that the skewness is zero i.e.,

$$C_3^x(\omega_1,\omega_2) = 0 \tag{3.20}$$

Hence, the BI of this process is zero. For non-Gaussian linear and nonlinear processes, the n[th] order moments are nonzero. Hence the BI is not zero but rather some finite value. The difference between these two processes is that for the former, the BI is constant at all frequencies and for the latter the BI varies and is dependent on the individual frequencies. In this manner, BI can easily distinguish between the three types of processes stated above. As part of this work, the BI calculation procedure has been implemented in

MATLAB. In the following chapters, we will quantitatively and qualitatively illustrate how the BI is able to distinguish such processes.

3.4.9 Surrogate Data Method

Most tests for nonlinearities are performed by specifying some well defined null hypothesis and then calculating a test statistic to test against this hypothesis. A common null hypothesis is that the data are generated by a linear Gaussian stochastic process (Schreiber and Schmitz, 2000). We will then attempt to reject this null hypothesis by comparing the value of a nonlinear parameter estimated from the data. This concept is known as the surrogate data method (SDM). Thus this is a two-fold task. Firstly, we have to find a nonlinear parameter that is able to veritably detect an existing deviation of the data from a given null hypothesis and we have to provide an array of randomized time series that accurately represents the null hypothesis. The latter is known as the surrogate data.

Surrogate data refers to random data that are generated in such a way that they have the same mean, variance and auto-correlation as the original data. This basically means that for both original and surrogate data, all first and second order statistics are exactly identical. There are three ways of generating surrogate data (Chang et al., 1995).

- **Phase randomized surrogates**: A phase-randomized surrogate is generated by randomizing the phases of the Fourier transform of the signal and then inverting it to time domain. The surrogate has identical first and second order statistics as the

original but has a different distribution of amplitudes (histogram) from the original. This method is implemented using the 'unwindowed Fourier transform' algorithm.

- **Gaussian-scaled surrogates:** In this method, the signal is shuffled based on the assumption that it is a Gaussian random process that is passed through a nonlinear filter. A Gaussian distributed random process is shuffled in the rank order of the experimental data, phase randomized and then the amplitudes of the original data are rank ordered and substituted. Since it is a shuffle of the original data, the histogram of the amplitudes is maintained. This method is implemented using the 'amplitude adjusted Fourier transform'.
- **Fourier shuffled surrogates:** The signal is shuffled by rank ordering the original data in the order of a phase-randomized surrogate. This surrogate usually approximates the power spectrum more closely than the Gaussian-scaled surrogate and still preserves the marginal distribution.

In this study, the first two methods have been implemented in Matlab to generate surrogate data sets.

3.4.10 Discriminating Statistics

For the purpose of nonlinearity testing, we need quantifiers that are particularly powerful in discriminating linear dynamics and weakly nonlinear entities. This is because strong nonlinearities are more easily detectable. An important objective criterion is the discriminating power of the resulting test. The power β is defined as the probability that

the null hypothesis is rejected when it is false. Taking this into consideration, a number of test statistics are available for discrimination. It is therefore important to choose a statistic that is easy to compute and achieves best performance for the purpose of discrimination. Examples of test statistics employed are the Brock, Declert and Scheinckman (BDS) statistic, time asymmetry (time reversal) and the Takens estimator for correlation dimension (Galka, 2000; Kantz and Schreiber, 1997). A number of investigations have been carried out to gauge the effectiveness of these test statistics in detecting nonlinearities. Some of these studies have shown that the BDS statistic and correlation dimension work poorly in detecting nonlinearities (Theiler et al., 1992; Galka, 2000).

3.4.11 Time reversibility

A simple and yet powerful discriminating technique is time reversibility (Diks et al., 1995). A time series is said to be reversible if its probabilistic properties are invariant with respect to time reversal. Whilst time reversibility is not a definitive indicator of linearity, time irreversibility indicates the presence of nonlinearities. There are many variations of the time reversibility (TR) test. The one used in this study is defined as:

$$T_{rev}(\{x_n\},\theta) = \frac{\left\langle (x_n - x_{n-\theta})^3 \right\rangle}{\left\langle (x_n - x_{n-\theta})^2 \right\rangle^{\frac{3}{2}}} \tag{3.21}$$

where θ is the delay. θ is determined from the method of mutual information which will be discussed in section 3.5.4.

3.4.12 Hypothesis Testing

With a large number of generated surrogates (the minimum recommended being 100), the T_{rev} histogram will tend toward a Gaussian distribution (Galka, 2000). If the signal is linear, the T_{rev} value of the original signal will lie well within the range of the surrogates because the generated surrogates are always time reversible. If the signal is not linear, T_{rev} value of the original signal will lie outside the range of the surrogates. This is a qualitative approach and it may work well for a strictly linear or highly nonlinear signal. However, it can fail for a mildly nonlinear signal as one may not be able to say confidently if the T_{rev} original lies within or outside the range of the surrogates. Hence, we need a rigorous method for categorizing linear and nonlinear processes as well as quantifying the degree of nonlinearity that is present in the data. Hypothesis testing is one such method that provides the means to achieve this. Hypothesis testing is a way to determine if a time series is nonlinear by combining the SDM and TR methods. It provides a quantitative way of determining whether or not results obtained are significant enough to conclude that nonlinearities are present. The strategy is as follows:

1. We first formulate a null hypothesis, i.e., we hypothesize that the data are produced by a Gaussian linear stochastic process.
2. We then generate 500 surrogate data sets from the original data set using one of the methods described earlier.
3. A suitable test statistic, e.g. TR, is calculated for the original data set ($T_{rev,ori}$) as well as the 500 surrogates ($T_{rev,surr}$).

4. A histogram of the 500 values is plotted to determine if the distribution is approximately Gaussian and then the mean (μ_{surr}) and standard deviation (σ_{surr}) of the surrogates are calculated.
5. The observed statistic is given by $\frac{T_{rev,ori} - \mu_{surr}}{\sigma_{surr}}$
6. A suitable level of significance is chosen and the hypothesis is either rejected or accepted. In order to reject the hypothesis at a 95% confidence level, the observed statistic should be at least 2. If the distribution is not Gaussian, we need between the observed statistic to be between 5 and 6 in order to reject the hypothesis (Galka, 2000).

The hypothesis testing procedure, combined with the TR and SDM has been coded in MATLAB as part of this research effort.

3.5 Tests for Chaos

In the previous section we discussed linearity and nonlinearity and how most real life systems and processes are nonlinear in nature. Linear systems are easier to solve both in principle and practice, with significant savings in computational time and cost. Therefore, most nonlinear systems are linearly approximated before solving them. However, for some cases, linear functions and equations are just not good approximations. This led to a new classification of highly nonlinear systems now known as chaotic systems and the phenomenon at the heart of this is chaos (Grebogi and Yorke, 1997). Chaos theory has been well explored in the fields of mathematics and theoretical physics compared

chemical engineering. However, some studies have shown chemical processes do exhibit chaotic behaviour under certain conditions (Abasaeed and Elnashaie, 1997; Abasaeed and Elnashaie, 1998). Hence this section aims to discuss the relevant statistical tools that detect chaos. It must be noted that although such tools and algorithms are designed to make this distinction, they are known to be unreliable and usually involve considerable human judgement. This is especially true for experimental time series data which are short in length and noisy (Tanake et al., 1993). Chaos quantifiers employed may be fooled into signaling chaos when there is none to begin with. One study has shown that it is plausible for one method to detect chaos and for another to show otherwise (Fraser, 1999). This problem is further intensified given the fact that there is a fine line between chaos and noise. Fluctuations that are mistaken for chaos may actually be due to nonchaotic but still nonlinear determinism, linear correlations and noise. The prerequisite of chaos is nonlinearity. In principle, any nonlinear system has the potential to exhibit chaos. Many chemical process systems are nonlinear and there are many ways of determining this. However, these chemical systems are not investigated for chaos. Therefore, we propose to implement several chaotic quantifiers that would confirm the presence of chaos. This knowledge would aid us in truly understanding the nature of the process. Therefore, identification of chaos and more importantly pin-pointing the degree of chaos using statistical tools would be the first steps in studying chaotic systems.

3.5.1 Chaos and Chaotic Systems

Chaos is the breakdown of predictability and represents a state of disorder. In the world of dynamics, chaos refers to the generation of random, unpredictable behaviour from a

simple, but nonlinear rule. A chaotic system is a highly nonlinear dynamical system that is very sensitive to initial conditions. Hence, subtle changes in its initial conditions lead to rapid divergence of the system from one trajectory to another amongst the many possible trajectories (Alligood et al., 1997). Such systems are also mathematically deterministic as in they follow precise laws but their irregular behavior can appear random to the casual observer.

3.5.2 Phase-Space Reconstruction

When testing for chaos, it is important to obtain the proper information from the time series data. Hence, a solution to extract geometric information from these time series data was proposed by Packard et al. 1980. The basic idea is that the state of an m-dimensional dynamical system can be uniquely characterized by m independent quantities. One such set of independent quantities are the phase space coordinates. However, this is not possible as the only data one has in the beginning is the one dimensional time series data. Hence, a one dimensional time series is expanded into a higher dimensional space using a technique called 'delayed coordinate embedding' (Takens, 1981). This creates a phase-space portrait of the dynamical system and transforms it into an m-dimensional system from which the correct information can be retrieved.

3.5.3 Delayed Coordinate Embedding

The process of delayed coordinate embedding can be summarized as follows. Each observation in the signal x(t) is substituted with a vector given by:

$$y(i) = \{x(i), x(i+\tau), x(i+2\tau), ..., x(i+(M-1)\tau)\} \tag{3.22}$$

where M = embedding dimension, τ = time delay, i = time index. Thus, the original signal can be represented as a set of vectors with each vector corresponding to a single state or an observation of the time series. The algorithm for delayed coordinate embedding has been developed in MATLAB. The embedding dimension and time delay are important parameters in determining an appropriate phase space representation from which useful information about signal structure can be derived. Algorithms exist for finding the optimal value of M and τ are described in the following sub-sections.

3.5.4 Average Mutual Information (AMI)

It is important to choose a good value of τ, the time delay. If the delay is too short, then x(t) is very similar to x(t+τ) and when plotted, all the data stays near the x(t) = x(t+τ) line. If the delay is too long, then the coordinates are essentially independent and no information can be gained from the plot. Therefore, the value of the time delay is chosen by plotting a graph of mutual information I(τ) between x(t) and x(t+τ) and finding the value for which I(τ) is a minimum (Fraser and Swinney, 1986). This algorithm has been implemented in MATLAB as part of this work.

3.5.5 False Nearest Neighbours (FNN)

The false nearest neighbours (FNN) method is used to find the optimal embedding dimension (Kennel et al., 1992). It works by finding the nearest neighbour of every point in the phase space for a given dimension and then checks to see if the points are close neighbours in the next higher dimension. If the distance between the two points (S_i and S_j)

in the higher dimension divided by the distance in the present dimension exceeds a given heuristic threshold (R_t), i.e.,

$$R_i = \frac{\left|S_{i+1} - S_{j+1}\right|}{\left\|S_i - S_j\right\|} > R_t \tag{3.23}$$

the point is marked as a false nearest neighbour. The percentage of false nearest neighbours should be at its minimum when the optimal embedding dimension is reached. Similar to the AMI algorithm, this algorithm has also been written in MATLAB.

3.5.6 Recurrence Plots

Recurrence plots are a useful qualitative tool for detecting the presence and amount of structure in a given dataset (Eckman et al., 1987). Once the phase-space representation of the signal is obtained, a recurrence plot can be used to show which vectors in the reconstructed space are close and far from each other by calculating the Euclidean distance between all pairs of vectors. The recurrence plot is then merely a colour-mapped representation of a 2-dimensional array where each element (i,j) represents the Euclidean distance between the vectors y(i) and y(j). It has been likened to a graphical representation of a correlation integral with the advantage that it preserves the temporal dependence of the time series (Eckman et al., 1987). The recurrence plot of a completely random signal (e.g. white noise) will show a uniform distribution of colours over the entire plot. On the other hand, a recurrence plot of a deterministic signal (e.g. a sine wave) will be more structured. Hence, a chaotic process would have a recurrence plot that has both a uniform and structured distribution of colours. Furthermore, the quality of the recurrence plot is affected by the choice of time delay and embedding dimension. Hence, optimal values of

these parameters using the methods described above may bring out the hidden structure of the data. The visual recurrence analysis (VRA) freeware is used to generate recurrence plots.

3.5.7 Spatio-Temporal Entropy

Spatio-temporal entropy provides a quantitative measure of the degree of structure in both space and time domain (Fan et al., 2001). It compares the distribution of colours over the whole recurrence plot with the distribution of colours over each diagonal line present in the plot. The higher the combined difference between the global distribution and the distribution over the individual lines, the more structured the image. In other words, it compares the distribution of distances between all pairs of vectors in the reconstructed space with that of the distances between different orbits evolving in time. The result is normalized and presented as a percentage of the maximum entropy. 100% entropy indicates the absence of any kind of structure whatsoever, i.e. pure randomness and thus a uniform distribution of colours. On the other hand, 0% entropy indicates complete determinism or perfect structure and thus distinct patterns and a high predictability. A chaotic process would incorporate both randomness and determinism and therefore, its spatio-temporal entropy will be in the mid range of 0% - 100%.

3.5.8 Return Maps

As seen in the earlier sections, the result of delayed coordinate embedding is a multi-dimensional plot in the phase space. This is known as an attractor which is defined to be the smallest unit that cannot be decomposed into two or more attractors with distinct

basins of attraction. Given that a time series data set is embedded into m dimensions, it has to be plotted in a plot that contains m axes for us to accurately visualize the attractor. However, it is complicated to construct a plot that is higher than three dimensions. Therefore, more often that not, attractors are visualized in a two or three dimensional plot. The unique characteristic of a chaotic process is that its attractor is known to be 'strange'. A strange attractor is an attractor whose variables never exactly repeat their value but always found to be within a restricted range of state space. This concept is analogous to the earlier tests where it was seen that a chaotic process is one that is neither completely stochastic nor completely deterministic.

3.5.9 Lyapunov Exponents

Lyapunov exponents are a measure of chaos (sensitivity to initial conditions), whose sign signifies chaos and whose value is a measure of the chaos. For an n dimensional chaotic system, there are n Lyapunov exponents that may be positive, negative or zero. The set of all the exponents is called the Lyapunov spectrum and the i^{th} Lyapunov exponent is defined as:

$$\lambda_i = \lim_{t\to\infty} \frac{1}{t} \log \frac{l_i(t)}{r(0)} \tag{3.24}$$

where λ_i = ith Lyapunov exponent, t = time and r = radius. A bounded system with a positive Lyapunov exponent is chaotic and the exponent measures the mean rate at which predictability is lost. Lyapunov exponents must be calculated numerically and the largest exponent is the most informative and important. Therefore it is useful to develop a generic numerical technique that works for any system in any dimension. Table 3.1 presents the characteristics of Lyapunov exponents (symbolized by λ) which are used in this study.

Table 3.1: General character of Lyapunov exponents

λ_1	λ_2	λ_3	attractor
negative	negative	negative	equilibrium point
0	negative	negative	limit cycle
0	0	negative	2-torus
positive	0	negative	strange (chaotic)
positive	positive	negative	noise

There are four kinds of attractors. 1) point, 2) periodic, 3) quasi-periodic and 4) chaotic, which encompass the various kinds of attractors seen in Table 3.1. Equilibrium point is the point attractor where a time series converges and there are no more oscillations. Limit cycle is an attractor in which orbits or trajectories converge, upon which trajectories are periodic. 2-torus which is quasi-periodic is defined to be the surface of a doughnut shaped compact manifold. Lastly, chaos is a strange attractor that has a fractal dimension (implying that a structure assumes a consistent pattern of self-similarity) whose trajectory appears to move around randomly. Thereafter, using the interpretations in Table 3.1, the exact nature of the data (most importantly if chaos is exhibited) can be determined. There are numerous algorithms available to calculate Lyapunov exponents. In our study, the method by Briggs is used to estimate the spectrum of Lyapunov exponents as this method is proven to produce more reliable results (Briggs, 1990). This algorithm has been implemented in FORTRAN / MATLAB.

3.5.10 Kaplan-Yorke Dimension

The Kaplan-Yorke (KY) dimension can be derived from the Lyapunov exponents as follows. If there are n Lyapunov exponents then:

$$KY = i + \frac{\sum_{a=1}^{i} \lambda_a}{|\lambda_{i+1}|} \tag{3.25}$$

where the λ_i are positive and arranged in descending order of magnitude, their sum is greater than zero and $\sum_{a=1}^{i+1} \lambda_a < 0$. For a chaotic signal, the KY dimension value would be similar to the correlation dimension of the signal.

3.5.11 Kolmogrov Entropy

Kolmogrov entropy of an attractor is a measure of the rate of information loss along the attractor, or a measure of the degree of predictability of points along the attractor, given an arbitrary initial point. It is related to the Lyapunov exponents as follows:

$$K = \sum_{i} \lambda_i \tag{3.26}$$

and it is the sum of all positive Lyapunov exponents. For a chaotic signal, K should be positive and finite.

3.5.12 Correlation Dimension

The correlation dimension method is a way to determine if a signal is chaotic (Grassberger and Procaccia, 1984). Chaotic attractors often have a complex and highly fractured structure that result in non-integer dimensions in the phase space called fractal dimensions. Before the correlation dimension is computed, it is necessary to reconstruct the one dimensional data into a multi-dimensional vector which was described in the earlier section. Subsequently, the correlation dimension can be calculated using the absolute distances between each pair of points in the set of N points.

$$s(i,j) = | X_i - X_j | \tag{3.27}$$

A correlation function C(r) is then calculated using,

$$C(r) = \frac{1}{N^2} \times (\text{number of pairs with (i,j) with s(i,j) < r}) \tag{3.28}$$

C(r) follows a power law of $C(r) = kr^D$. Therefore, correlation dimension (CD) can be found with the estimation techniques derived from the formula:

$$CD = \lim_{r \to 0} \frac{\log(C(r))}{\log(r)} \tag{3.29}$$

C(r) written in mathematical form is as follows:

$$C(r) = \frac{\lim}{N \to \infty} \frac{1}{N^2} \sum_{j=1}^{N} \sum_{i=j+1}^{N} \theta(r - |X_i - X_j|) \tag{3.30}$$

where θ is the Heaviside function step function described as,

$$\theta(r - |X_i - X_j|) = \{1, 0 \le (r - |X_i - X_j|)\} or \{0, 0 > (r - |X_i - X_j|)\} \tag{3.31}$$

For determining chaotic dynamics in a system, the correlation exponent has to be plotted as a function of the embedding dimension. A code that implementes these computations has been developed in MATLAB.

3.5.13 Auto-Correlation Function (ACF)

Through the shape of the auto-correlation function, a perfunctory detection of deterministic chaos in the time series may be done. If the ACF falls quickly to zero, then most probably the time series is stochastic and exhibits no determinism, implying that the value at each point is independent of all other values in the series. One such example is random Gaussian white noise. However, the ACF of a signal which has chaotic dynamics decreases very slowly and even more slowly than in an exponential manner. This is due to

the fact that the points are dependant and self-similar. An example of such a system is the Lorenz attractor. More details will be covered in chapter 4. A function that computes the ACF has been implemented in MATLAB.

3.6 Noise Removal Techniques

Time series data from chemical systems often display fluctuations in the measured variables. Much effort has been put into determining if this variability reflects determinism or stochastic "noise". The output from these systems is the result of both the internal dynamics of the system and the inputs to the system from the surroundings. This implies that the system should be viewed as consisting of both stochastic and deterministic components. To analyze the "true" signal, it is important to characterize the determinism in the signal. However, the stochastic components cause the chaos quantifiers to give spurious results (Gong and Lai, 2000). This would lead us to the wrong conclusions about the nature of the signal which would have severe ramifications when we try to implement a suitable control strategy for the signal. Therefore, when the signal is too noisy, it is important to use some techniques to de-noise the signal and recover the true signal. Frequency domain filtering techniques can be applied to remove noise if the frequency characteristics of the signal are known. The latter can be found from the power spectrum analysis. Hence, low-pass, high-pass and band pass finite impulse response (FIR) filters have been implemented in MATLAB to achieve the objective of removing noise. A technique that smoothes noise (by evening out the noise) across the entire frequency range of the signal has also been implemented. Lastly, another de-noising

technique is discussed in this study, which is the concept of wavelets. Fourier smoothing has long been the method of choice to limit noise, but recently methods based on wavelet transformation have been surfacing. The reason is that they are more flexible in analyzing data. The advantage of wavelets lies in the additional spatial resolution of the transformed signal. In contrast to the Fourier transformation, the signal is decomposed into waves of finite length, hence the name wavelets. The wavelet transformation of a one dimensional signal has two independent variables, a frequency and a spatial location variable. It leads to the decomposition of a spectrum into a series of spectra at finer and coarser resolutions. Hence, the wavelet transformation furnishes us with the frequency of a signal at every spatial location (Mallat, 1989). To perform this transformation, the wavelet toolbox (wavmenu) in MATLAB is utilized. The utility of this tool will be shown in chapter 4.

3.7 Summary

In this chapter, we outlined many statistical and graphical methods that are used for the purpose of data analysis. The next chapter will present the application of these methods to various industrial data sets.

CHAPTER 4

ANALYSIS OF ROUTINE OPERATING DATA

This chapter contains sections on closed-loop systems, a simulation example, results of analyzing various key variables from routine operating data and applying noise removal techniques to the riser temperature data.

4.1 Introduction

Data analysis is the process of systematically applying statistical and mathematical techniques to data. In the context of this work, the purpose of doing this is to comprehend the meaning, structure and origin of the data which would help in understanding reasons for poor control loop performance and subsequently controlling the key variables within specified boundaries. Our current investigation is on an industrial FCC unit in which a temperature control loop is exhibiting less than satisfactory performance. We will examine routine and experimental data of various key variables to make appropriate structural and parametric decisions for the control system using the methods described in chapter 3.

4.2 Previous Studies

In this section, we present some of the related work that provides us the motivation to implement a comprehensive data analysis framework (including testing for chaos) of key

variables in the FCC unit. Abasaeed and Elnashaie (1997, 1998) showed that the external periodic forcing of the regenerator air temperature, can lead to chaotic behavior in the gasoline yield. Han and Chung (2001) then reported sensitivity in initial conditions leading to inverse responses and nonlinear behavior of the riser and the regenerator in the FCC unit. Even in other units, such phenomena were observed. Morud and Skogestad (1998) observed the occurrence of oscillations and instability in an ammonia reactor. Mosdorf and Shoji (2003) also observed chaos for bubbling in a submerged orifice.

4.3 Closed-Loop Systems

The presence of chaos in mathematical and physical systems has been extensively demonstrated and is very common (Ott et al., 1990). Amongst all these systems, the Lorenz system proposed by Lorenz (1963) is the one of the simplest system of three equations (for certain specific parameter values) to exhibit chaos. It must be noted however, that these systems are investigated under open-loop conditions. On the contrary, most chemical systems (such as the one which is the focus of this study) function as closed-loop systems due to the commonly employed feedback control. Hence, it is important to consider the effect of the controller, disturbance and noise, on chaos (if any). Hitherto, there doesn't exist much literature on the investigation of chaos of closed-loop systems. Therefore, in this study, we will focus on such systems.

4.4 Results and Discussion

For consistency, three sets of routine operating data (when the plant is in closed-loop) taken on the first day of consecutive weeks are analyzed. Each set is sampled at every 5 seconds and for the purpose of our analysis, 4096 data points are used.

4.4.1 Simulation Example

Let us consider the Lorenz system (Lorenz, 1963):

$$\begin{aligned} \frac{dx}{dt} &= -\sigma(x-y) \\ \frac{dy}{dt} &= rx - y - xz \\ \frac{dz}{dt} &= xy - bz \end{aligned} \tag{4.1}$$

The following are chosen as values for the different parameters: σ = 10, r = 28 and b = 8/3. These values are known to result in chaotic behavior (Lorenz, 1963).

The three system equilibria are:

$$\begin{aligned} [x,y,z]^{(1)} &= [0,0,0]^T \\ [x,y,z]^{(2)} &= [+6\sqrt{2},+6\sqrt{2},27]^T \\ [x,y,z]^{(3)} &= [-6\sqrt{2},-6\sqrt{2},27]^T \end{aligned}$$

which are all unstable. This implies that when the outputs (x, y and z) evolve over time, they are unable to achieve steady state but rather tend to undergo permanent transience from one equilibrium to another. This is the open-loop analysis of the Lorenz system and results from various chaotic quantifiers confirm the presence of chaos (Sprott, 1993). In our study, we aspire to investigate the closed-loop configuration of the Lorenz system.

Therefore, we consider the same system but add a feedback PID controller (with arbitrary tuning parameters) and random noise of mean 0 and variance 0.1. For this closed-loop system, the state variable 'x' is chosen as the controlled variable. 'σ' which is the Prandtl number (a dimensionless parameter that can be varied depending on the choice of kinematic viscosity and thermal diffusivity) is the manipulated variable. We compare the Lyapunov exponents obtained from both open-loop and closed-loop configurations to determine if the closed-loop Lorenz system also exhibits chaos. In this thesis, the Lorenz system (open-loop and closed-loop) is simulated in Simulink using the differential equation editor (DEE) block, with a sampling rate of 1 unit of time and 4096 data points. Results are presented in Table 4.1.

Table 4.1: Lyapunov exponents (LE) of the open-loop and closed-loop Lorenz system

LE of an open-loop Lorenz system			LE of a closed-loop Lorenz system without noise			LE of a closed-loop Lorenz system with noise		
LE_1	LE_2	LE_3	LE_1	LE_2	LE_3	LE_1	LE_2	LE_3
0.906	0	-1.572	0.924	0	-1.553	1.126	0.030	-1.478

Results from Table 4.1 show that the LE_1 of the open-loop Lorenz system is positive, LE_2 is zero, LE_3 is negative and that the sum of all LEs is negative. This signifies that chaos is present and this is consistent with the results reported in the literature. This pattern is also evident in the LEs of the closed-loop Lorenz system without noise. This implies that the control action is unable to mitigate the chaotic fluctuations exhibited by the process variable. We observe that the LE_1 of the closed-loop system with noise is 0.22 more than that of the open-loop system. This increase could be due to chaos and / or noise but a clear distinction cannot be made as LEs are often not able to distinguish between chaos and

noise (Gong and Lai, 2000). However, based on the LE_2 of the closed-loop system, we note that the value has increased from 0 to 0.03. For a purely chaotic system, LE_2 is expected to be zero (as demonstrated by the open-loop and closed-loop without noise Lorenz systems). Therefore, this increase is due to the noise in the system which is also likely to have caused the increase in LE_1. LE_3 is negative which is typical of a chaotic system. Therefore, results clearly show that the closed-loop Lorenz system with noise also exhibits chaos and the marginal difference in results compared to the open-loop and closed-loop without noise systems is mainly due to noise.

The observed chaos in the closed-loop Lorenz system is dependent on the controller tuning parameters selected. It can be seen that for this particular set of tuning parameters, chaos is observed. This suggests that even with a linear feedback controller, the phenomenon of chaos may be still inherent as the controller is unable to eliminate the chaotic components in the system. This also provides us the justification to examine routine operating data under closed-loop conditions as we have shown that it is indeed possible for a closed-loop system to exhibit chaos. It must be noted that the purpose of a controller in an unstable and chaotic system, is to stabilize the system equilibria and ensure that the output doesn't fluctuate between the equilibrium coordinates. Tian et al. (2002) have shown that it is possible to mitigate chaotic fluctuations in the controlled Lorenz system via a special form of chaos control called the bang-bang control. However, there have been no studies which have reported the mitigation of chaotic fluctuations via feedback control using conventional PID controllers. In this chapter, we do not aspire to show that such feedback control can quench chaos but rather we purport to show that even

under this type of feedback control, chaotic behavior can occur. In the next sub-section, we will critically examine several key variables of the FCC unit.

4.4.2 Riser Temperature

In this section, we utilize our framework (refer to Appendix B) and present results of analyzing the riser temperature data and various key variables of the FCC unit. This framework is not applied to the simulation example of the Lorenz system, as it is a mathematical system that is already known to exhibit chaos. Figure 4.1 shows the dynamics of the riser temperature (plotted as deviation from the set-point for proprietary reasons).

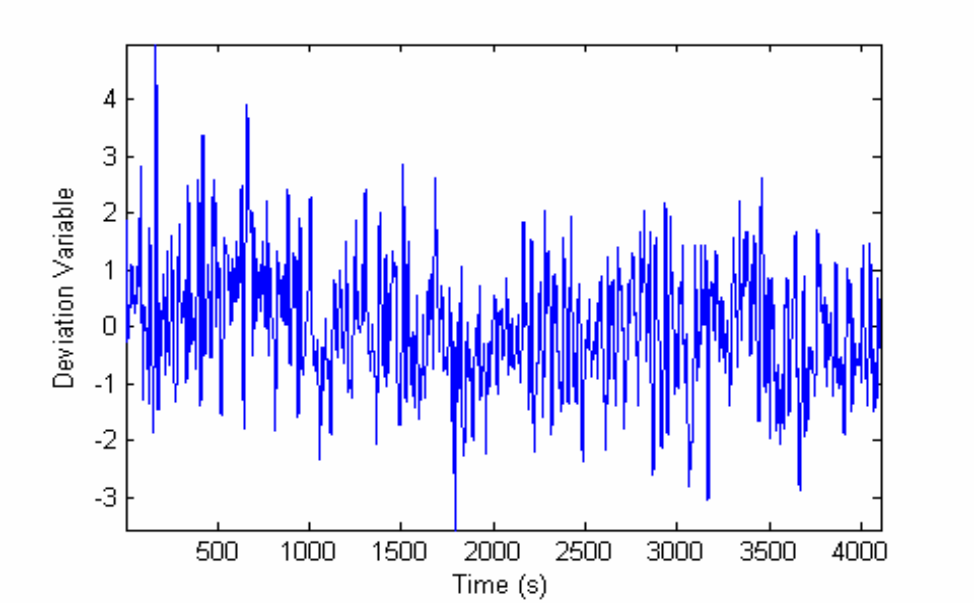

Figure 4.1: Graph of riser temperature against time (set 1)

From Figure 4.1, we can observe the higher than desired fluctuations in the riser temperature, which may be a result of poor control, poor process design or other causes.

Table 4.2 presents the results from the tests of stationarity and Gaussianity on the riser temperature data.

Table 4.2: Results from tests of stationarity and Gaussianity for riser temperature

Index	Indicator	Metric for Set 1	Metric for Set 2	Metric for Set 3
1	Runs Test	11 (97)*	2 (92)*	2 (91)*
2	Reverse Arrangements Test	1724 (2243)*	3553 (2764)*	3345 (2651)*
3	Kurtosis	1.4215	1.0319	1.3369

*The metric in brackets is for the differenced data

Results from Table 4.2 show that for all three sets, the data are not stationary. This is confirmed by both the runs and reverse arrangement tests. Hence, the data are differenced (as described by the method in chapter 3) to ensure stationarity. This is indicated by the metric values for the differenced data which are in brackets. Hereafter, the new differenced data sets are used in our analysis. The Kurtosis of all three sets is more than 1 and this indicates a non-Gaussian distribution. From this, we can infer that first and second order statistics are not sufficient to characterize the dynamics of the riser temperature. Hence, HOS have to be implemented. Furthermore, since the data are non-Gaussian, the assumption of linearity is not justified and testing for nonlinearities should be carried out. This is because only a positive test for Gaussianity implies linearity (Rao and Gabr, 1980, 1984; Hinich, 1982). Table 4.3 presents the results obtained from the two tests (BI and SDM) for nonlinearities.

Table 4.3: Results from tests of nonlinearities for riser temperature

Index	Indicator	Metric for Set 1	Metric for Set 2	Metric for Set 3
1	BI (f_1,f_2)	0.373 (-0.031, -0.445)	0.473 (-0.468, -0.476)	0.465 (-0.328, -0.335)
2	$T_{rev,ori}$	0.0030	0.0034	0.0031
3	μ_{surr}	-4.843E-5	-4.725E-5	-4.678E-5
4	Observed Statistic	3.711	3.342	3.366

It can be seen that the BI of all three sets is between 0.37 and 0.47. This implies that the data are nonlinear with the magnitude of the BI's indicating the degree of interaction of the nonlinearities at the two independent frequencies shown in brackets. For a visual depiction of this, refer to Figure 4.2.

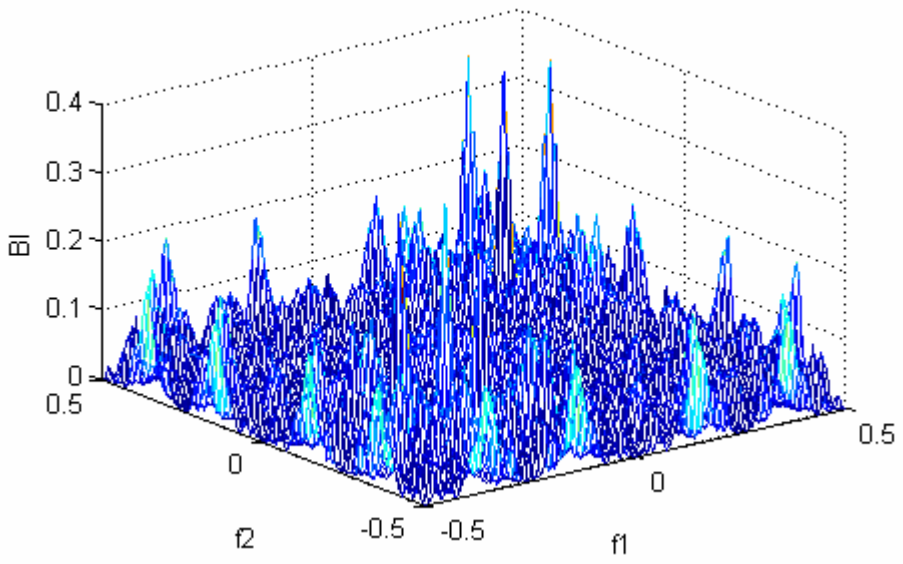

Figure 4.2: BI of riser temperature (set 1)

Figure 4.2 shows the interaction at the various bi-frequencies and the highest peak (which is caused by a nonlinearity) is observed at (-0.031, -0.445) and its magnitude is 0.373.

From Table 4.3, we also observe that the observed statistic of all three sets is more than 2. This insinuates that the null hypothesis is rejected and provides evidence that the data are nonlinear. Figure 4.3 shows the SDM in graphical form.

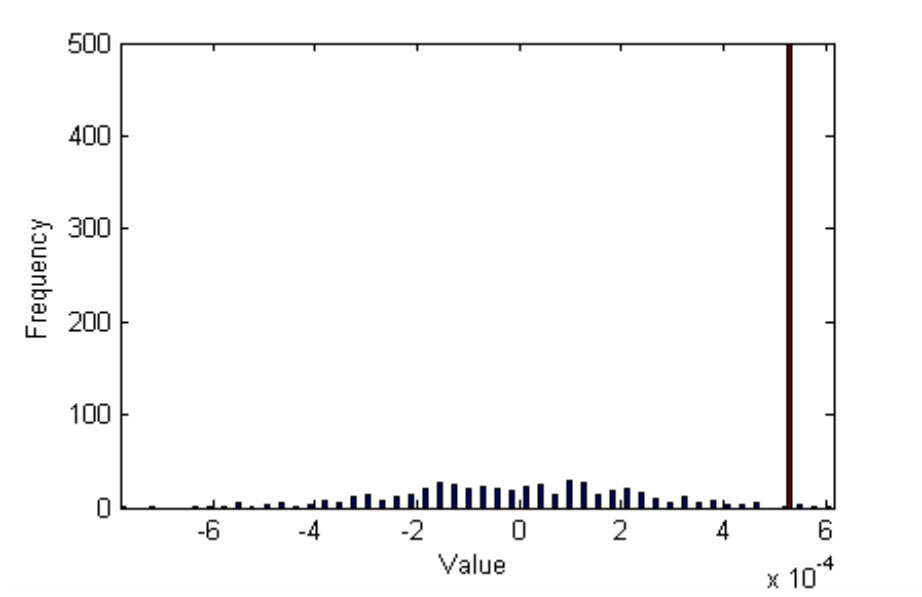

Figure 4.3: Surrogate data plot of riser temperature (set 1)

Figure 4.3 shows the time reversal value of the original (differenced) data (indicated by the tallest bar) and the time reversal values of all the surrogate data which are indicated by the numerous shorter bars. We can clearly see that the time reversal value of the original data ($T_{rev,ori}$) lies well outside the range of that of the mean of the surrogates (μ_{surr}). This implies that the data are nonlinear and this is confirmed by the hypothesis testing and calculation of the observed statistic. Since both tests (BI and SDM) confirm the presence of nonlinearities, this paves the way for testing for chaos, as nonlinearities are the precursors of chaos. Table 4.4 presents the results from the various chaos quantifiers.

Table 4.4: Results from tests of chaos for riser temperature

Index	Indicator	Metric for Set 1	Metric for Set 2	Metric for Set 3
1	LE_1	0.5421	0.5031	0.3861
2	LE_2	0.0392	0.0281	0.0166
3	LE_3	-0.8907	-0.8654	-0.8196
4	STE	84%	85%	85%
5	K	0.5813	0.5312	0.4027
6	CD	3.60	3.65	3.50
7	KY	2.64	2.55	2.45
8	OED	8	8	8
9	AMI	3	3	3

It can be seen that the first and second LE for all the three sets are positive. A positive LE_1 is an indicator of chaos and / or correlated noise and a positive LE_2 indicates that random noise is present as well. Since the riser temperature data are embedded in three dimensions, LE_2 is expected to be zero if the data are purely chaotic. LE_3 is negative for all three sets and this is expected as the third exponent is always negative for any data set. The theoretical value of LE_1 for a purely random signal is infinity (http://sprott.physics.wisc.edu/ phys505/lect09.htm, accessed on 08/07/05) but in practice this is not achieved. Instead, a typically high value (higher than that of chaos, but of no specific value) is registered. For the riser temperature data, the LE_1 is not high enough to be classified as pure noise. Hence, this is a good indication that there are chaotic fluctuations present in the riser temperature.

The spatio-temporal entropy (STE) of the three sets, indicates that the data are mostly random but with some hidden structure. This reinforces our belief that chaos may be present as this is the typical nature of a chaotic attractor. The Kolmogrov entropy (K) that is calculated for all three sets is positive and finite and this also suggests that chaos is

present. The correlation dimension (CD) of the riser temperature (set 1) is shown in Figure 4.4.

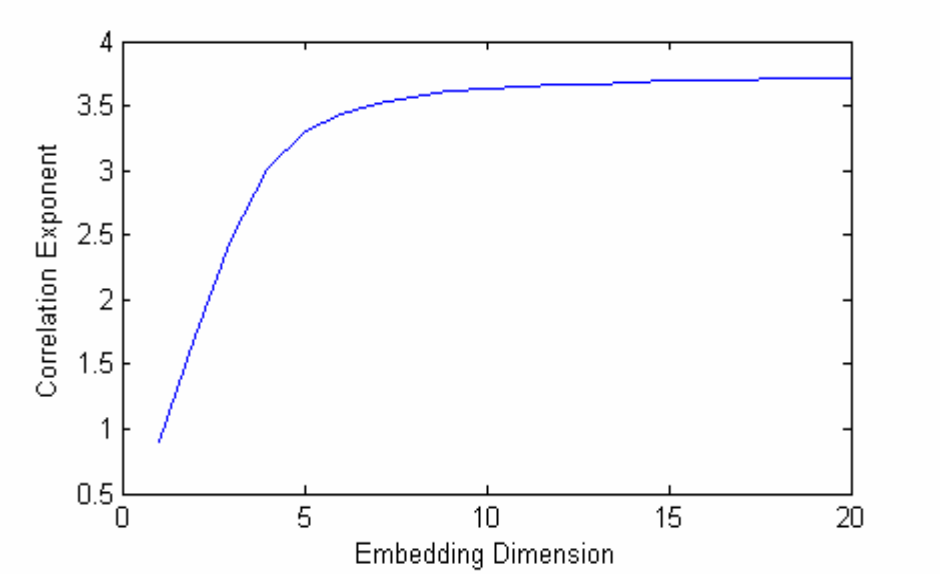

Figure 4.4: Correlation dimension of riser temperature (set 1)

From Figure 4.4, we observe that the rate of increase of the correlation exponent decreases as the embedding dimension increases. This type of saturation is typical of what is observed in a chaotic process as described in chapter 3. This inference and the trend in Figure 4.4 are also similar to those for the experimental data reported in literature (Mosdorf and Shoji, 2003). Furthermore, we observe that CD, which is the correlation exponent at the saturation point, is approximately 3.60. This implies that the data has a fractal dimension which is also a criterion for a chaotic process. We also note that the CD for data sets 2 and 3 are also fractal. In evaluating the CD, we stop at an embedding dimension of 20 so as to save on computational time (following the approach employed by Mosdorf and Shoji (2003)).

From Table 4.4, we can also see that the Kaplan-Yorke (KY) dimension is similar in value to the CD. For a chaotic process, the KY should be the same as or similar to the CD. Hence, this also shows evidence of chaotic behavior. The values of average mutual information (AMI) and optimal embedding dimension (OED) in Table 4.4 are used in determining the graphical chaos quantifiers. We now present some quantifiers that detect chaos via graphical means. Refer to Figures 4.5 to 4.7.

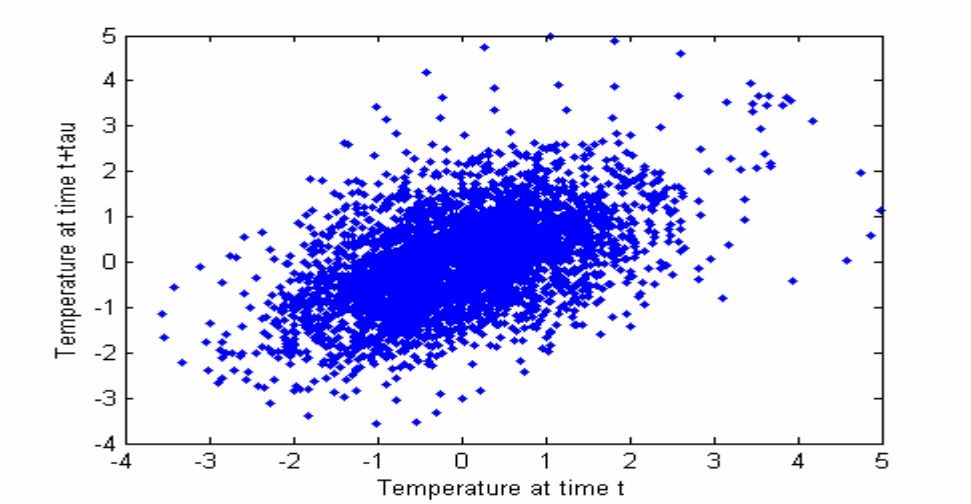

Figure 4.5: Return map of riser temperature (set 1)

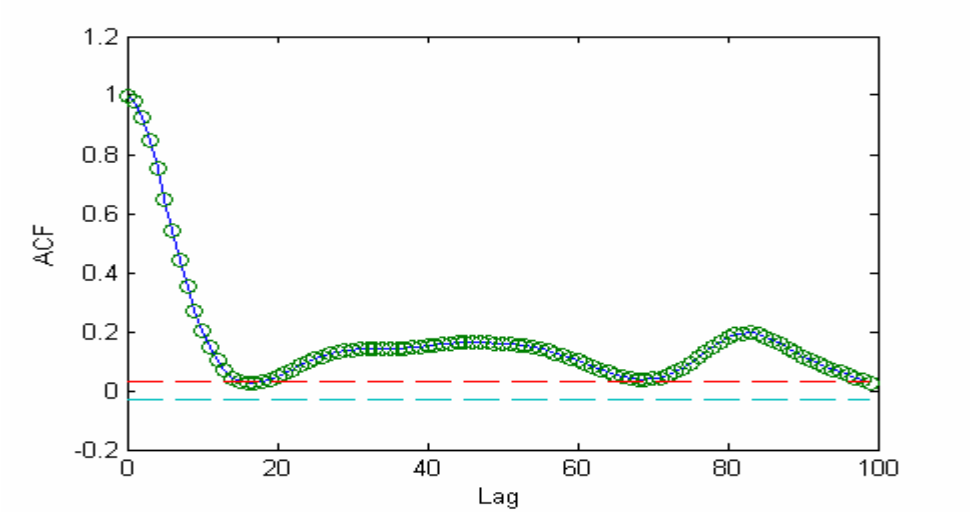

Figure 4.6: ACF of riser temperature (set 1)

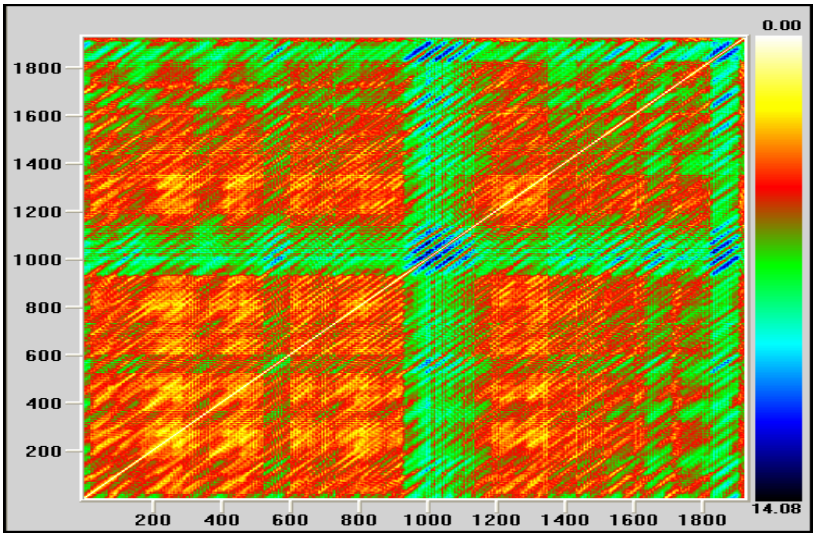

Figure 4.7: Recurrence plot of riser temperature data (set 1) using Lyapunov color scheme

Figures 4.5 to 4.7 depict the return map, ACF and recurrence plot of the riser temperature data taken in the first week (set 1). Figure 4.5 shows that the data are not entirely random and some structure is present. Whilst this is not a confirmation of chaos, it is nevertheless indicative that chaos could be present. The ACF plot (Figure 4.6) of the data shows that the ACF decreases slowly as lag increases. However, the trend in this plot does not decrease in an exponential manner as observed in the trend for the Lorenz data (http://cecwi.fsv.cvut.cz/jiz/stehlik/det_chao.htm, accessed on 08/07/05). While the ACF test may work well for chaotic mathematical systems, they often fail for chaotic experimental systems. This is attributed to the fact that for experimental systems, the reconstruction of chaotic attractors is not as good as compared to the attractors of mathematical systems

(http://www.cmp.caltech.edu/~mcc/Chaos_Course/Lesson12/Experiment.pdf, accessed on 08/07/05). In Figure 4.7, we observe that the data are mostly random (as indicated by the distribution of the red color) but at the same time there is some structure inherent (as

indicated by the green color). It must be noted that AMI, OED and the choice of color scheme (in this example, the Lyapunov color scheme is used) are vital in obtaining the complete structure (or the lack of) of the data. This suggests that the data have chaotic origins.

In summary, the above analysis shows that the riser temperature has a non-Gaussian distribution which implies that HOS techniques should be utilized to extract more useful geometric information. Based on the two formal tests of nonlinearities, we can conclude that the data are nonlinear in the operating region. This is important because some studies assume that chemical processes may be linear in a narrow operating region (Eskinat et al., 1991) but in this case, it is not true. After confirming the presence of nonlinearities, several statistical tools for characterizing chaos are implemented and results from most chaos quantifiers indicate the presence of chaos. Based on this, we can conclude that two of the causes of the large fluctuations in the riser temperature are the presence of nonlinearities and chaos. To understand more about the causes of these fluctuations, dynamics of other key variables of the FCC unit are characterized in the following sub-sections. Data for all these variables are presented in the rest of this thesis as deviation variables for proprietary reasons.

4.4.3 Feed Flowrate

The feed flowrate is known to be one of the dominant variables affecting the riser temperature. The fluctuations inherent in the feed flowrate may propagate and cause the nonlinear and chaotic fluctuations seen in the riser temperature. Figure 4.8 shows the time

series of the feed flowrate. From this, one can observe that there are some fluctuations in the feed flowrate.

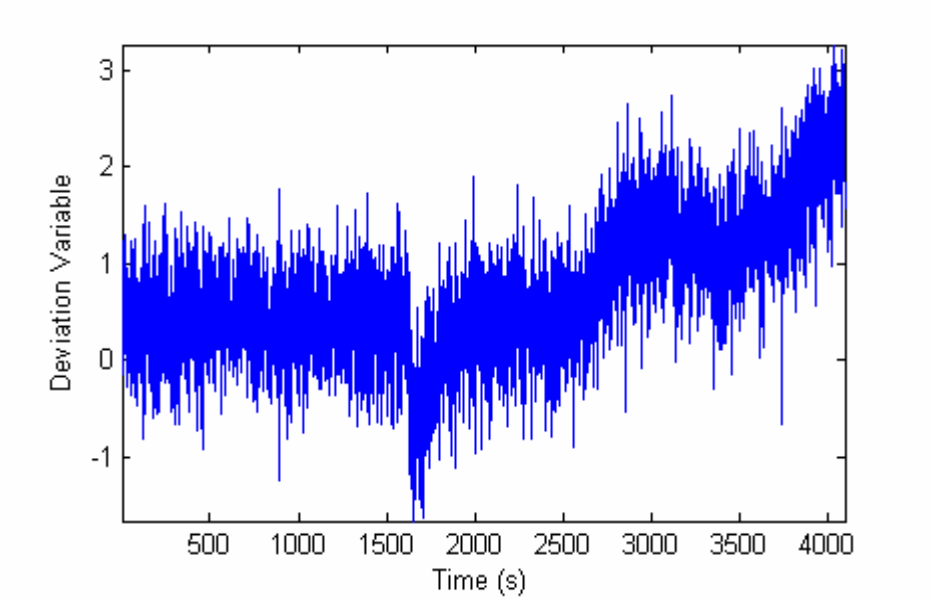

Figure 4.8: Graph of feed flowrate against time (set 1)

Table 4.5 presents the results of testing for stationarity, nonlinearity and Gaussianity for the fluctuations in the feed flowrate. These results show that the feed flowrate data are not stationary. Hence, differencing is carried out and stationarity is ensured as seen by the metric values in brackets. The data are then tested for Gaussianity and although the Kurtosis of all three sets is lower than that of the riser temperature data, Gaussianity cannot be assumed. Hence, this shows that HOS have to be used and the data are then tested for nonlinearities. The low non-zero BI values indicate that the data are non-Gaussian but linear. The linearity of the data is further confirmed by the SDM as the observed statistic for all three sets is in the range of -2 to 2. Therefore, the null hypothesis that the data are linear is not rejected. Subsequently, since no nonlinearity is observed in

the feed flowrate data, testing for chaos is not necessary as nonlinearity is a prerequisite for chaos. From the above analysis, we can see that the feed flowrate acts as a linear disturbance to the riser temperature and hence this might be one of the causes of the large fluctuations in the riser temperature.

Table 4.5: Results from tests of stationarity, Gaussianity and nonlinearity for feed flowrate

Index	Indicator	Metric for Set 1	Metric for Set 2	Metric for Set 3
1	Runs Test	3 (98)*	8 (106)*	11 (89)*
2	Reverse Arrangements Test	1418 (2247)*	3167 (2678)*	2862 (2546)*
3	Kurtosis	0.1932	0.2246	0.2563
4	BI (f_1,f_2)	0.1146 (0,0)	0.0799 (-0.398, -0.398)	0.0853 (0.390, -0.406)
5	TR_{ori}	-2.077E-4	-2.756E-4	3.816E-4
6	μ_{surr}	2.5432E-5	2.340E-5	-7.448E-6
7	Observed Statistic	0.4607	0.5356	0.6723

* The metric in brackets is for the differenced data.

4.4.4 Feed Temperature

The temperature of the feed entering the riser is the other dominant variable that may have an effect on the riser temperature. Similar to that of the feed flowrate, the fluctuations present in the feed temperature may contribute to the fluctuations in the riser temperature and result in the higher than desired fluctuations. Fluctuations in the feed temperature are evident from the feed temperature data (set 1) in Figure 4.9. Table 4.6 presents the results from the characterization of these fluctuations.

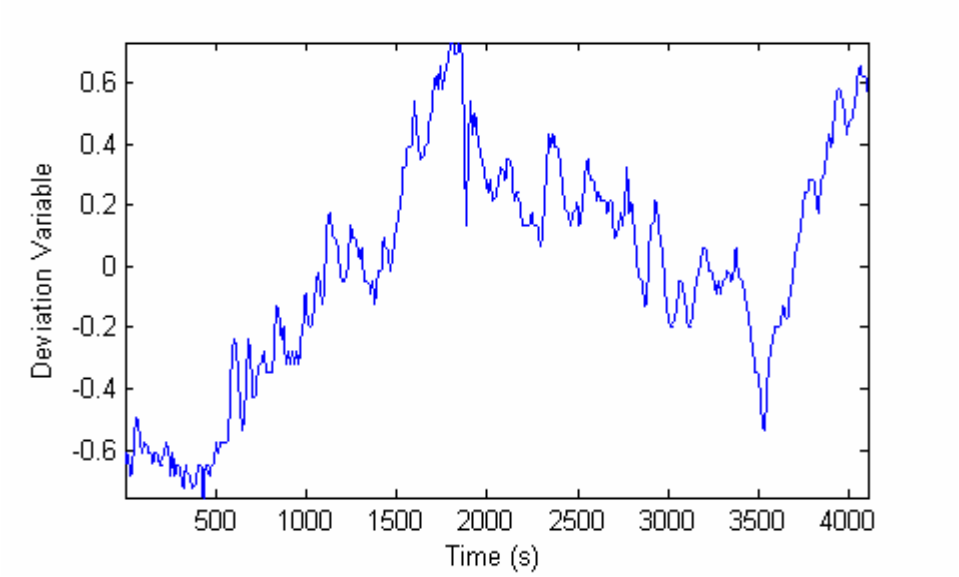

Figure 4.9: Graph of feed temperature against time (set 1)

Table 4.6: Results from tests of stationarity, Gaussianity and nonlinearity for feed temperature

Index	Indicator	Metric for Set 1	Metric for Set 2	Metric for Set 3
1	Runs Test	2 (90)*	19 (113)*	5 (94)*
2	Reverse Arrangements Test	1202 (2278)*	2081 (2369)*	4498 (2698)*
3	Kurtosis	-0.6908	-0.7392	-0.7230
4	BI (f_1,f_2)	0.0900 (0,0)	0.0799 (-0.398, -0.398)	0.0853 (0.390, -0.406)
5	TR_{ori}	2.9696E-4	2.6572E-4	2.7361E-4
6	μ_{surr}	2.4890E-5	2.4311E-5	2.2295E-5
7	Observed Statistic	0.2826	0.3356	0.2723

* The metric in brackets is for the differenced data.

Results from Table 4.6, show that the feed temperature data are neither stationary nor Gaussian. Hence, the data are differenced and tested for nonlinearities with both the BI and the observed statistic from the SDM showing that the data are linear. This suggests that the feed temperature is acting as a linear disturbance to the riser temperature. These results are very similar to that seen in the case of the feed flowrate data.

4.4.5 Pressure of 2nd Stage Regenerator

Pressure of the 2nd stage regenerator is not considered to be one of the dominant variables in the FCC unit. However, it is known to adversely affect the riser temperature if poorly controlled. Figure 4.10 shows the dynamics of the 2nd stage regenerator pressure. We can observe that there are some fluctuations in the regenerator pressure. Table 4.7 presents the results from the characterization of these fluctuations.

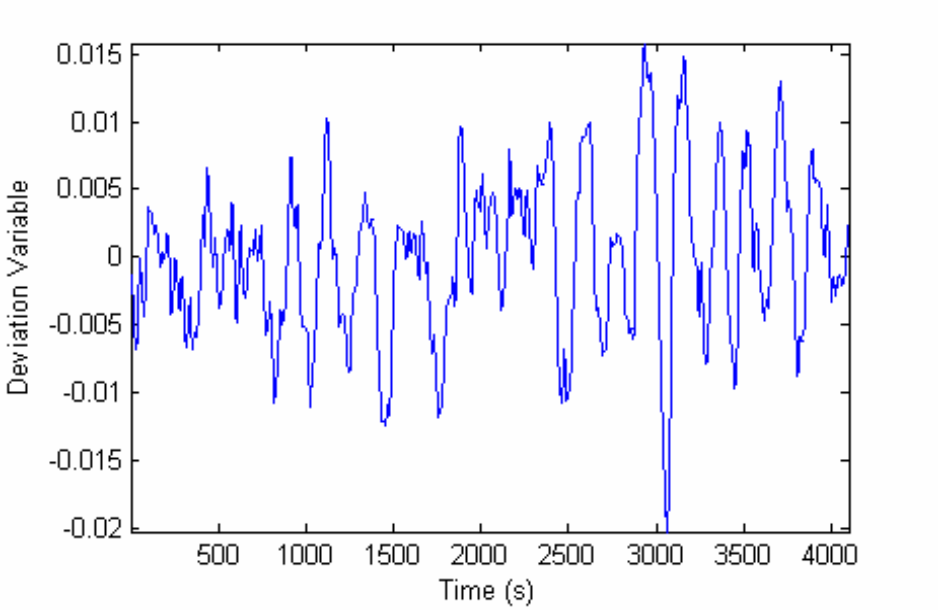

Figure 4.10: Graph of the 2nd stage regenerator pressure against time (set 1)

Table 4.7: Results from tests of stationarity, Gaussianity and nonlinearity for regenerator pressure

Index	Indicator	Metric for Set 1	Metric for Set 2	Metric for Set 3
1	Runs Test	86	97	90
2	Reverse Arrangements Test	2280	2519	2616
3	Kurtosis	0.1896	0.2296	-0.7230
4	BI (f_1,f_2)	0.1232 (0.007, -0.085)	0.1691 (0.0546, -0.1093)	0.1745 (0.340, -0.435)
5	TR_{ori}	0.0042	0.0040	0.0037
6	μ_{surr}	-7.3754E-5	-7.3947E-5	-7.4192E-5
7	Observed Statistic	2.2259	2.2736	2.3481

Results in Table 4.7, show that the 2nd stage regenerator pressure data are stationary. Hence differencing need not be carried out and the original data can be used for further testing. The Kurtosis values indicate that the data are not Gaussian and so the data are tested for nonlinearities using HOS techniques. The BI values are between 0.12 and 0.18 which are typical of a mildly nonlinear signal (Choudhury et al., 2004). Subsequently, the observed statistic from the SDM was tabulated to be in the range of 2.20 to 2.35. This implies that although the null hypothesis is rejected, it is nevertheless close to 2 and hence the data can only be classified as mildly nonlinear. Therefore, both BI and SDM show that the data are mildly nonlinear in their operating range. Since the data are shown to be nonlinear, this requires us to test the data for chaos as that could be a contributing factor to the fluctuations in the riser temperature. Table 4.8 presents these results.

Table 4.8: Results from tests of chaos for the regenerator pressure

Index	Indicator	Metric for Set 1	Metric for Set 2	Metric for Set 3
1	LE_1	1.7580	1.8235	1.8964
2	LE_2	0.1129	0.1276	0.1340
3	LE_3	-0.3355	-0.3497	-0.3622
4	Σ LE	1.5354	1.6014	1.6682

Table 4.8 presents the calculated LEs for the three different sets of data. Results show that for all the three sets, LE_1 and LE_2 are positive and LE_3 is negative. This pattern is similar to what we observed for the riser temperature data. However, in this case, we note that the LE_1 for each set is quite high (above 1) compared to what is normally observed for a chaotic process and this implies that noise is present. This is confirmed by the positive value of the LE_2 for each set. At this juncture, it seems that both chaos and noise are present with the large value of LE_1 suggesting that more noise than chaos is present. However, the sum of LE's is positive which rules out chaos. Therefore, we can conclude that the data is not chaotic and that the fluctuations are due to noise and nonlinearities. Although Lyapunov exponents are known to give a false indication of chaos at times, they are accurate in detecting the absence of chaos. This negates the usage of other quantifiers of chaos to verify that no chaotic fluctuations are present. Overall, results show that the 2nd stage regenerator pressure acts as a nonlinear disturbance toward the riser temperature.

4.4.6 Pressure Differential between the 1st and 2nd Stage Regenerator

The pressure differential between the 1st and 2nd stage regenerator is not considered to be one of the dominant variables in the FCC unit. However, it is also known to adversely affect the riser temperature if poorly controlled. From the pressure differential data in

Figure 4.11, we can observe that there are some fluctuations in the pressure differential. Table 4.9 presents the results from the characterization of these fluctuations.

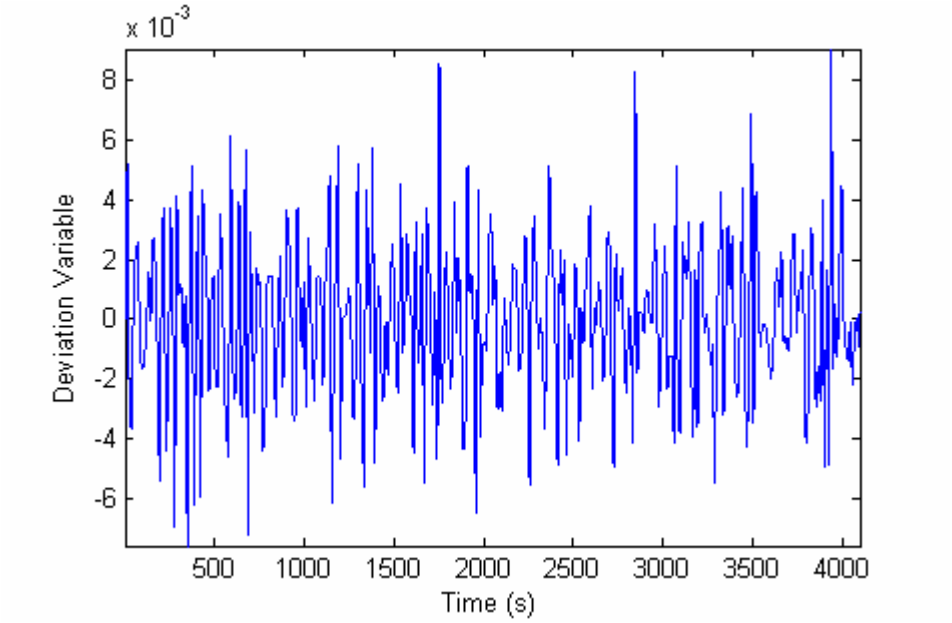

Figure 4.11: Graph of the regenerator pressure differential against time (set 1)

Table 4.9: Results from tests of stationarity, Gaussianity and nonlinearity for regenerator pressure differential

Index	Indicator	Metric for Set 1	Metric for Set 2	Metric for Set 3
1	Runs Test	114	109	113
2	Reverse Arrangements Test	2421	2561	2590
3	Kurtosis	0.1910	0.1996	0.2523
4	BI (f_1,f_2)	0.0960 (0.054, -0.109)	0.1092 (0.044, -0.091)	0.0844 (0.430, -0.438)
5	TR_{ori}	0.0015	0.0012	0.0018
6	μ_{surr}	4.288E-5	4.0276E-5	3.975E-5
7	Observed Statistic	1.2622	1.2043	1.1487

Results in Table 4.9 show that the pressure differential data are stationary and non-Gaussian. Hence, differencing need not be carried out and the original data can be used to

test for nonlinearities. Both BI and the observed statistic from the SDM show that the data are linear and therefore, testing for chaos need not be undertaken. Similar to the feed flowrate and feed temperature data, the pressure differential is also a linear disturbance that could be affecting the riser temperature variable.

4.4.7 Saturated Steam Flowrate

Similar to the 2nd stage regenerator pressure and 1st and 2nd stage regenerator pressure differential data, the saturated steam flowrate is also not a dominant variable. However, it is still tested for any effect on the riser temperature. From Figure 4.12, we can observe that there are some fluctuations in the saturated steam flowrate. Table 4.10 presents the results from the characterization of these fluctuations.

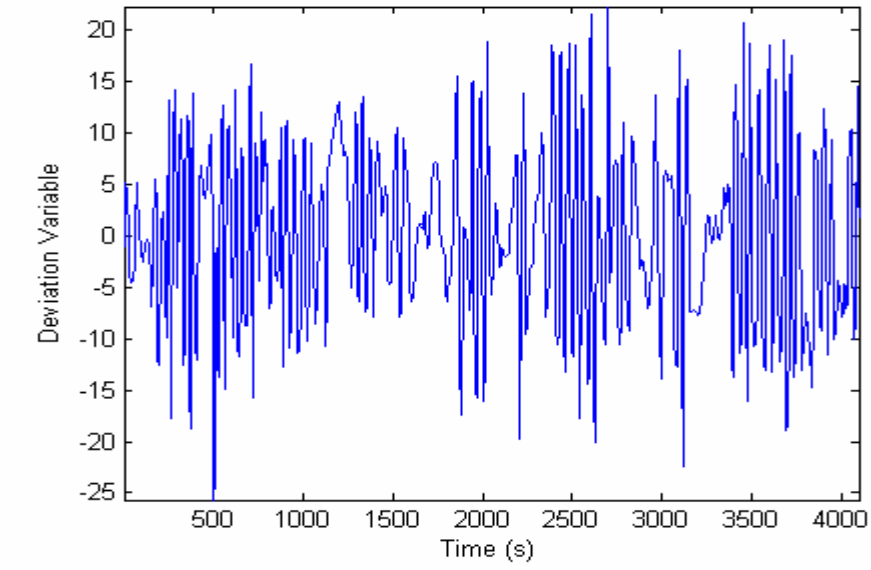

Figure 4.12: Graph of saturated steam flowrate against time (set 1)

Table 4.10: Results from tests of stationarity, Gaussianity and nonlinearity for saturated steam flowrate

Index	Indicator	Metric for Set 1	Metric for Set 2	Metric for Set 3
1	Runs Test	102	92	104
2	Reverse Arrangements Test	2564	2627	2609
3	Kurtosis	-0.5317	0.1996	0.2523
4	BI (f_1,f_2)	0.3066 (0.054, -0.109)	0.2894 (0.054, -0.022)	0.3249 (0.341, -0.497)
5	TR_{ori}	0.0075	0.0072	0.0079
6	μ_{surr}	-4.643E-5	-4.359E-5	-3.946E-5
7	Observed Statistic	3.0654	3.1262	3.1478

Results in Table 4.10 show that the data are stationary and non-Gaussian. Hence, HOS techniques are applied to the original data sets and both SDM and BI confirm the presence of nonlinearities. Compared to the values obtained for the 2nd stage regenerator pressure data, the BI and observed statistic for the saturated steam flowrate are higher. This implies that this data are comparatively more nonlinear. Subsequently, the saturated steam flowrate data are tested for chaos and results are presented in Table 4.11.

Table 4.11: Results from tests of chaos for saturated steam flowrate

Index	Indicator	Metric for Set 1	Metric for Set 2	Metric for Set 3
1	LE_1	1.5765	1.6253	1.5993
2	LE_2	0.1125	0.1216	0.1104
3	LE_3	-0.4206	-0.4394	-0.3923
4	Σ LE	1.2684	1.3075	1.3174

Results in Table 4.11, show that for all sets, LE_1 and LE_2 are positive, LE_3 is negative and the summation of LEs are positive. This is similar to the situation and discussion about the 2nd stage regenerator pressure data (refer to section 4.4.5). Although chaos can be misconstrued from the results, the Σ LE metrics indicate that it is actually absent and the

data are merely contaminated with noise. Overall, results show that the saturated steam flowrate acts as a nonlinear disturbance toward the riser temperature.

4.4.8 Overall Analysis

In this sub-section, we consider the implication of our analysis of the key variables of the FCC unit. The riser temperature is seen to be nonlinear and have chaotic fluctuations. This can be fathomed as one of the reasons for its poor regulation by the feedback control loop. Aside from the innate nature of the riser temperature dynamics, other disturbance variables are observed to contribute to the fluctuations in the riser temperature. Three variables: feed flowrate, feed temperature and pressure differential between the 1^{st} and 2^{nd} stage regenerator, are identified as linear disturbances. The other two variables: 2^{nd} stage regenerator pressure and saturated steam flowrate are identified as nonlinear disturbances; but they are found to be non-chaotic. The combination of these linear and nonlinear disturbances coupled with the riser temperature dynamics, may have led to the chaotic fluctuations in the riser temperature. Hence the riser temperature (which is the controlled variable) is poorly regulated. This revelation is important in investigating the root cause of the poor control loop performance observed in the riser temperature loop. The control aspect of the FCC unit will be dealt with in chapter 5.

4.5 Noise Removal Techniques applied to Riser Temperature Data

In this section, we apply some of the noise removal techniques described in chapter 3 to the riser temperature data. Let us consider the riser temperature data in Figure 4.1. Figure 4.13 illustrates the power spectrum of the riser temperature data. All the power of the riser temperature signal lies between 0 and 60Hz (normalized frequency of 0.06). This implies that a low-pass filter of cut-off frequency of 60 Hz would be an ideal choice for noise-removal. Figure 4.14 shows the signal characteristics of the riser temperature after the low-pass filtering.

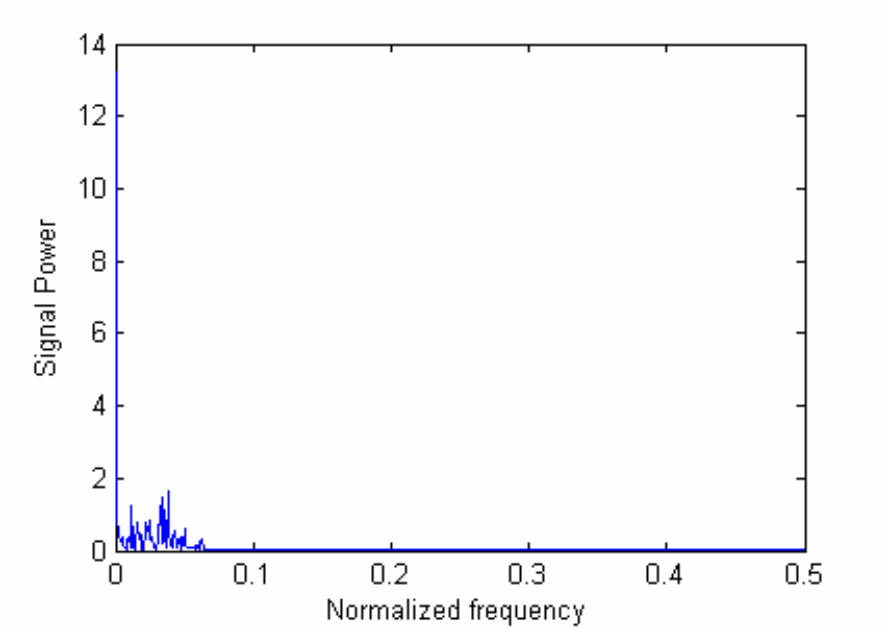

Figure 4.13: Power spectrum of riser temperature

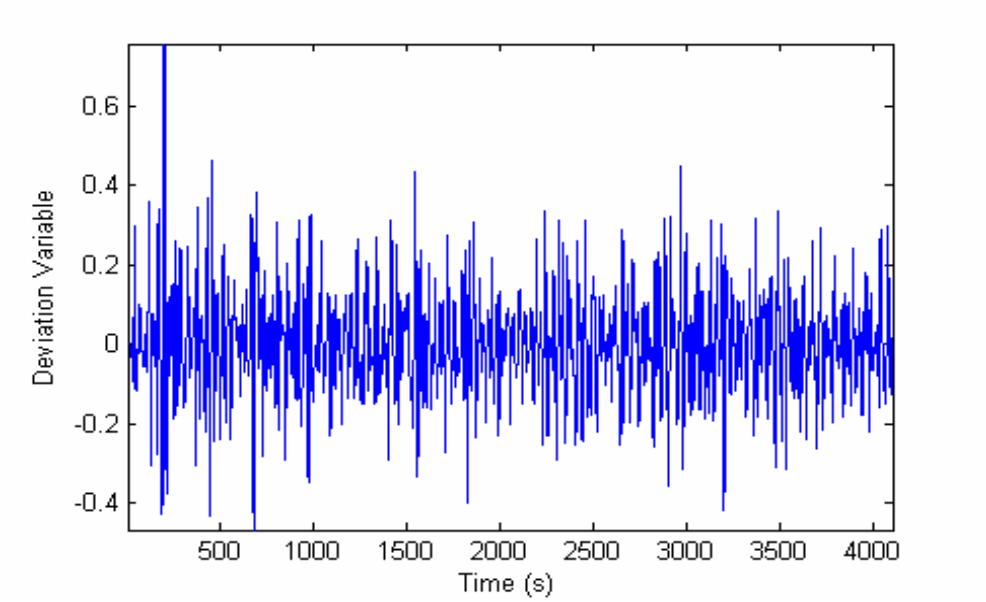

Figure 4.14: Graph of riser temperature after low-pass filtering

The next noise removal technique to be applied to the raw data is the smoothing technique, described in chapter 3. Figure 4.15 shows the signal characteristics of the riser temperature after smoothing by this technique.

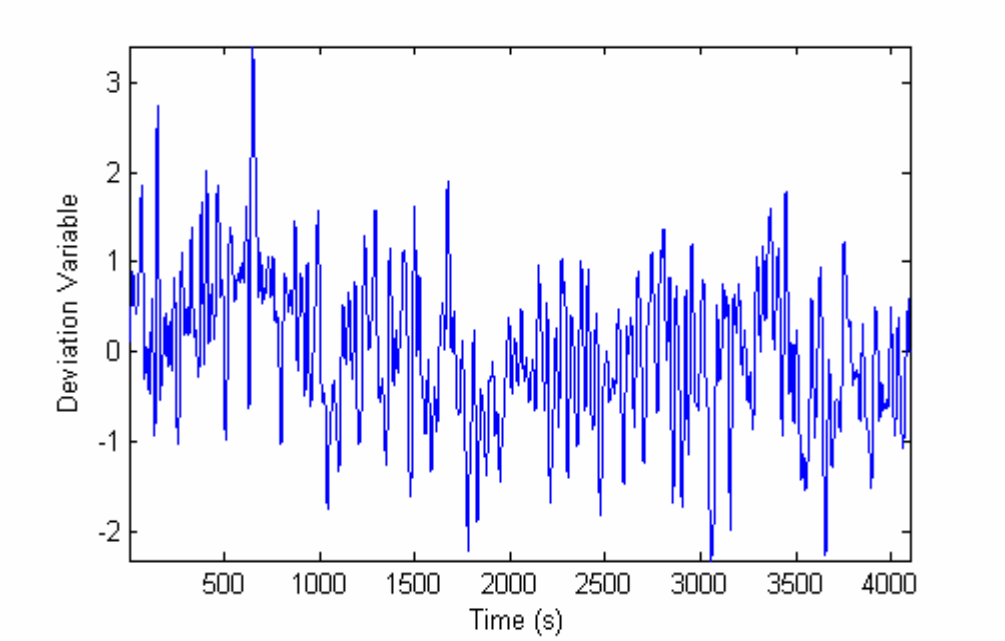

Figure 4.15: Graph of riser temperature after smoothing

After the low-pass filtering and smoothing techniques are applied to the riser temperature data, we attempt to characterize the chaotic fluctuations of the de-noised data by recalculating the Lyapunov exponents. Results in Table 4.12 show that the LE_1 for both data are positive and less than that of the original riser temperature data. This implies that some of the noise from the original data has been suppressed and this is reflected in the lower LE_1. Also, the positive values of the LE_1 indicate the presence of chaos which is expected since the original data are deemed to be chaotic. We observe that the LE_2 for both the de-noised data to be approximately zero. This suggests that virtually all the noise is suppressed as for a noisy system LE_2 is expected to be positive, as seen in the case of the original riser temperature data (Table 4.1). LE_3 is negative for both the de-noised data and this is expected as well. Overall, taking into consideration that the LE_1 is positive, LE_2 is virtually zero and that the sum of LEs is negative, we can conclude that the de-noised data also exhibits chaotic dynamics. Results also show that most of the noise is eliminated through filtering / smoothing and what is captured is mostly pure chaos. Therefore, for the case of the riser temperature data, the low-pass filtering and smoothing techniques seem to work well in suppressing the noise and recovering the true chaotic signal.

Table 4.12: Lyapunov exponents of the de-noised riser temperature data

Lyapunov exponents (LE) for the low-pass filtered data			Lyapunov exponents (LE) for the smoothed data		
LE_1	LE_2	LE_3	LE_1	LE_2	LE_3
0.3382	0.0065	-0.6138	0.1286	-0.0051	-0.1460

It must be noted that the LE values for both sets of filtered data are different but the conclusions drawn from them are the same. This shows that the recovered signal after de-noising is different (due to different techniques implemented) and that we cannot determine which method recovers the more accurate signal. If the conclusions drawn from the two methods are different, we could have formed a judgment as to which method is better. We can observe (refer to Figure 4.15) that the smoothing technique has suppressed more noise than the low-pass filtering technique. This however shouldn't be an indication of it being a better method. This is because in suppressing some of the noise, it may have inadvertently eliminated some of the true dynamics of the signal which would then impede the results obtained.

For a consummate discussion on noise removal techniques, we also present results obtained from a wavelet transformation of the riser temperature signal (refer to chapter 3). Figure 4.16 shows this transformation. As before, we attempt to characterize the dynamics of the riser temperature data after wavelet transformation. Table 4.13 presents these results.

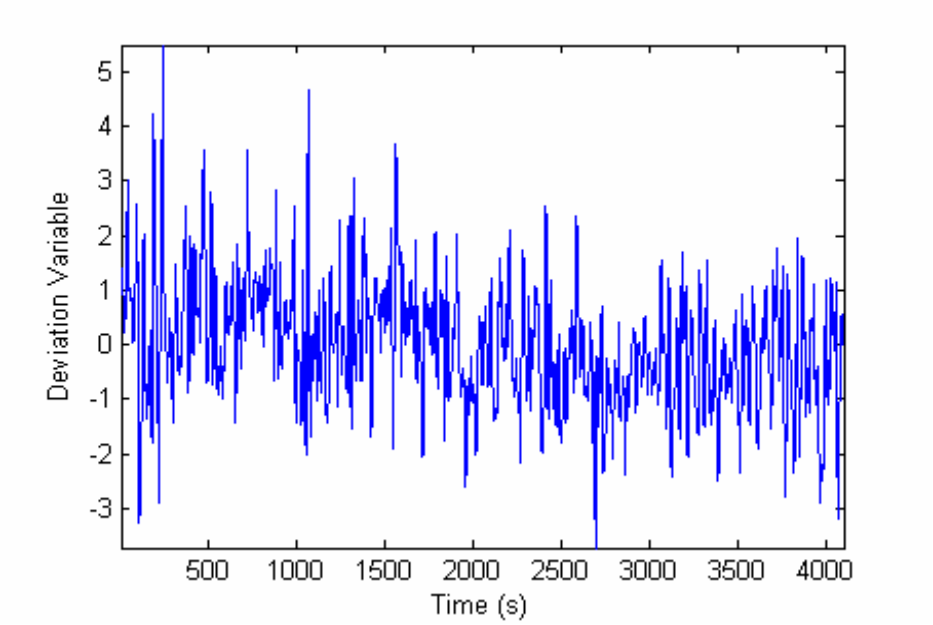

Figure 4.16: Graph of riser temperature after wavelet transformation

Table 4.13: Lyapunov exponents of the wavelet transformed riser temperature data

Lyapunov exponents (LE) for wavelet transformed data		
LE_1	LE_2	LE_3
0.3871	-0.0499	-0.8703

Results in Table 4.13, show that the LE_1 is positive, LE_2 is almost zero, LE_3 is negative and the sum of them is also negative. This proves that the de-noised data are found to exhibit chaotic fluctuations and this is expected since the original data are chaotic. Results also show that the LE values in this case are closer to those for the original data, compared to the values obtained for the low-pass filtered and smoothed data. Since wavelet analysis is known to be a superior method compared to other filtering methods, we can expect its results to be more accurate (Padmanabhan, 2004). Therefore, since the LE values of the original data and wavelet transformed data are not that different, we can conclude that the original data did not contain much noise to begin with. We can also

conclude that the low-pass filtering and smoothing techniques may have over compensated to remove noise as well as some of the true characteristics of the signal

Based on the above analysis, we can see that all three techniques work well in mitigating noise (and perhaps some of the characteristics of the signal) to recover the dynamics of the true signal. Characterizing the true nature of the signal would aid us in comprehending reasons for poor control performance. It must be noted that the true signal can never be completely known and hence we can only infer which method is more superior, either from results or prior knowledge of the efficiency of the method. Recovering the true signal is also important in cases where the systems are too noisy and the abundance of noise results in a false indication of chaos. We note that tests for stationarity, Gaussianity and nonlinearity are more robust than that of chaos and are able to yield good results even in the presence of noise. Therefore, if a signal is found not to be chaotic, there is no need to apply noise removal techniques to it. Hence, in this study, de-noising techniques are only applied to the riser temperature data since it is the only signal to exhibit chaotic dynamics.

4.6 Summary

This chapter applied a rigorous statistical framework to comprehensively characterize the dynamics of the riser temperature and other important variables in the FCC unit. The feature of this framework is that all analyses utilize only routine operating data which is easily available. The results clearly show that the riser temperature exhibits nonlinear and

chaotic fluctuations. Hence, it is deduced that a linear PI controller is unable to mitigate these fluctuations and thus large fluctuations are still inherent. To further understand why such fluctuations are present, other variables that may vicariously affect the riser temperature are investigated using the same statistical framework. Results show that there are linear fluctuations in feed flowrate, feed temperature and pressure differential between the 1st and 2nd stage regenerator and nonlinear fluctuations in the 2nd stage regenerator pressure and saturated steam flowrate all of which may contribute to the chaotic fluctuations observed in the riser temperature. In conclusion, via data analysis, we fully understand why the riser temperature control loop is performing poorly. The next step is to propose remedial actions that may help reduce these fluctuations and improve control loop performance. This will be discussed in chapter 5. We also tested three noise removal techniques for the riser temperature data and the results show that they could be useful in recovering the true nature of the signal. Results also reveal that the true signal is chaotic and this is important because this shows that our implemented methods are efficient in detecting chaos in the original signal although it is contaminated with some noise. In the next chapter, we will discuss the modeling and control aspect of the FCC unit and attempt to reduce the fluctuations seen in the riser temperature.

CHAPTER 5

MODELING AND CONTROL ENHANCEMENT OF THE FCC UNIT

This chapter provides the background information followed by a review of available FCC models. Subsequently, modification and implementation of one selected FCC model, its validation, followed by several strategies to improve the control of the FCC unit are presented.

5.1 Introduction

The fluid catalytic cracking (FCC) process is one of the most important processes in a modern refinery. To recapitulate, the FCC unit is constituted basically of two interconnected reactors (riser and regenerator) supported by ancillary equipment. In the riser, the catalytic cracking of the feed takes place whilst in the other, deactivated catalyst is reactivated by coke combustion. The interacting effects of these two units pose several challenges related to the stability and control of the FCC process. This was seen in chapter four, where results showed that the nonlinear and / or chaotic fluctuations in several key variable(s) of the FCC unit were the plausible causes of poor control of the riser temperature. In this chapter, the modeling and control aspect of the FCC unit will be discussed in order to ameliorate the control loop performance of the riser temperature. The first step towards this goal will be to develop an accurate model that realistically represents the characteristics of the process.

5.2 Previous Studies

Numerous studies dealing with the modeling, simulation, kinetics, multiplicity of steady states, chaotic behavior, online optimization and control of FCC units have been reported in the open literature (Kasat and Gupta, 2003). Several studies on the multiplicity of steady states and chaotic behavior were presented in chapter four and in this chapter, we present some of the related work on the modeling and control of FCC units. The literature is relatively rich in modeling and control studies of FCC units. A few of these models are developed using fundamental principles, while other FCC studies are based on empirical or semi-empirical models (Viera et al., 2005). A detailed review of these models is provided by Arbel et al. (1995) while their merits and demerits have been critically reviewed by Elshishini and Elnashaie (1990). Based on these, it has been suggested that one can possibly use any reasonable model, even if empirical, for simulation and control, as long as experimental or industrial data are used to tune the parameters associated with the model. This clearly implies that the model can be tuned to match the industrial FCC process. Going by the availability of several FCC models, it can be concluded that deriving a new FCC model from first principles to accurately model our industrial FCC process is redundant. Therefore, for the purpose of this thesis, we propose to utilize an existing FCC model and fine tune it, to accurately depict the industrial FCC process.

5.3 Review of FCC Models

FCC processes are known to be difficult to model well because of the large scale nature of the process, complicated hydrodynamics and complex kinetics of both cracking and coke burning reactions. Numerous papers on FCC modeling have had widely varying scope and level of modeling rigor. Some papers focus on specific parts of the units while others are only concerned with reaction kinetics or steady state behavior. Several studies on dynamic modeling of the whole FCC unit, as reported by Han and Chung (2001), have had limited applicability due to the outdated type of process or the over-simplified and unrealistic assumptions introduced in the modeling effort. Empirical and semi-empirical models are adequate and conform well to the real industrial process over a small operating range. However, when the operating conditions change, their validity may fail. Many of these models also do not describe or include important variations in variables, like pressure effects (Balchen and Strand, 1992; Hovd and Skogestad, 1993) and use over-simplified kinetics (Ansari and Tade, 2000). It is also not possible to investigate nonlinearities and chaos in empirical models, as these models are generally linear models obtained from system identification. If nonlinear models are identified, we may be able to capture phenomena such as chaos and bifurcation. Dynamical models (from first principles) are able to capture the nonlinearity and chaos (if any) of a process and therefore would be deemed more suitable for this study. These models have been developed in several studies for certain parts of the FCC process. For the purpose of this study, we will restrict our review of FCC models that model the riser and regenerator. Arbel et al. (1995) have developed a model that can describe both the steady state and

dynamic behavior of a FCC unit (consisting of the riser and regenerator) being operated in both partial and full combustion modes. Ali and Rohani (1997) presented a more detailed dynamic model that consists of several ordinary differential and algebraic equations. Han and Chung (2001) presented an even more detailed model of the FCC unit which consists of ordinary and partial differential equations. The latter is used to simulate the effect of the dense bed and freeboard both of which are not included in this study. Furthermore, the model proposed by Han and Chung (2001), incorporates too much complexity for the purpose of control studies. Furthermore, partial differential equations are not always necessary when time scales are of large varying orders (Jia et al., 2003). Thus, an adequate reduced model would suffice for the purpose of this study. Hence, the model proposed by Ali et al. (1997) is employed in this study as it is of adequate complexity and yet it captures most of the important variables we wish to investigate. For more details of this model, the reader is directed to the paper by Ali and et al. (1997).

5.4 Modification and Implementation of the FCC model

The model for the FCC unit proposed by Ali et al. (1997) consists of sixteen differential equations coupled with twenty four algebraic equations. The steady state model involves both ordinary differential equations (riser equations) and algebraic equations (regenerator equations). Riser ordinary differential equations are solved using MATLAB ODE functions. All the output variables are integrated with respect to axial length of the riser. The output variables are the product distribution (species composition) and temperature of the riser. The regenerator nonlinear algebraic equations are solved using Newton-Raphson

method. When solving the dynamic model, the steady state variables are first calculated and then used as the initial conditions to obtain the transient response. The riser and regenerator equations are solved using MATLAB's ODE integrating functions (ode15s, ode45 etc). The integrating step size is set to one second. The model equations are implemented in a MATLAB code, which is provided by Jia et al. (2003) in a softcopy format. There is also a slight difference in the design between the industrial FCC unit and the FCC model of Jia et al. (2003). The latter does not account for a purge stream entering the riser along with the feed. Hence, suitable modifications are made to the mass and energy balances, to account for the purge stream. At this juncture, from a design point of view, the model is an apt representation of the industrial FCC unit. The next step would be to tune the FCC model to match with the measured operating data.

5.5 Validation of the FCC model

The FCC model is tuned by matching the measured operating data of the following variables: (1) riser temperature, (2) pressure of 2nd stage regenerator and (3) gasoline yield. Although the main focus of our investigation is the riser temperature, the added validation of (2) and (3) would lend credence to the validity of the FCC model as a good representation of the industrial FCC process. The manipulated variable for (1) is the regenerated catalyst flow rate and that of (2) is the spent catalyst flow rate. Gasoline yield is uncontrolled. The feed flowrate, feed temperature and saturated steam flowrate are selected as the disturbances, as mentioned in chapter 2. Industrial data of these

disturbances are used in estimating model parameters and model validation, which consists of the following steps:

1. Input all industrial FCC unit design and operating parameters (i.e., riser and regenerator dimensions, feed properties, disturbance and manipulated variables) into the model. These parameters are not listed or shown due to proprietary reasons.
2. Select operating parameters that would influence the riser temperature, regenerator pressure and gasoline yield, for estimating to match the measured data of the variables. These parameters are heats of reaction of the riser temperature and gasoline yield, heat of vaporization of the feed oil, voidage factors of emulsion and bubble phases in the regenerator. In total, there are 5 parameters.
3. Perform parameter estimation by implementing an optimization algorithm that would optimize these selected operating parameters to ensure a good fit of the model to the process data. The FMINCON function in MATLAB is used as the optimization routine in our study. The voidage factors are bounded between zero to one, the heats of reaction are bounded to be less than or equal to zero and the heat of vaporization is bounded to be non-negative. Settings such bounds in the optimization routine would ensure that only feasible solutions are obtained.

5.5.1 Results and Discussion

We consider three sets of riser temperature, 2nd stage regenerator and gasoline yield data, taken on the first day of consecutive weeks. The first set of data (set 1) is used to tune the

FCC model, i.e., estimate parameters in the model. Conventionally, a model is deemed to be a good fit to the process if the sum of squared error (SSE) is minimal. However, in our study, it is essential that the model is able to capture the dynamics of the process. Therefore, after finding optimal parameter values by minimizing SSE, we calculate the control loop performance index (CLPI, refer to chapter 6 for more details), BI and the observed statistic from SDM to ensure that the dynamics of our model typifies that of the process. Figures 5.1 to 5.3 show the fit of the FCC model to the process for riser temperature, regenerator pressure and gasoline yield. The corresponding SSE values are 0.8934, 0.7373 and 1.1699 respectively. These values appear low but they do not necessarily indicate that the model is a good fit to the process. However, Figures 5.1 to 5.3 indicate that the model is able to approximately capture the range of fluctuations of the process. As the FCC unit is very complex, the model cannot be expected to account for every peak or trough exhibited by the process. It is more important that the model be able to capture the dynamics of the process which are determined by the CLPI, BI and observed statistic.

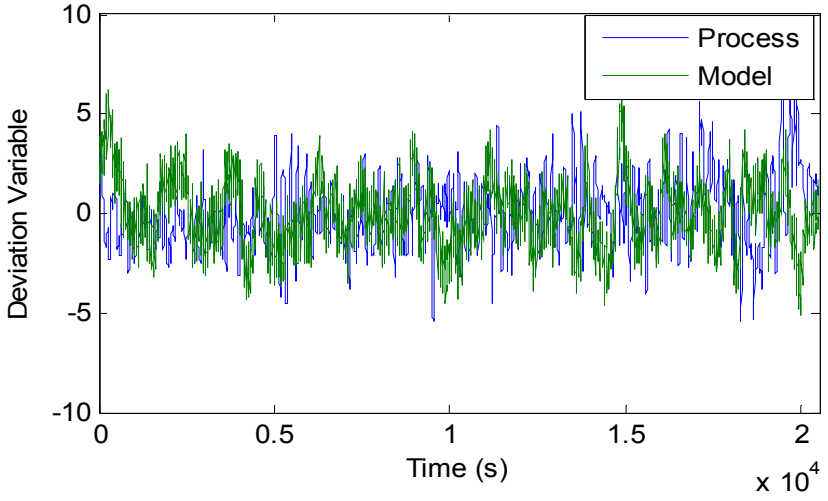

Figure 5.1: Graph of riser temperature against time (set 1)

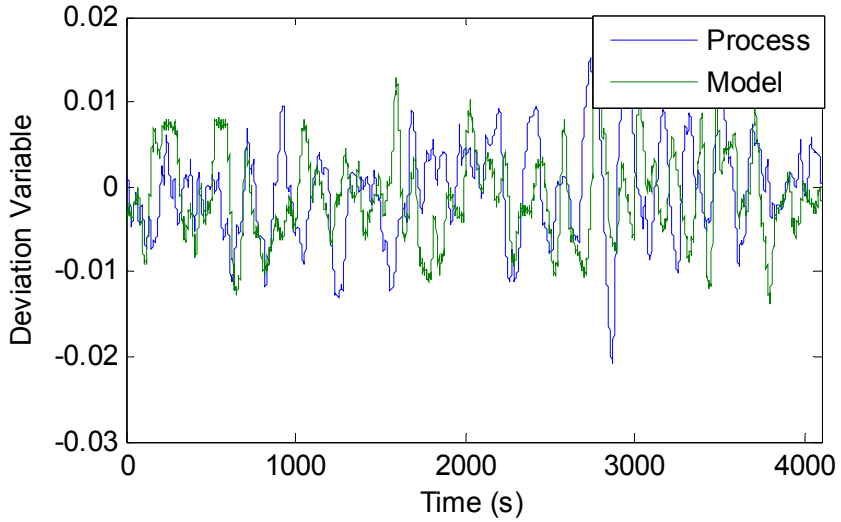

Figure 5.2: Graph of regenerator pressure against time (set 1)

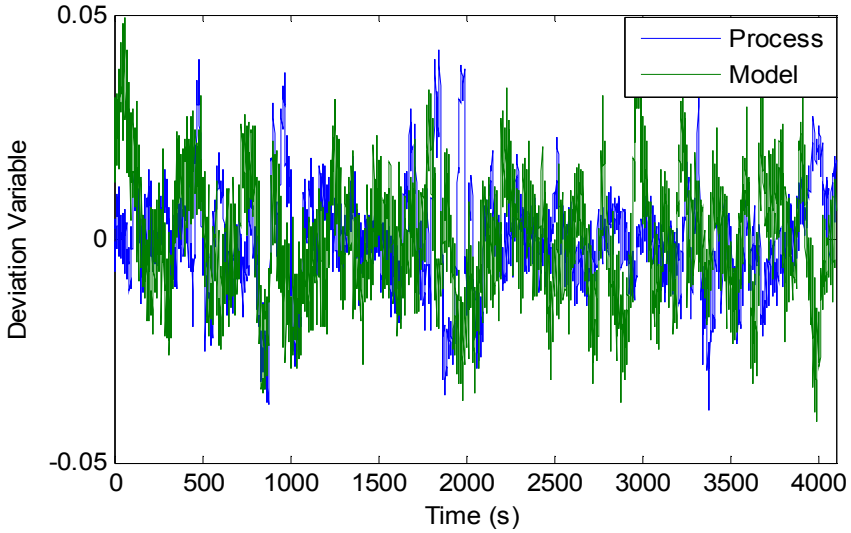

Figure 5.3: Graph of gasoline yield against time (set 1)

Table 5.1 presents the CLPI, BI and observed statistic for the riser temperature data. Results show that for set 1, the CLPI of the riser temperature from the FCC model is 0.034 higher than that of the riser temperature from the process. This 11.5% difference

shows that the model is able to capture the approximate control loop performance of the riser temperature process variable. Similarly, the BI and observed statistic values of set 1 indicate that the FCC model is able to capture the nonlinearity in the riser temperature of the FCC process. To ensure that our FCC model (that was fitted using only data set 1) is robust, it is imperative that we validate it for other sets of data which would signify a change in operating conditions. Results in Table 5.1 show that for sets 2 and 3, the CLPI, BI and observed statistic of both the process and model are similar. This demonstrates that the model is able to capture the dynamics of the process on different days.

Table 5.1: CLPI, BI and SDM results for the riser temperature, both measured in the process and predicted by the model

Set	CLPI ($\theta = 5$)*		BI		Observed Statistic	
	Process	Model	Process	Model	Process	Model
1	0.294	0.328	0.528	0.640	3.501	3.057
2	0.291	0.333	0.473	0.526	3.342	3.114
3	0.326	0.338	0.465	0.554	3.666	3.268

* The metric in brackets indicates the time delay for the FCC process

A similar analysis is presented for the regenerator pressure and gasoline yield. Tables 5.2 and 5.3 present the BI and observed statistic results for these variables. Results in Table 5.2 show that for set 1, the BI and observed statistics are marginally higher for the model predicted data than those for the measured data in the process. This shows that the model is able to capture the nonlinearity exhibited by the process variable. This is substantiated by the results in sets 2 and 3 whose values are similar for both the process and model. Likewise, results in Table 5.3 show that for all three sets, the BI and observed statistic

values are comparable. This implies that the model is able to capture the dynamics of the gasoline yield process variable.

Table 5.2: CLPI, BI and SDM results for the regenerator pressure, both measured in the process and predicted by the model

Set	BI		Observed Statistic	
	Process	Model	Process	Model
1	0.123	0.147	2.226	2.672
2	0.169	0.185	2.273	2.714
3	0.174	0.226	2.348	2.812

Table 5.3: CLPI, BI and SDM results for the gasoline yield, both measured in the process and predicted by the model

Set	BI		Observed Statistic	
	Process	Model	Process	Model
1	0.669	0.641	2.643	2.847
2	0.621	0.587	2.712	2.901
3	0.604	0.557	2.547	2.834

In summary, results in Tables 5.1 to 5.3 show that for all the three variables (riser temperature, regenerator pressure and gasoline yield) the FCC model is able to adequately predict the behaviour of the actual process. Therefore, the tuned FCC model can be deemed to be a good working model. Henceforth, this model will be utilized and all our analysis will be carried out in silico (i.e., on the computer).

5.6 Control Loop Performance Enhancement

Our focus in this study is to ameliorate the control loop performance (CLP) of the riser temperature. In this section, we analyze the CLP of the riser temperature (set 1) and present some strategies that may enhance its loop performance. As established in section 5.5, the CLPI of the riser temperature is 0.328. This CLPI is deemed poor and this is confirmed by the ACF plot (Figure 5.4). It can be seen that the ACF falls slowly to zero as the lag increases. This signifies that the time series of the regulated riser temperature is serially correlated which is an indication of poor CLP.

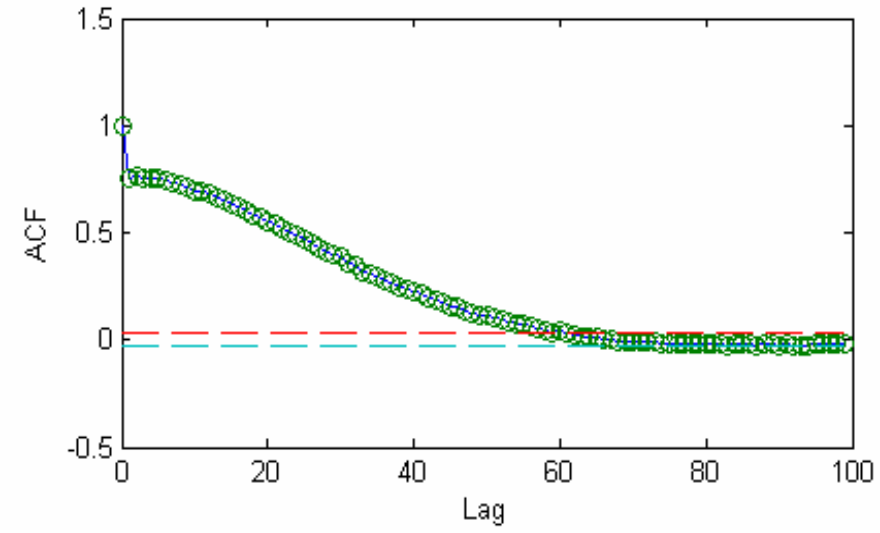

Figure 5.4: ACF of riser temperature

There could be several causes for the poor control loop performance exhibited by the riser temperature, which are namely: (1) poor controller tuning, (2) valve nonlinearities, (3)

process nonlinearities, (4) linear disturbances and (5) nonlinear disturbances. In this chapter, we will examine (1), (4) and (5) and attempt to improve the overall CLP by tackling these issues. (2) and (3) are not examined due to limitations in the data obtained. However, the nonlinearity issues will be re-examined in chapter 6 in greater detail by considering several realistic simulations and industrial case studies.

5.6.1 Results and Discussion

In any chemical plant, the rudimentary method of attempting to improve poor control performance in a loop is to re-tune the controller. For the purpose of this thesis, we will only be looking at "regulatory level" PID controllers operating in a feedback configuration. In section 5.5, the FCC model was established to be a good representative of the FCC process. Using this model, we incorporate a closed-loop control strategy using two PID controllers to regulate the two controlled variables (riser temperature and regenerator pressure). Our objective is to optimize the six tuning parameters (k_c, τ_i and τ_d in each controller) to maximize CLPI of the riser temperature, using our CLPI optimization algorithm which has been implemented in MATLAB. After re-tuning the controller, the next logical option would be to examine any linear or nonlinear disturbances that may enter the loop and degrade control loop performance. In our model, we consider three disturbances which are, the feed flowrate, the feed temperature and the saturated steam flowrate. Prior results in chapter 4 have categorized them as linear, linear and nonlinear disturbances respectively. At this juncture, we can easily see that mitigating the nonlinear disturbance into the loop would be the primary focus, after controller re-tuning. The linear disturbances although less harmful than the nonlinear disturbance could

still be the reasons for the poor performance exhibited by the riser temperature. Table 5.4 presents the CLPI results after controller tuning and removal of linear / nonlinear disturbances.

Table 5.4: CLPIs after various strategies are implemented in the riser temperature loop

No.	Strategy Implemented	CLPI	Increase in CLPI (%)
1	None	0.328	-
2	Re-tune the controller to maximize CLPI	0.369	13.2
3	Remove fluctuations in saturated steam flowrate + re-tuning	0.479	35.4
4	Remove fluctuations in feed flowrate + re-tuning	0.568	28.6
5	Remove fluctuations in feed temperature + re-tuning	0.639	22.8

Results in Table 5.4 show that when no strategy is implemented, the status quo remains and the CLPI is 0.328. After optimizing the controller tuning parameters, we note that the CLPI increases to 0.369. This new CLPI indicates that for this control loop, this is the best possible index that can be achieved. This is because the control loop is still afflicted with other problems such as process and / or valve nonlinearities and linear / nonlinear disturbances. Thereafter, we remove the nonlinear fluctuations in the saturated steam flowrate disturbance. We liken this to better regulation of the upstream saturated steam flowrate such that perfect control is achieved. Subsequently, we note that the CLPI has further increased to 0.479. It must be noted that after every strategy is implemented, the controller has to be re-tuned to register the best possible CLPI. This is because if something is altered in a control loop that previously had served to hinder loop performance, the existing tuning parameters may result in aggressive control action which would then exacerbate the CLPI. Hence, re-tuning is vital. The third strategy implemented

is mitigating the fluctuations in the feed flowrate. Once this is carried out, it is observed that the CLPI increases from 0.479 to 0.568. Lastly, the fluctuations in the feed temperature are attenuated and it can be seen that the CLPI now increases from 0.568 to 0.639. Through these strategies, the CLPI has increased from 0.328 to 0.639 which is a 94.8% increase and is deemed to be fairly substantial.

The CLPI cannot be increased beyond 0.639 because the control loop may still be afflicted with some valve and / or process nonlinearities or because the best possible performance with a PID controller has been achieved. If these problems are dealt with, it may be possible to increase the CLPI further. It is also important to apportion the effect of each control strategy on the CLPI. Results in Table 5.4 show that better upstream control of the saturated steam flowrate would account for a 35.4% improvement to the CLPI. This is followed by better control of the feed flowrate followed by better control of feed temperature. Finally, re-tuning the controller accounts for 13.2% increase to CLPI. This last statement is testament to why many critical variables in chemical plants are poorly regulated. It is noted that when a control loop is subject to nonlinear and linear disturbances (which could be contributing to chaotic fluctuations as shown in chapter 4), the effect of re-tuning the controller is minimal. Therefore, this should not be the only focus when attempting to improve the loop performance. Figure 5.5 shows the plot of the riser temperature after implementing all the various strategies. It can be seen that the fluctuations have reduced to $\pm 1.5^0 C$, which is a marked improvement from the original fluctuations of $\pm 5^0 C$ (Figure 4.1).

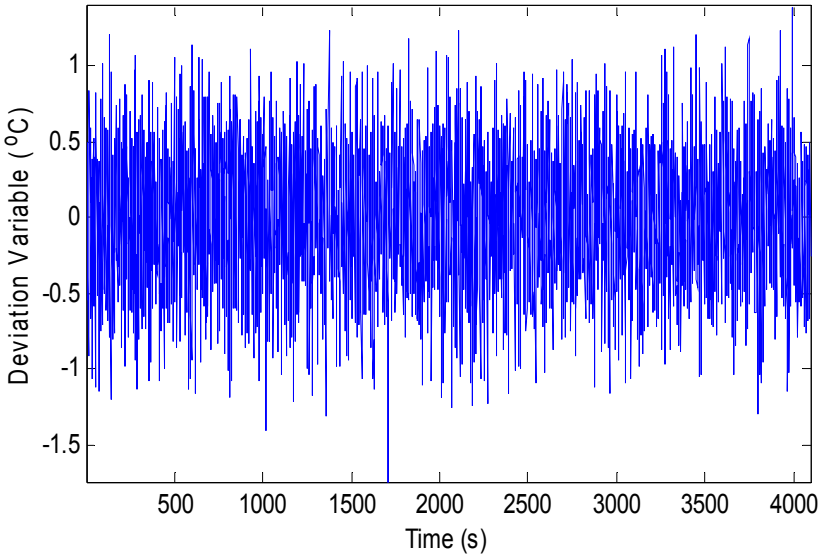

Figure 5.5: Graph of riser temperature (model) against time after implementation of various strategies

5.7 Summary

In this chapter, we review some of the latest FCC models that are available in literature and then select a suitable FCC model to model our industrial FCC process. Using industrial data and various statistical indices, the model is tuned and validated for different operating conditions. Results show that the model is able to realistically capture the dynamics of three critical variables in the FCC unit, with the riser temperature being the most important. Upon validation of the model, various strategies to ameliorate control loop performance are implemented. From the results obtained, it can be clearly seen that removal of the nonlinear disturbance would have the most significant impact on CLPI. More importantly, from our results, a control engineer would be able to determine how each strategy would improve the CLPI and this would enable him or her to make an informed decision when it comes to rectifying a poorly performing control loop. In the

next chapter, we present an even more detailed framework on control loop performance assessment which will look into the added adverse effect of process and / or valve nonlinearities, on CLPI.

CHAPTER 6

CONTROL LOOP PERFORMANCE ASSESSMENT AND ENHANCEMENT

This chapter contains sections on control loop performance assessment and enhancement with emphasis on the minimum variance benchmark, causes of poor control loop performance, mathematical models of valve nonlinearities, Hammerstein models, motivation, proposed framework for control loop enhancement, previous studies, effects of nonlinearities on control loop performance index, simulation examples, effect of poor data selection and industrial case studies.

6.1 Introduction

A typical chemical plant consists of several hundreds to thousands of process control loops. Although these "regulatory level" loops form the kernel of automatic and advanced process control, they are more often than not superseded by advanced control strategies such as model predictive control (MPC) and real-time optimization (RTO). This is because the performance capabilities of the "regulatory level" controllers which are mostly PI and PID algorithms, are limited and more sophisticated strategies such as the advanced control options must be implemented for better process control and economic optimization of the process. However, the limitations of these "regulatory level" controllers belie their importance as it is imperative that their performance be maintained at optimum levels for the advanced control strategies to perform well and achieve the

plants' overall objectives. At the time of commissioning, the controllers at the regulatory level may perform well but their performance can deteriorate over time due to changing operating conditions. Given such a scenario and particularly with the ready availability of routine operating plant data, there is good reason to develop tools and procedures for the purpose of control loop performance assessment (CLPA). For the purpose of this study, routine data encompasses (1) process variable (PV) data, (2) controller output (OP) data and (3) set-point (SP) data. From these data, the error (e) can be determined by calculating PV-SP.

6.2 Control Loop Performance

The performance of various control loops in a plant may be very good when commissioned. However, over time this performance is compromised due to external disturbances, changes in process dynamics, limits on the manipulated variables and even degradation of control system hardware. This necessitates the periodic monitoring of the plant to ensure that it runs efficiently and without any hitches. Hence, the fundamental idea in CLPA is to define a performance metric. This metric can then be used to compare the current control loop performance against a user defined benchmark. If the comparison is favorable, the loop under investigation is deemed to be functioning well. If not, the loop is subject to a more detailed analysis and appropriate rectification actions are carried out. The main features of this metric are that it should not interfere with the nominal operation of the plant, it should detect performance degradation quantitatively and it should be non-invasive meaning that it should utilize only routine operating data. In the control

literature, there are several measures that exist for the purpose of control loop performance assessment. Astrom (1967) proposed the auto-correlation function method (ACF), DeVries and Wu (1978) proposed the spectral analysis method and Harris (1989) came up with minimum variance controller (MVC) benchmark. The methodology developed by Harris (1989) is theoretically sound, reliable, efficient, easily interpretable and computationally simple (Goradia, 2004). However, it is usually undesirable to install a MVC in practical applications as it may result in excessive or aggressive control actions that may damage control valves and limit their life span. The MVC also is not very robust to changing operating conditions and if a process has non-invertible zeros (zeros outside the unit circle), it is not possible to design a MVC. However, despite these demerits, one can exploit the fact that the MVC provides the best possible control under feedback conditions. With only the knowledge of process delay, the MVC benchmark represents a powerful tool in the analysis of control loops to determine if they are performing to the standard of the MVC benchmark. Today, taking into consideration the various advantages and disadvantages, the MVC is the most popular benchmark used for the purpose of CLPA. It also forms the major core of commercially available control loop performance monitoring software such as 'LoopScout' (Honeywell) and 'ProcessDoctor' (Matrikon). Hence, this metric will be used in this study.

6.3 Control Loop Performance Index (CLPI) using the MVC benchmark

This method computes an index known as the CLPI which is a measure of the performance of the control loop. The derivation of this index is shown below:

Let us consider a conventional feedback control loop (refer to Figure 6.1) where

- Q is the feedback controller.
- T is the process transfer function whereby $\tilde{T}$ is the delay free transfer function and $z^{-\theta}$ is the pure delay portion such that $T = \tilde{T} z^{-\theta}$
- N is the disturbance or load transfer function.
- T, Q and N are polynomials in z^{-1}
- y is the process output.
- w_t is a white noise signal that feeds the disturbance transfer function and is the signal driving the closed loop system.

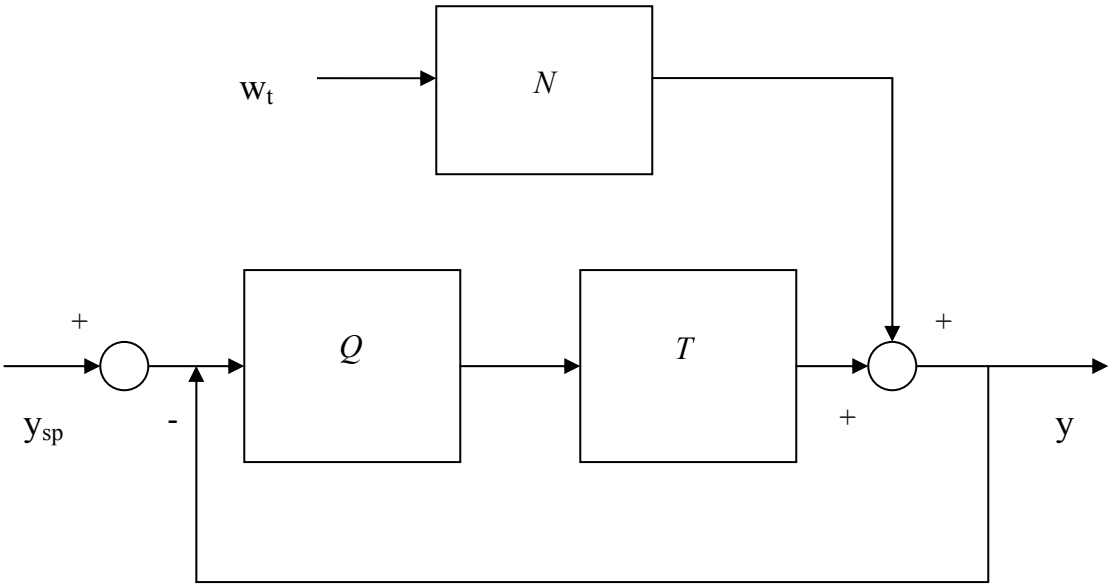

Figure 6.1: Block diagram of a conventional feedback loop

The process output (y) can be expressed in terms of the transfer functions (labeled in Figure 6.1) and white noise (w_t) as:

$$y = \left\{ \frac{N}{1 + TQ} \right\} w_t = \left\{ \frac{N}{1 + z^{-\theta} \tilde{TQ}} \right\} w_t \tag{6.1}$$

Factor the transfer function N as

$$N = F + z^{-\theta} R \tag{6.2}$$

where $F = F_0 + F_1 z^{-1} + ... + F_{\theta-1} z^{-(\theta-1)}$ and R is an appropriate transfer function that is yet to be determined. y may now be written as

$$y = Fw_t + \left\{ \frac{(R - F\tilde{TQ}}{1 + z^{-\theta} \tilde{TQ}} \right\} w_{t-\theta} = Fw_t + Lw_{t-\theta} \tag{6.3}$$

where L is a polynomial in terms of z^{-1}. The polynomial F is now independent of the controller Q and hence characterizes the controller invariant portion of y. The polynomial L is dependent on the controller. If $Q = \frac{R}{\tilde{TF}}$, then L = 0, which implies that $y = Fw_t$. This selection of Q yields the MVC. The output variance for the MVC is:

$$\sigma^2_{MVC} = \text{var}(y_{MVC}) = (F_0^2 + F_1^2 + ... + F_{\theta-1}^2)\sigma_w^2 \tag{6.4}$$

For any other choice of Q, $L \neq 0$ and we have the output variance

$$\sigma_y^2 = \text{var}(y) = (F_0^2 + ... + F_{\theta-1}^2 + L_0^2 + L_1^2 + ...)\sigma_w^2 \tag{6.5}$$

The CLPI (η) using the MVC benchmark is given as

$$\eta(\theta) = \frac{\sigma^2_{MVC}}{\sigma_y^2} \tag{6.6}$$

implying the index is a function of process delay (θ). The CLPI is the ratio of the sum of squares of the first 'θ' closed loop disturbance impulse response (IR) coefficients to the

sum of squares of all closed loop disturbance IR coefficients. To evaluate CLPI, only the knowledge of process delay and closed loop disturbance impulse response are needed. The CLPI is bounded between 0 and 1 where 0 indicates the worst performance and 1 indicates the best performance. For detailed calculations, refer to Huang and Shah (1999). The codes for CLPI calculation and design of a MVC have been implemented in MATLAB.

6.4 Causes of Poor Control Loop Performance

Hitherto, we have discussed a performance metric (CLPI using MVC) that is able to quantitatively detect performance degradation. Assuming that the current CLPI shows poor performance, it is important for us to firstly diagnose the cause of this performance degradation and secondly to suggest suitable corrective action. In control literature, these two points have not received much attention and remains an open area for research. Poor performance of control loop can be caused by various factors. In this study we will consider the four main causes which are (1) poor controller tuning, (2) oscillations (due to external disturbances and / or aggressively tuned controllers), (3) nonlinearities and (4) combination of (1), (2) and (3).

6.4.1 Poor Controller Tuning

Since most of the regulatory level controllers are PI or PID, there are at least two or three parameters that require to be correctly tuned. In most industries, there is computer software that tunes these parameters based on system identification of linear models from

step responses. However, given the changing operating conditions and process dynamics, these tuning parameters may become sub-optimal and new tuning parameters are required. However, the tuning parameters are not routinely updated and often they are manually adjusted by the shift operators. This results in the controller being either conservatively tuned (resulting in sluggish closed-loop response) or the controller being tightly tuned (resulting in large oscillations and overshoot). Both however, contribute to poor performance.

6.4.2 Oscillations

Oscillations can be caused by a tightly tuned controller as described in the above sub-section. They are also caused by external disturbances which affect the process variable and hence result in poor control. It is worthwhile to note that these external disturbances may be linear or nonlinear. If the disturbances can be measured, it is possible to distinguish linear disturbances from nonlinear ones. This is important because the impact of nonlinear disturbances on control loop performance is more severe than that of linear disturbances. If the disturbances are unmeasured, it is virtually impossible to infer anything about their linearity or nonlinearity. Therefore, in such instances, they are assumed to be linear. For the purpose of this thesis, we will also assume that these linear external oscillations are in the form of random white noise, integrated white noise or colored noise (a random signal passing through a first order filter to give it structure).

6.4.3 Nonlinearities

Nonlinearities are often the cause of poor control loop performance. This is because controllers are tuned based on linear algorithms and nonlinearities would render these tuning parameters inaccurate. Nonlinearities in a control loop may appear as follows:

- The process may be nonlinear (process nonlinearity).
- The control valve may have a nonlinear characteristic (valve nonlinearity).
- The valve may contain nonlinear faults (valve nonlinearity).
- A nonlinear disturbance enters the loop.

Although most chemical processes are nonlinear in nature, it is often assumed that given the narrow operating conditions within which they operate, the process operates linearly. However, it is still possible that process nonlinearities affect control loop performance. Since the control valve may be innately nonlinear and given that over time they develop faults which augment the nonlinearities, valve nonlinearities are predominantly the cause for poor control loop performance. There are also cases where process nonlinearities and valve nonlinearities combine (known as system nonlinearities) and result in poor control loop performance (Choudhury, 2004).

6.5 Mathematical Models of Valve Nonlinearities

In the previous sub-section we discussed valve nonlinearities and how nonlinearities in general affect control loop performance. In this section we discuss and develop the types of valve nonlinearities via mathematical models.

6.5.1 Stiction

Stiction is the resistance to the start of the motion, usually measured as the difference between the driving values required to overcome static friction. The word stiction is a combination of the words **sti**ck and fri**ction**, created to emphasize the difference between static and dynamic friction. Stiction exists when the static (starting) friction exceeds the dynamic (moving) friction inside the valve. Stiction describes the valves stem (or shaft) sticking when small changes are attempted. Friction of a moving object is less than when it is stationary. Therefore, stiction can keep the stem from moving for small control input changes and then the stem moves when there is sufficient force to free it. The result of stiction is that the force required to get the stem to move is more than that required to go to the desired stem position. Hence, in the presence of stiction, the movement is jumpy as shown by the dashed lines in Figure 6.2.

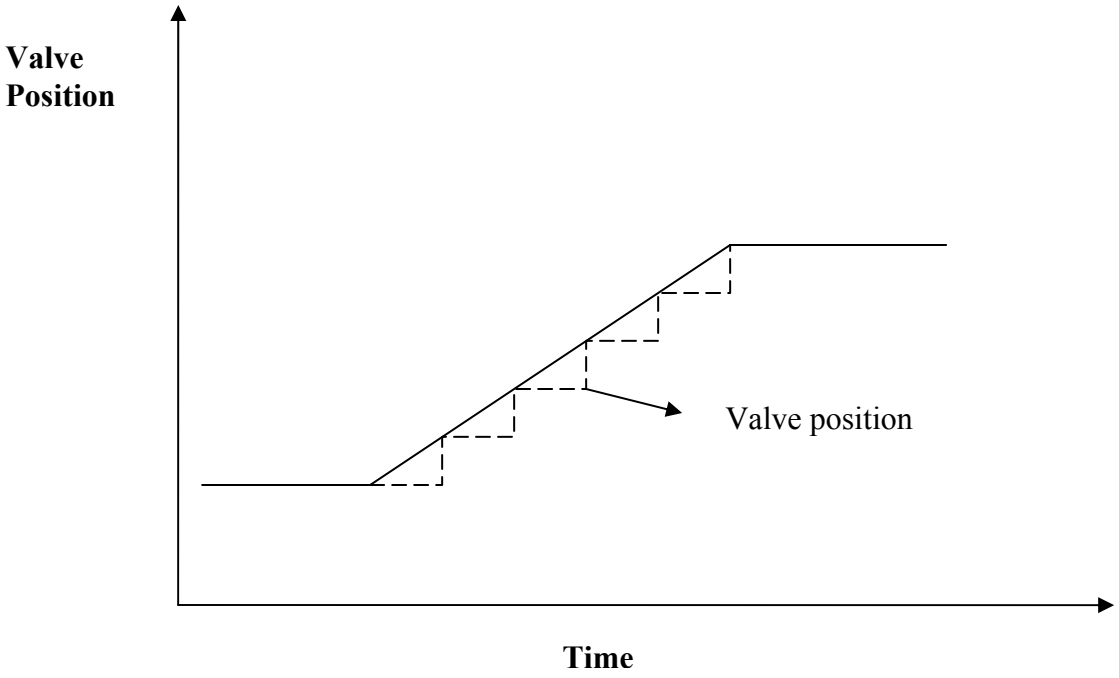

Figure 6.2: Valve position against time under stiction conditions

Valve stiction in a control loop will cause problems. In a control loop, stiction causes the loop to cycle and any amount of stiction will degrade the performance of the control loop. Hence identification of stiction is the first step in circumventing this problem and this is achieved by means of mathematical models of stiction. In literature, several friction models that can model stiction are available (Karnopp, 1985). Each model has its merits and demerits and in this study we implement the classical and simple stiction model.

6.5.1.1 Classical Stiction model

In this sub-section we will discuss the classical stiction model based on a friction model proposed by Karnopp (1985) that includes static and dynamic friction. For a pneumatic

sliding stem valve, the force balance equation based on Newton's second law is written as:

$$M\frac{d^2x}{dt^2} = \sum Forces = F_a + F_r + F_f + F_p + F_i \tag{6.7}$$

where M is the mass of moving parts, x is the relative stem position, F_a = Au is the force by pneumatic actuator where A is the area of the diaphragm and u is the actuator air pressure or the valve input signal. F_r = -kx is the spring force where k is the spring constant, F_p = -αΔP is the force due to fluid pressure drop where α is the plug unbalance area and ΔP is the fluid pressure drop across the valve, F_i is the extra force required to force the valve to be into the seat and F_f is the friction force. F_i and F_p will be assumed to be zero because of their negligible contribution to the model (Kayihan and Doyle III, 2000). The expression for the moving friction, F_f (in the first line of equation 6.8) is as follows:

$$F_f = \begin{cases} -F_c\,\mathrm{sgn}(v) - vF_v & if\ v \neq 0 \\ -(F_a + F_r) & if\ v = 0\ and\ \left|F_a + F_r\right| \leq F_s \\ -F_s\,\mathrm{sgn}(F_a + F_r) & if\ v = 0\ and\ \left|F_a + F_r\right| > F_s \end{cases} \tag{6.8}$$

It comprises of a velocity independent term F_c known as Coulomb friction and a viscous friction term vF_v that depends linearly on velocity (v). Both act in opposition to the velocity, as shown by the negative signs. The second line in equation 6.8 depicts the case when the valve is stuck whereby F_s is the maximum static friction. The velocity of the stuck valve is zero and is not changing, so therefore the acceleration is also zero. Hence, the right hand side of Newton's law is zero, so F_f = - (F_a+F_r). The third line in equation 6.8 represents the instance the valve breaks free and moves. At this instant, the sum of the

forces is $(F_a + F_r) - F_s - F_s \operatorname{sgn}(F_a + F_r)$, which is not zero if $|F_a+F_r| > F_s$. Hence, the acceleration is non-zero and the valve begins to move.

This classical stiction model although very detailed, has numerous parameters that have to be identified from routine operating data and identifying all the parameters accurately is a tedious task. Oftentimes, due to the fallibility of numerical optimization routines, it is not possible to identify the parameters at all. Hence, this paves the way for a simpler stiction model that would be easier to solve and be a reasonably good substitute to the classical stiction model. The classical stiction model has been implemented in MATLAB using the S-function algorithm.

6.5.1.2 Simple Stiction Model

In this sub-section we present a simple stiction one parameter model that is proposed by Hagglund (2002). This simple model is given as follows:

$$x_t = \begin{cases} x_{t-1} & if \ |u_t - x_{t-1}| \le d \\ u_t & otherwise \end{cases} \tag{6.9}$$

Here, x_t and x_{t-1} are present and past valve outputs, u_t is the present controller output and d is the valve stiction band. Srinivasan and Rengaswamy (2004) have shown that this simple model is able to capture stiction phenomena by matching the data generated by the classical model with reasonable accuracy. The algorithm for the simple stiction model has been developed in MATLAB (Simulink).

6.5.2 Hysteresis

Hysteresis is a highly nonlinear phenomenon that affects the control valves in many industrial process control systems. As a parameter that represents some property of a system is increased, the behaviour makes a sudden jump at a particular value of the parameter. But as the parameter is then decreased, the jump back to the original behaviour does not occur until a much lower value. In the region between the two jumps, the system is bi-stable. Figure 6.3 depicts the input output behavior of a loop that is exhibiting hysteresis.

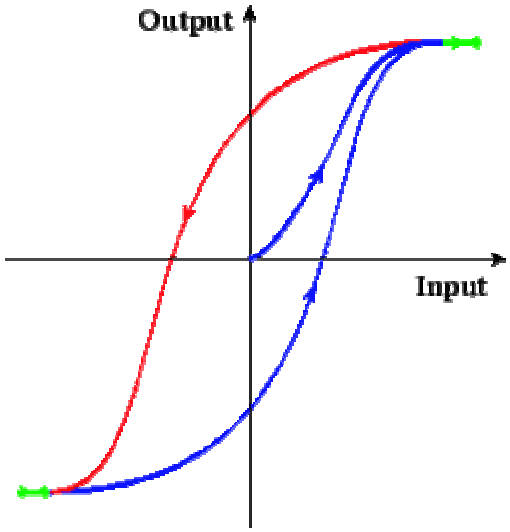

Figure 6.3: Input output behaviour of hysteresis

For the purpose of this thesis, we present the Weiss model of hysteresis.

Suppose we have some relays:

$$R^j = R_{\alpha j,\beta j}, 1 \le j \le N \tag{6.10}$$

Consider a parallel connection of the relays R^j with the weights $\mu_j = \mu(j) > 0$:

$$y(t) = y[t_0, \eta_0](t) = \sum_{j=1}^{N} \mu_j R^j [t_0, \eta_0(j)] x(t), t \geq t_0 \qquad (6.11)$$

Figure 6.4 illustrates this situation. This is the Weiss model of hysteresis where u(t) represents the controller output and x(t) represents the valve output. This model has been developed in MATLAB (Simulink).

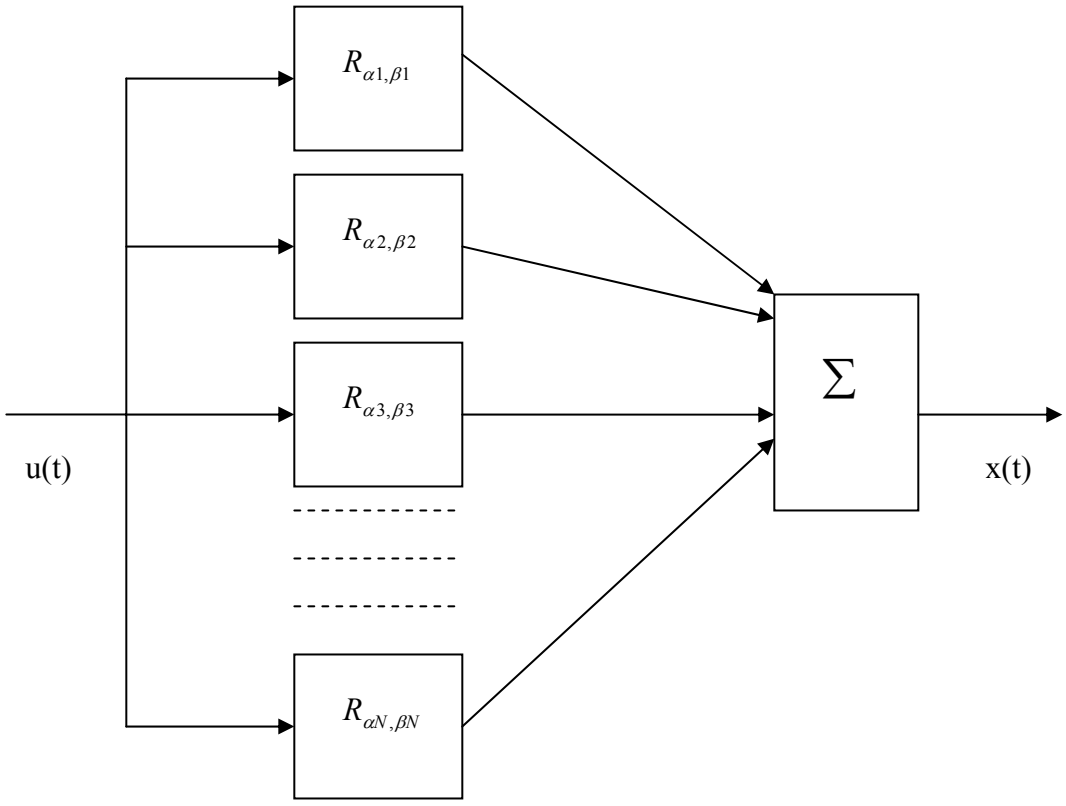

Figure 6.4: Weighted parallel connection of a finite number of nonideal relays

6.5.3 Backlash

In process instrumentation, backlash is the relative movement between interacting mechanical parts, resulting from looseness, when the motion is reversed. This can be due

to play in the fittings of the control valve. Backlash can lead to oscillations in closed-loop configurations and should not be confused with hysteresis (refer to Figure 6.5). A one parameter model of backlash is available in Simulink and it will be used in this study.

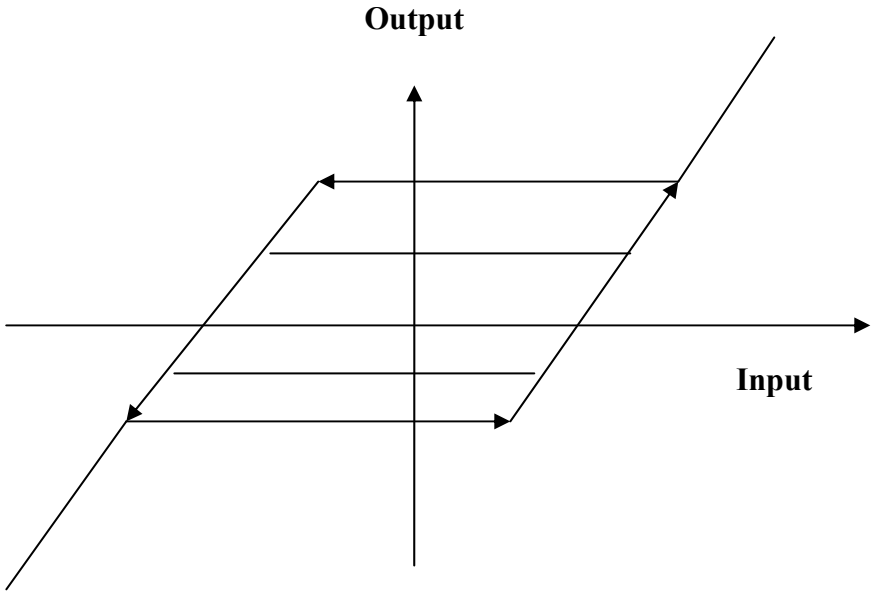

Figure 6.5: Input output behaviour of backlash

6.5.4 Deadzone

In process instrumentation, a dead zone is the range through which an input signal may be varied, upon reversal of direction, without causing an observable change in the output signal (refer to Figure 6.6). Similar to backlash, a one parameter model of dead zone is available in Simulink and it will be used in this study.

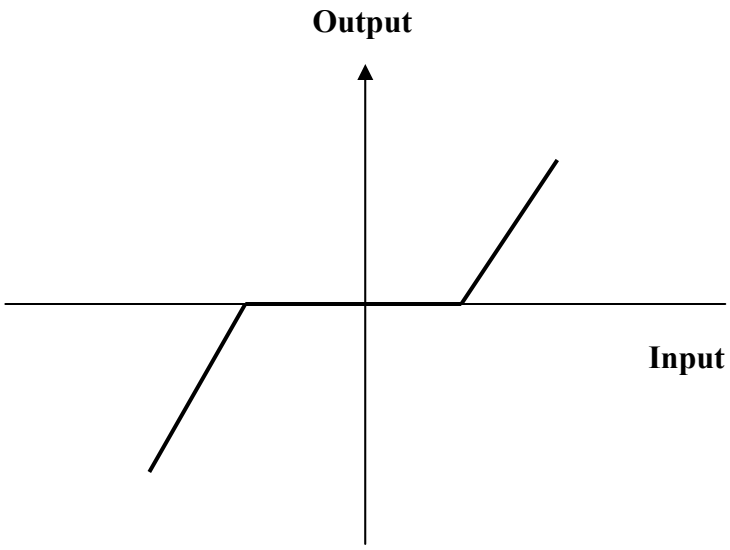

Figure 6.6: Input output behaviour of deadzone

6.6 Hammerstein Models

Nonlinear behavior is the rule rather than the exception in the dynamic behavior of chemical processes. In these chemical processes, understanding the inherent nonlinear characteristics is vital for proper design of controllers. One way to comprehend the nonlinear behavior is to form a mathematical model of the process. This approach has often been used to model nonlinear processes and is very useful. Owing to the relatively high effort in modeling systems from first principles, empirical modeling using process data is convenient for process control purposes. Therefore, system identification makes use of input / output data of the process to build an empirical model that represents the process and the crucial step in this method is the selection of the model structure. The vast majority of research done on system identification is for linear model structures which may suffice in modeling linear and mildly nonlinear systems. However, there is still a

need to obtain empirical models that are able to capture the nonlinearities by identifying a nonlinear model from input / output data. One useful representation for nonlinear processes is the block oriented models. The popular representation of this family of models is the Hammerstein model. This model structure is considered because of its high relevance to the current work.

The Hammerstein model of a nonlinear system is shown in Figure 6.7. The static NL element takes in the input u(t) and transforms it to x(t) and the dynamics are modeled by a linear discrete transfer function $G(z^{-1})$, with y(t) as the resulting output. The Hammerstein model captures the effects of the nonlinearity as an input dependent gain nonlinearity and the gradient of this nonlinearity at a particular operating point is the instantaneous gain of the system.

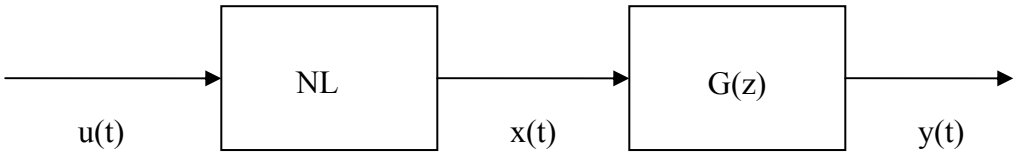

Figure 6.7: Hammerstein model

For the Hammerstein model, the mathematical representation is developed as follows:
If the static NL element is assumed to be approximated by a finite polynomial expansion, the Hammerstein model can be described by the following equations:

$$y(t) + a_1 y(t-1) + \ldots + a_n y(t-n) = b_1 x(t-1) + b_2 x(t-2) + \ldots + b_n x(t-n) \qquad (6.12)$$

$$x(t) = \gamma_1 u(t) + \gamma_2 u^2(t) + \ldots + \gamma_m u^m(t) \qquad (6.13)$$

The intermediate variable x(t) cannot be measured but it can be eliminated from the equations. Substituting the second equation into the first we obtain:

$$\begin{aligned} &y(t) + a_1 y(t-1) + \ldots + a_n y(t-n) = \\ &b_1\gamma_1 u(t) + \ldots + b_1\gamma_m u^m(t) + \ldots + b_n\gamma_1 u(t-n) + \ldots + b_n\gamma_m u^m(t-n) \end{aligned} \tag{6.14}$$

We can write the above equation in operator form as:

$$y(t) = \frac{B(q^{-1})}{A(q^{-1})}\sum_{i=1}^{m}\gamma_i u^i(t) \tag{6.15}$$

where the polynomials $A(q^{-1})$ and $B(q^{-1})$ are:

$$\begin{aligned} A(q^{-1}) &= 1 + a_1 q^{-1} + \ldots + a_n q^{-n} \\ B(q^{-1}) &= b_1 q^{-1} + \ldots + b_n q^{-n} \end{aligned} \tag{6.16}$$

The orders of the polynomial are assumed to be the same and in our study we will represent the NL element as a third order polynomial.

6.6.1 Parameter Estimation Methods for Hammerstein Models

It is possible to estimate the parameters of the Hammerstein model separately because of a special property of the Hammerstein model structure. Several algorithms exist for this parameter estimation and they include (1) prediction error method, (2) recursive prediction error method and (3) Narendra-Gallman algorithm. Eskinat et al. (1991) have reported that the Narendra-Gallman algorithm is the most robust amongst the three methods. Hence, this method is used in this study. Details of the method can be found in the paper by Eskinat et al. (1991). The algorithm for identifying Hammerstein models has been developed in MATLAB.

6.6.2 Identification of Hammerstein Models from Closed-Loop Data

The plethora of methods for identification of linear models has been based on open-loop identification and is deemed to work well. However, most of these methods fail when applied to closed loop data (Forssell and Ljung, 1999). The problem lies with the correlation between the immeasurable noise and the input in the closed-loop configuration. This is because, as long as the feedback controller is not identically zero, the noise and input will be correlated. In spite of these problems, performing experiments under closed loop conditions may be required for safety or economic reasons. This is especially pertinent for chemical processes. This conundrum led to the advent of several closed-loop identification methods for system identification which are namely the direct, indirect and joint input-output methods (Forssell and Ljung, 1999). In this study, we propose to use the direct approach, as the plant input 'u' which is now the controller output for the closed-loop case and the plant output 'y' are treated exactly the same way as in the open-loop case. While Forssell and Ljung limited their analysis to the identification of linear models, we extend this approach to the identification of Hammerstein models. The direct approach is also advantageous since apriori information such as the nature of the controller, tuning parameters and noise models are not accurately obtainable.

6.6.3 Persistence of Excitation

To identify good Hammerstein models, the system must be sufficiently excited. This is more so for closed-loop systems because the correlation between the input and noise must be broken and this can be done only if the system is persistently excited over a length of

time. Eskinat et al, (1991) made use of random noise as the input to the system to achieve the required excitation and showed that good Hammerstein models may be obtained. However, the scope of that paper is limited to open-loop simulations. In our study, we extend the concept of system identification using Hammerstein models, to closed-loop industrial data. This is more challenging because such data may not be persistently excited especially if they are operating near the steady state for a long period of time. Also, given that the data are obtained from industrial processes and not computer simulations, it is neither possible nor feasible to inject random noise in the loop to excite the data. Therefore, in this study, we propose an alternate means of data excitation which encompass a series of step changes applied to the set-point. The magnitude of the change and the time frame for which the changes are made, are carefully selected to ensure that the data are sufficiently excited. Such set-point changes are more realistic in industrial plants as opposed to injection of random noise. At times, when a particular unit operation becomes unstable due to changes in feed or operating conditions, the operator has to step in and manually adjust the controller to regulate the process variable. During this period, the operator makes fairly significant set-point changes and data collected over this time frame would be beneficial in identifying Hammerstein models via the direct identification method.

6.7 Motivation

The motivation behind presenting the above mentioned concepts and techniques is to introduce a novel framework that will detect, diagnose and rectify poor control loop performance (if any). Such a consummate approach to control loop performance

assessment would ensure that the appropriate rectification actions are carried out when control loops are not performing up to expectations. Oftentimes, when a loop is performing poorly, the cause for this poor performance is attributed to the wrong reason. Hence, the rectification action that is implemented is unable to improve the control loop performance and the process variable continues to be poorly controlled.

6.8 Proposed Framework

A detailed framework on control loop performance assessment is depicted in Figure 6.8. Firstly, a set of control loop data (error, e = PV-SP) is analyzed and tested for Gaussianity. If the error signal is found to be Gaussian, the signal generating process is assumed to be linear (Rao and Gabr, 1980; Hinich, 1982). In this case, if the CLPI and / or other means of assessing control loop performance are deemed to be poor, the causes of this would be linear external oscillations and / or poor control loop tuning. The controller can then be re-tuned and / or the linear external oscillations can be mitigated by investigating the disturbance variables for the CLPI to be improved. If the error data are found to be non-Gaussian, this implies that the data may or may not be linear and hence, a test for linearity should be implemented. If the data are nonlinear, the poor CLPI would be due to the system nonlinearities present in the loop. Given our assumption that a chemical process may be linear over a narrow operating range, the major contribution of the nonlinearities would be due to valve problems such as those discussed in the earlier section. With this knowledge, the valves may then be serviced and an acceptable loop performance may be restored.

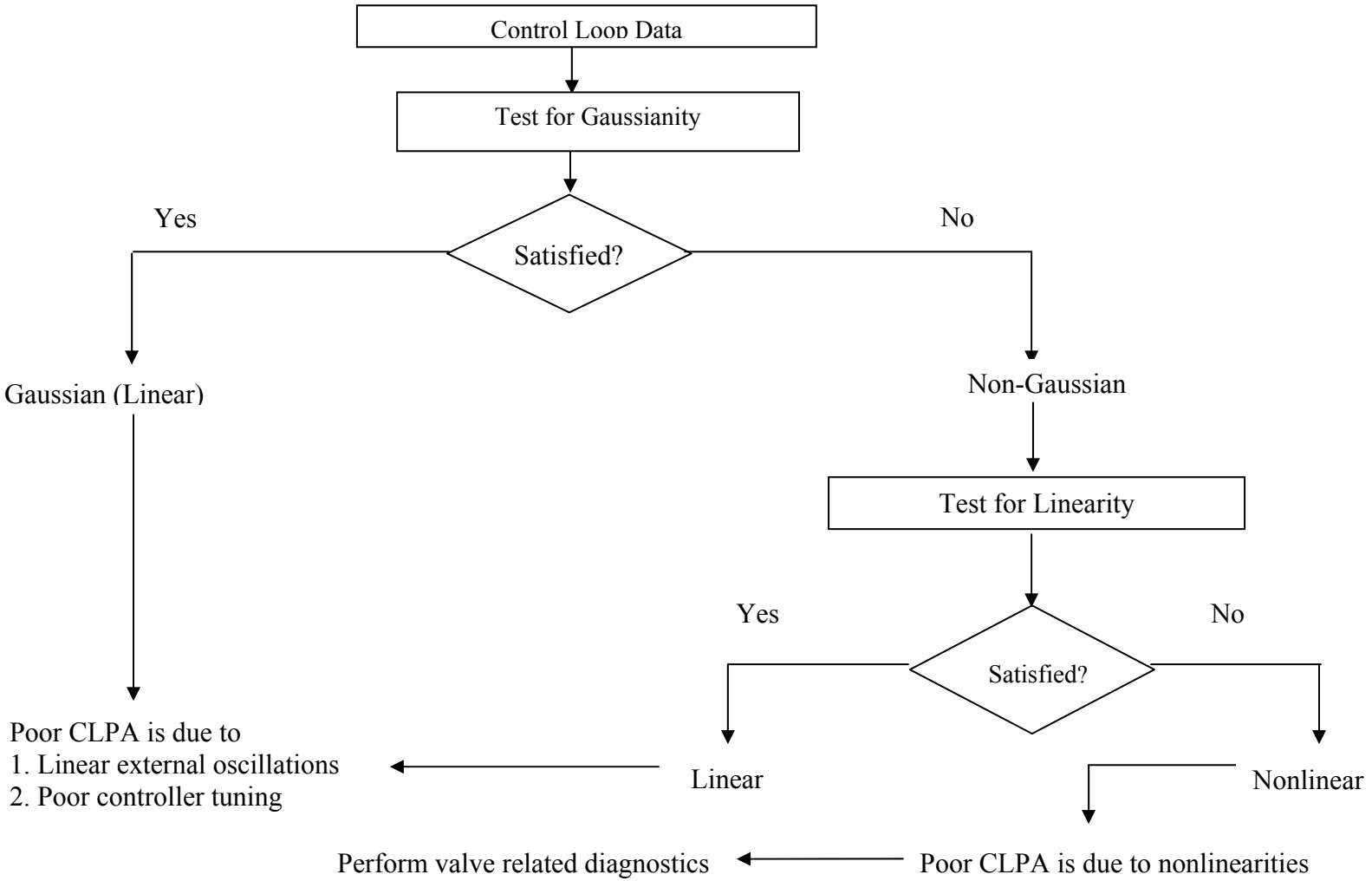

Figure 6.8: Flow diagram of proposed framework

We now consider the case where the poor CLPI is a result of poor controller tuning, linear external oscillations and valve nonlinearities. This is a much more challenging issue because for the control engineer to make the right decision, he / she has to ascertain the main cause for the poor CLPI and also the individual contribution of each possible cause of the poor CLPI. Many times in the chemical industries, a valve problem (due to the valve nonlinearity) is untreated as the cost of rectifying the problem is thought to outweigh the benefit of having the valve serviced and treated. However, there is no real way of measuring the increase in CLPI in a control loop when a valve is treated. Control engineers would be interested to quantify the potential improvement in loop performance if a certain problematic valve is serviced. Only if the increase in control loop performance is significant, would it make for good economic sense. We outline the main features in our proposed method that would enable the control engineer to detect, diagnose and rectify poor control loop performance when a loop is afflicted with poor tuning, linear external oscillations and valve nonlinearities.

- A control loop that is performing poorly is identified by calculating the CLPI.
- If the data are linear this means that the poor CLPI is a result of poor controller tuning and / or linear external oscillations.
- If the data are nonlinear, this means that the poor CLPI is a result of poor controller tunings, linear external oscillations and / or valve nonlinearities.
- Using the PV, OP and SP data, we identify a Hammerstein model of the system which should be a good representation of the real system (process and valve dynamics together). A low sum of squared error (SSE) would indicate a good fit.

CLPI, BI and the observed statistic from SDM will also be recalculated. If these indices are similar to that of the process, the model is deemed to be a good fit to the process.

- Since we are able to separate this system into a linear and nonlinear component, we assume the entire nonlinear polynomial term represents the valve nonlinearity.
- Since controller re-tuning is the common method of attempting to improve control loop performance, at this juncture we re-tune the controller (using an optimization algorithm that we implemented in MATLAB) by maximizing the CLPI. Any increase in CLPI would be solely due to re-tuning of the parameters and the effect of the tuning parameters on CLPI can be quantified.
- We then remove the nonlinear term (which signifies that the valve has been serviced to remove any nonlinearity) and calculate the new CLPI after further re-tuning is carried out. Any increase in CLPI would be now solely due to the removal of the valve nonlinearity. The increase in CLPI would indicate the degree of the valve nonlinearity that is affecting the control loop performance.
- The new CLPI may still not be optimal as linear external oscillations (resulting in some noise structure) may still limit the control loop performance. Subsequently, we remove the noise structure and re-tune the controller. This new CLPI would now be higher than the earlier CLPI that was calculated as we expect a noise model to adversely affect the CLPI. The absence of the noise structure indicates that all possible disturbance variables (which could be controlled variables in upstream units) are controlled better such that significant variance / structure are not propagated into the downstream unit. To separate the effect of the tuning

parameters, valve nonlinearity and linear external oscillations we determine the difference between the CLPI (after re-tuning), the CLPI (valve nonlinearity removal + re-tuning) and CLPI (valve nonlinearity + noise structure removal + re-tuning). This would aid us in determining the percentage improvement to CLPI after each control loop problem (poor controller tuning, valve nonlinearity and noise structure) is dealt with.

- In summary, the individual effect of valve nonlinearities, poor controller tuning and linear external oscillations (noise structure) can be found.

Therefore, the above mentioned framework would provide accurate and relevant information to a control engineer who needs to make appropriate structural and parametric decisions in improving control loop performance. We will implement this proposed framework with realistic simulations and industrial case studies in sections 6.11 and 6.12. For the latter, several realistic noise models will be considered.

6.8.1 Parameter Estimation

In our framework, we propose to model the valve nonlinearities accurately by means of a third order polynomial model as this has shown to suffice in modeling nonlinearities in system identification via Hammerstein models (Eskinat et al., 1991). However, this is merely a mathematical representation of the valve nonlinearity and has no physical meaning. For our method to work, a mathematical representation is sufficient. Nevertheless, it is important to the control engineer to know the kind of valve nonlinearity (valve problem) that is affecting the performance of the loop. Therefore, in

our method we propose to utilize the Hammerstein model and routine operating data to accurately identify the valve problems (stiction, hysteresis, deadzone and backlash). Such knowledge would be useful because now it will be known that this loop suffers from this particular kind of valve problem and appropriate measures may then be taken to avoid this occurrence in future. This proposed method will be implemented and discussed in the section on simulation examples. For the purpose of parameter estimation, most of the local optimization methods fail to converge, thus giving poor results. This could be attributed to the discontinuities present in the mathematical models of stiction and hysteresis. Hence, we use the genetic algorithm (GA) toolbox in MATLAB as the optimization routine in our codes.

6.9 Previous Studies

Before we present the results in this chapter, we present a brief summary of the related work. As seen in section 6.2, CLPA has been a popular area of research for many years and there exists an abundant amount of literature on it. In this section we discuss some of the latest work that has been carried out in this field and how our study aims to address some of the issues that have not been adequately addressed but are nevertheless important. In the recent past, the focus on CLPA has shifted from identifying poorly performing control loops to finding out the causes of poor control loop performance. This has resulted in a spate of research papers identifying valve problems as a chief cause of poor performance. Most of these papers concentrate on identification of stiction as the valve nonlinearity. Rossi and Scali (2004) used a cross-correlation technique to detect

stiction in routine operating data. Aside from this, a generalized definition of valve stiction based on the real plant data has also been proposed and validated, and results show that it works well in detecting stiction (Choudhury et al., 2004b). This model was subsequently modified to deal with stochastic inputs as well (Kano et al., 2004). Singhal and Salsbury (2004) then went on to present a simple and new method for detecting valve stiction in an oscillating control loop. This method is based on the calculation of areas before and after the peak of an oscillating signal. There exist other methods for stiction diagnosis but in this chapter, we present only the latest related work. Based on the available literature, it can be seen that the valve problems are limited to stiction detection only and other valve problems which are described in the earlier sections are not researched. Furthermore, efforts were made in detecting stiction but there was no mention as to how stiction really affects control loop performance. Also, the research so far focuses more on identifying stiction via graphical means rather than parameter estimation which would be more accurate. Hence, in this study we aspire to fill in the gaps by addressing these pertinent issues which until now have not received much attention.

6.10 Effect of Nonlinearities on CLPI

In this section, a perfunctory analysis of the effects of nonlinearities on CLPI will be carried out. Such a study gives credence to the next section when we examine other simulation examples and industrial case studies with regard to our proposed framework. We consider an example with the following process, noise and controller transfer functions respectively.

$$T(z^{-1}) = \frac{z^{-1}}{1-0.8z^{-1}},\ N(z^{-1}) = \frac{1-0.2z^{-1}}{1-z^{-1}} \&\ Q(z^{-1}) = \frac{0.8-0.64z^{-1}}{1-z^{-1}}$$

Q is the minimum variance controller designed for the above mentioned first order plus time delay (FOPDT) transfer function, with the corresponding noise model. For this system, an optimal PID controller is also designed in MATLAB, based on maximizing the CLPI. The digital controller transfer function is $G_c = \frac{0.933 + 0.777z^{-1} + 1.56e^{-3}z^{-2}}{1-z^{-1}}$.

Table 6.1 presents the effect of stiction on the CLPI of both the MVC and PID controllers.

Table 6.1: Effect of stiction on CLPI

No.	Stiction Interval (d)	BI	$CLPI_{MVC}$	$CLPI_{PID}$
1	0	0.0697	0.9977	0.9976
2	2	0.0954	0.8688	0.8531
3	4	0.1317	0.6121	0.5958
4	7	0.1619	0.4323	0.4128
5	12	0.4591	0.2928	0.2681

Table 6.1 presents the first case where no stiction is present (d=0) and this is confirmed by the BI whose value indicates the absence of any nonlinearity. For such a case, both the CLPI of the MVC and PID controllers are very close to 1 indicating excellent performance. From a theoretical perspective, the $CLPI_{MVC}$ should be exactly 1 but due to round-off inaccuracies in the computer program, this is not practically achievable. Therefore, the value of 0.9977 for the MVC case is the best possible performance this system can exhibit. The $CLPI_{PID}$ is 0.9976 and this is only a fraction less than the MVC case. This augurs well with our expectations, because the performance of an optimally tuned PID controller can never be as good as a MVC but for a simple FOPDT system it

can be extremely close. We can also observe that as the level of nonlinearity is increased in the system, the difference between the $CLPI_{MVC}$ and $CLPI_{PID}$ increases. This suggests that as the degree of complexity increases in any system, the optimal PID controller is not able to perform as well as its MVC counterpart. The implications of this will be seen later on.

In the second to fifth cases, stiction (using the 1 parameter simple stiction model) is introduced into the system and is slowly increased by varying the stiction interval (d). As the stiction level is increased, the degree of nonlinearity is also increasing as seen by the BI. In the second case, the level of stiction is mild as seen by a BI of 0.0954 but nevertheless, the $CLPI_{MVC}$ is reduced to 0.8688 and the $CLPI_{PID}$ to 0.8531. In the fifth case, where the BI is now 0.4591 (which signifies a much higher level of nonlinearity) the CLPI for both cases is drastically reduced to less than 0.30. This clearly illustrates the effect of stiction on CLPI and as mentioned earlier, the implications of this are:

1. Even for a simple FOPDT system with a MVC, stiction could comprehensively degrade performance.
2. Most industrial processes are regulated using PID controllers and not MVC's. Therefore, we expect the CLPI to be worse off due to this.
3. Most industrial processes are more complex than that of a FOPDT process and this complexity would serve to exacerbate the CLPI.

Therefore, the rationale behind using this simple example and a MVC is to show that if stiction can have such an adverse effect on this simple system performing at its best, it would have an even more adverse effect on higher order systems that are regulated by PID controllers. For a more consummate study on the effects of nonlinearities on CLPI, we consider the same example but now we introduce separately, hysteresis, backlash and deadzone into the system. Tables 6.2, 6.3 and 6.4 present these results respectively.

Table 6.2: Effect of hysteresis on CLPI

No.	Hysteresis Interval (a)	BI	$CLPI_{MVC}$	$CLPI_{PID}$
1	0	0.0697	0.9977	0.9976
2	0.3	0.1609	0.9615	0.9553
3	0.5	0.1721	0.8687	0.8592
4	0.7	0.2108	0.6744	0.6636
5	0.9	0.3699	0.3011	0.2949

Table 6.3: Effect of backlash on CLPI

No.	Backlash Interval (b)	BI	$CLPI_{MVC}$	$CLPI_{PID}$
1	0	0.0697	0.9977	0.9976
2	5	0.0932	0.3157	0.3095
3	7	0.2382	0.2243	0.2182
4	9	0.3444	0.1869	0.1861
5	11	0.7447	0.1535	0.1470

Table 6.4: Effect of deadzone on CLPI

No.	Deadzone Range (r)	BI	$CLPI_{MVC}$	$CLPI_{PID}$
1	0	0.0697	0.9977	0.9976
2	-2.5 to 2.5	0.8552	0.9688	0.9645
3	-5 to 5	1.2132	0.9085	0.9022
4	-7.5 to 7.5	1.3677	0.8553	0.8478
5	-12.5 to 12.5	2.3446	0.7380	0.7295

Results in Tables 6.2 to 6.4 also show that as the degree of nonlinearity increases, CLPI is reduced. It can also be seen that the effect of backlash and hysteresis is much more severe than that of deadzone on the CLPI. Overall the results show that nonlinear valves are a major cause for concern as their drastically degrade control loop performance

6.11 Simulation Examples

In this section we implement our proposed framework on fifteen realistic simulations which are shown below. For each of these examples, the process is modeled as a FOPDT transfer function with gain (K) = 1, time constant (τ) = 10 and time-delay (θ) = 2, represented as FOPDT (1, 10, 2). It must be noted that the simulations are only used to generate PV, OP and SP data. Using only these data, we carry out pertinent analyses and identify a suitable linear / nonlinear model to represent the process. Thereafter, any further analysis, diagnosis, modifications and improvements to CLPI are carried out in silico. If controller tuning parameters are known, they will be used in our computer simulations. Noise models which are generally unknown, will be assumed.

Examples:

1. FOPDT (1, 10, 2); PI Controller; White noise; 0.05 minutes sampling
2. FOPDT (1, 10, 2); PI Controller; Colored noise; 0.05 minutes sampling
3. FOPDT (1, 10, 2); PI Controller; Integrated white noise; 0.05 minutes sampling
4. FOPDT (1, 10, 2); Marginally stable PI Controller; White noise; 0.05 minutes sampling

5. FOPDT (1, 10, 2); Marginally stable PI Controller; Colored noise; 0.05 minutes sampling
6. FOPDT (1, 10, 2); Marginally stable PI Controller; Integrated white noise; 0.05 minutes sampling
7. FOPDT (1, 10, 2); PI Controller; (White noise + Periodic noise through filter); 0.05 minutes sampling
8. FOPDT (1, 10, 2); PI Controller; (White noise + Periodic noise through filter) passing through an integrator; 0.05 minutes sampling
9. FOPDT (1, 10, 2); PI Controller; (White noise + Periodic noise through filter) passing through a first order filter; 0.05 minutes sampling
10. Nonlinearity + FOPDT (1, 10, 2); PI Controller; White noise; 0.05 minutes sampling
11. Nonlinearity + FOPDT (1, 10, 2); PI Controller; Colored noise; 0.05 minutes sampling
12. Nonlinearity + FOPDT (1, 10, 2); PI Controller; Integrated white noise; 0.05 minutes sampling
13. Nonlinearity + FOPDT (1, 10, 2); PI Controller; (White noise + Periodic noise through filter); 0.05 minutes sampling
14. Nonlinearity + FOPDT (1, 10, 2); PI Controller; (White noise + Periodic noise through filter) passing through integrator; 0.05 minutes sampling
15. Nonlinearity + FOPDT (1, 10, 2); PI Controller; (White noise + Periodic noise through filter) passing through first order filter; 0.05 minutes sampling

In our simulations, we assume the process model to be a FOPDT model and the controller to be of PI form. Since most industrial controllers are PI controllers and industrial processes can be accurately modeled as FOPDT transfer functions in many cases, our examples (while not exhaustive) are able to realistically cover a range of industrial processes. The sampling time of 0.05 minutes is also realistic as given major advances in measurement technology and cheaper hardware, process variables are able to be sampled at such fast rates. Furthermore, in our examples, we incorporate various noise models to make the situations even more realistic. Different controller tuning parameters are also considered to augment the reality of the situation. Examples 1 to 9 are linear cases and examples 10 to 15 are nonlinear cases. This is to ensure that our proposed methodology works wells in linear and nonlinear situations. For the purpose of our analysis, we have grouped the fifteen examples into sets of five, with the first three examples comprising of set 1, second three examples comprising of set 2 and so on so forth. Details of each set and its examples will be discussed in the next sub-sections.

6.11.1 Simulation Set 1

In this set, our proposed framework is implemented on the first three examples. The system in example 1 is driven by white noise of mean 0 and variance 0.05. The controller tuning parameters are $k_c = 0.909$, $\tau_i = 10$ and $\tau_d = 0$. These tuning parameters are selected by manual tuning such that reasonably good control loop performance is observed. This typifies the method of controller tuning in most industries. The CLPI for this example is calculated to be 0.9657 and the ACF of the process is shown in Figure 6.9.

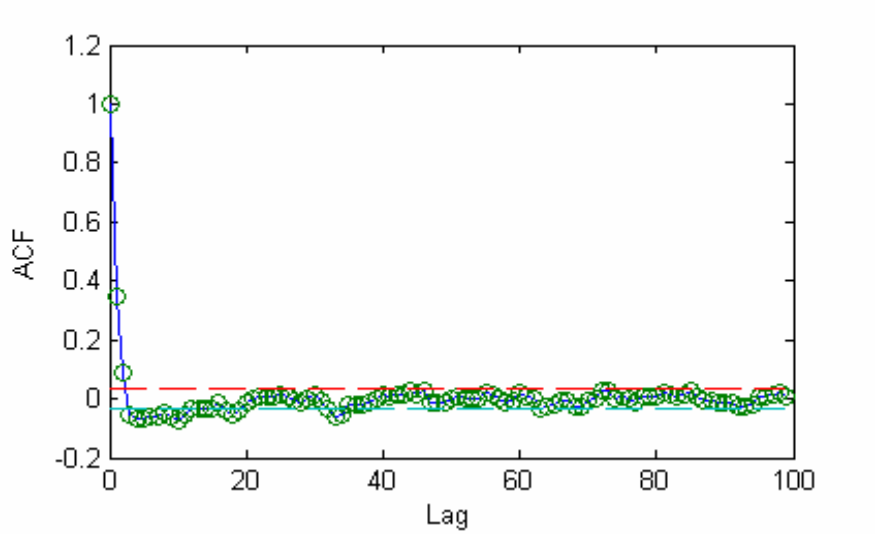

Figure 6.9: ACF of process variable (y) in example 1

From Figure 6.9, we observe that the ACF falls quickly to zero as the lag increases. This suggests that the output has very little determinism which is a sign of good control. Ideally, the ACF should fall to zero at a lag of two. Therefore, we can conclude that although the controller is performing well, there is still marginal room to ameliorate its performance. This is substantiated by the fact that although the CLPI is very high, it can still be made to increase slightly such that it tends to 1.

Assuming that no prior process knowledge is known, we calculate the Kurtosis and implement the BI and SDM test for nonlinearities. Figures 6.10 and 6.11 show the results from the BI and SDM tests.

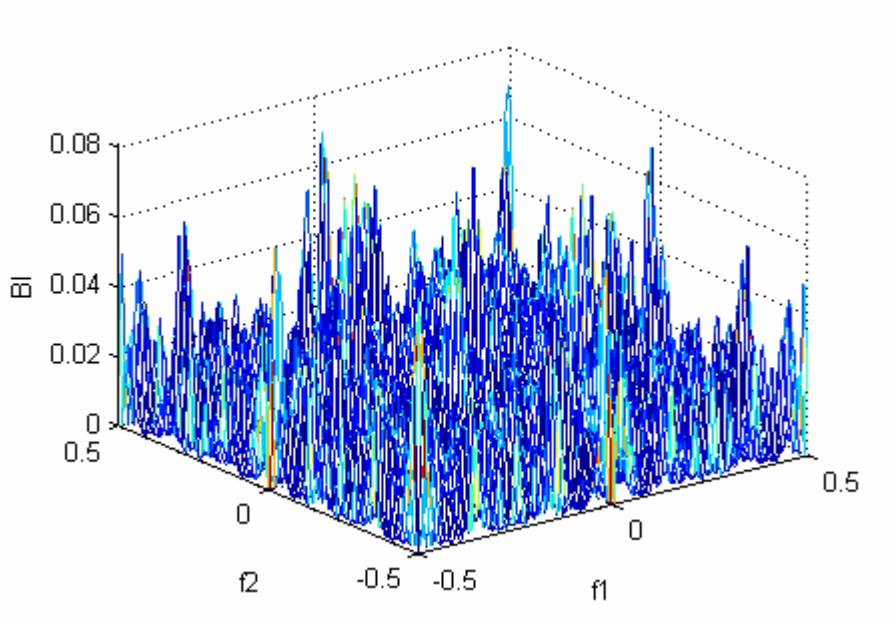

Figure 6.10: BI of process variable (y) in example 1

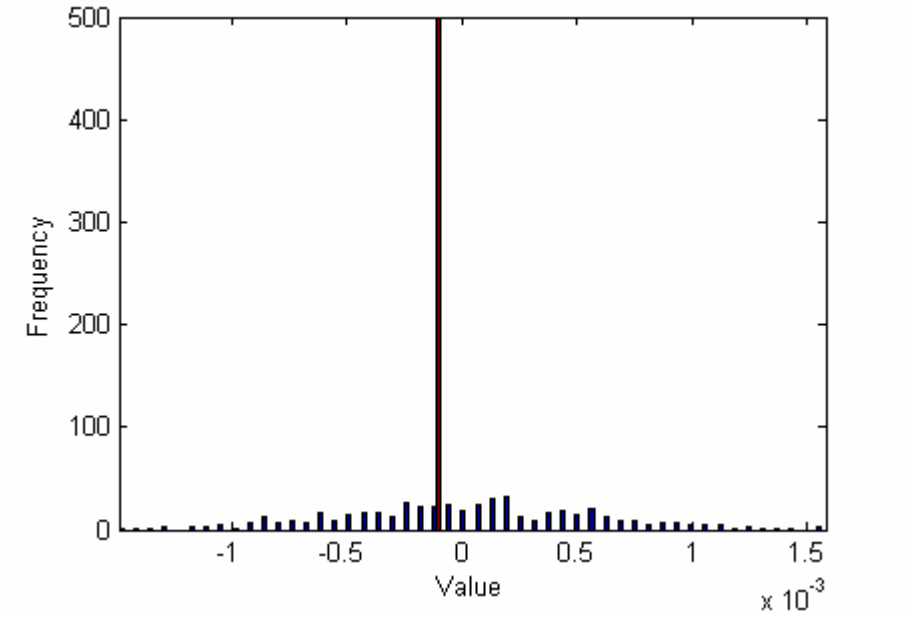

Figure 6.11: Surrogate data plot of process variable (y) in example 1

Kurtosis is determined to be -0.0513 which implies that the data distribution is mostly Gaussian and hence the process is linear. From Figure 6.10, we note that the maximum BI is 0.0640 which occurs at the bifrequencies of 0.453 and -0.484. From Figure 6.11, we see that the observed statistic from hypothesis testing is 0.2415. Hence, both methods demonstrate that the data are linear. Since the data are linear, it is not necessary to identify a Hammerstein model for the process. However, we still perform system identification using our Hammerstein model algorithm. This is to ensure that a good linear dynamic model is identified under linear circumstances. We also expect our algorithm not to identify a spurious nonlinear static polynomial model in such a situation. Figure 6.12 illustrates these results.

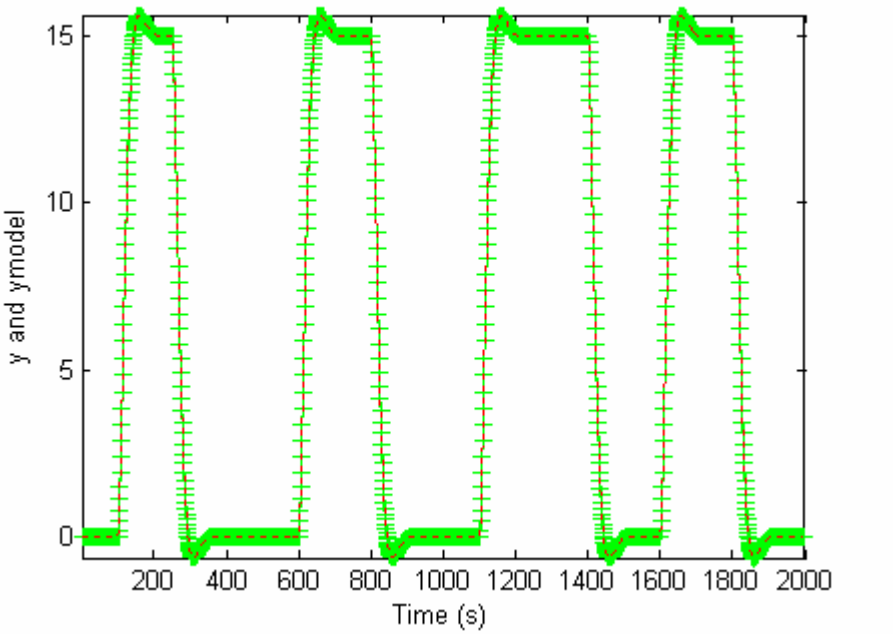

Figure 6.12: Plot of y (continuous line) and ymodel ('+') in example 1

From Figure 6.12, we can see that the Hammerstein model is an excellent fit to the process with a sum of squared error (SSE) value of 8.478E-5. The parameters of the linear dynamic model (which is in the form of $G_m = \frac{\beta z^{-2}}{1-\alpha z^{-1}}$) are α = 0.9097 and β = 0.0858. The parameters for the nonlinear static polynomial (which is in the form of $u^* = au + bu^2 + cu^3$) are a = 1, b = 0.0107 and c = 0. For a linear process, a, b and c should be 1, 0 and 0 respectively such that u* = u. In this example, only b is marginally inaccurate but even then it is almost zero. The identification results for this example show that a linear model is adequate. This also confirms the absence of any nonlinearity just as the BI and observed statistic from the SDM predicted.

Hence, any improvement to the CLPI can only be made by re-tuning the controller. Using our algorithm that calculates tuning parameters based on maximizing the CLPI, we find that the maximum CLPI for this process is 0.9946 with K_c = 0.060, τ_i = 10.015 and τ_d = 0.566. Therefore, we can see that for a simple case of a linear process, our method can ascertain that there is marginal room for improvement of control loop performance by re-tuning the controller. In the next two examples, we will consider the same process and controller (original tuning parameters) but now with two different noise models. Example 2 consists of random noise (of mean 0 and variance 0.05) passing through an integrator ($G_n = \frac{1}{s}$) and example 3 consists of the same random noise passing through a colored noise transfer function ($G_n = \frac{10}{s+1}$). Results are presented in Table 6.5.

Table 6.5: CLPI results for simulation set 1

Example	CLPI(original)	CLPI(after re-tuning)	CLPI(after noise structure is removed + re-tuning)
1	0.9794	0.9974	0.9974
2	0.3112	0.8896	0.9974
3	0.9657	0.9946	0.9974

In Table 6.5, the original CLPI of example 1 is the highest and that re-tuning of the controller increases it to 0.9974 (as discussed earlier). The original CLPI of example 2 is 0.3112 and this poor CLPI is due to the effect of the integrator and possibly poor selection of tuning parameters. After re-tuning is carried out, the CLPI is 0.8896 and this is the best possible performance exhibited by this system under feedback PID control. Assuming now that the linear external oscillations are mitigated and that the noise structure is removed (and the controller re-tuned), the CLPI further increases to 0.9974. This shows that no matter how much re-tuning is carried out, the CLPI can only increase to 0.8896 and for any further increase, it is imperative that the noise structure is altered or removed. Therefore, considering the overall increase in CLPI from 0.3112 to 0.9974 and the individual increases in CLPI by re-tuning and noise structure removal, re-tuning is responsible for 84.3% improvement in CLPI. This percentage is calculated by dividing the difference of CLPI (after re-tuning) and CLPI (original) with the difference of CLPI (after noise structure removal + re-tuning) and CLPI (original), multiplied by 100. Similarly, removing the noise structure is responsible for the balance 16.7% improvement in CLPI.

We analyze example 3 in a similar fashion and find that in this case the original CLPI of 0.9657 is only slightly less than that of example 1 but much greater than that of example

2. This highlights the more benign effect of colored noise compared to integrated white noise. Results also show that re-tuning contributes to 91.2% increase in CLPI and noise structure removal results in the balance 8.8% improvement to CLPI. Given that example 2 and 3 have different noise models it is imperative that our methods are able to detect the absence of nonlinearities in them, as they did for example 1. Table 6.6 presents the results from the nonlinearity tests.

Table 6.6: Kurtosis, BI and SDM results for simulation set 1

Example	Kurtosis	BI (f_1,f_2)	SDM (Observed Statistic)
1	-0.0513	0.0640 (0.453,-0.484)	0.2415
2	-0.8632	0.0816(0,0)	0.9715
3	0.1213	0.0784(-0.492,-0.492)	0.2998

Table 6.6 shows that Kurtosis for example 2 is inconclusive but that of example 3 insinuates linearity. BI values for both example 2 and 3 are less than 0.09 and the observed statistic from hypothesis testing is less than 2. Overall results indicate the absence of any nonlinearity in the system.

6.11.2 Simulation Set 2

In this simulation set, we present a similar analysis to what is seen in set 1. The difference is now that we use a marginally stable PI controller as opposed to the more optimal one in set 1. We purport to show that our methods are robust and work well for different controller settings. The controller tuning parameters selected are $K_c = 4$, $\tau_i = 1000$ and $\tau_d = 0$. The data are first tested for Gaussianity and nonlinearity with results presented in Table 6.7.

Table 6.7: Kurtosis, BI and SDM results for simulation set 2

Example	Kurtosis	BI (f_1,f_2)	SDM (Observed Statistic)
4	0.0767	0.0726 (0.109,-0.218)	0.3587
5	-0.5342	0.100 (0,0)	0.6169
6	0.0749	0.0740 (0,0)	0.2548

Table 6.7 shows that the Kurtosis for examples 4 and 6 are close to zero which means that the signal distribution is Gaussian and hence the system is linear. This is further confirmed by the BI and observed statistic values. For example 5, the Kurtosis is inconclusive but BI and the observed statistic are able to show that data originates from a linear system. Once linearity is established, we look into the CLPI indices of the various examples and these are presented in Table 6.8.

Table 6.8: CLPI results for simulation set 2

Example	CLPI(original)	CLPI(after re-tuning)	CLPI(after noise structure is removed + re-tuning)
4	0.7531	0.9974	0.9974
5	0.1984	0.8896	0.9974
6	0.7158	0.9946	0.9974

Table 6.8 shows that the original CLPI for example 4 is the highest and that CLPI of example 2 is the lowest. This once again reflects the negative effect of integrated white noise compared to colored noise. The CLPI (after re-tuning) and CLPI (after noise structure is removed + re-tuning) results for all three examples are the same as that of simulation set 1. This is expected as time-delay and noise models have not changed between the sets. We then apportion the effect of improvement to CLPI for each factor for examples 5 and 6. In example 5, there is an 86.5% increase in CLPI after re-tuning the

controller and a 13.5% increase after the noise structure is removed and then re-tuned. Similarly in example 6, the effect is 99% and 1% respectively.

6.11.3 Simulation Set 3

In this simulation set, we now use the same PI controller settings as of example 1 but modify the same noise models by combining them with periodic noise through a filter. Table 6.9 presents results from tests of Gaussianity and nonlinearity.

Table 6.9: Kurtosis, BI and SDM results for simulation set 3

Example	Kurtosis	BI (f_1,f_2)	SDM (Observed Statistic)
7	-0.0487	0.0698 (0.109,-0.218)	0.2306
8	-0.6513	0.0786 (0,0)	0.7557
9	0.2025	0.0804 (0,0)	0.2548

Results from Table 6.9 show that the data distribution for example 7 is almost Gaussian, implying linearity and this is confirmed by both the BI and observed statistic. Results also show that although the Kurtosis value is inconclusive for examples 8 and 9, BI and the observed statistic demonstrates that signal generating process is linear. Table 6.10 presents the various CLPI indices for this simulation set.

Table 6.10: CLPI results for simulation set 3

Example	CLPI(original)	CLPI(after re-tuning)	CLPI(after noise structure is removed + re-tuning)
7	0.9794	0.9884	0.9974
8	0.0353	0.2314	0.9974
9	0.6061	0.6581	0.9974

Results in Table 6.10 show that the CLPI (original) for example 7 is 0.9794 which is similar to that in set 1. This leads us to believe that in the case of example 7, the controller is still able to perform well even when extra periodic noise through a filter is added. For example 8, the CLPI (original) drastically reduces to 0.0353 and this shows that the combined effect of periodic and integrated noise adversely affects control loop performance. Upon controller re-tuning, the performance is increased to 0.2314 which implies that for this system, this is the best possible performance for a feedback PID controller. Similar to the analysis in example 8, the original CLPI for example 9 is 0.6061 which indicates that the extra periodic noise degrades performance (as compared to the performance in example 3). Upon re-tuning, the performance is able to improve to a maximum CLPI of 0.6581. We then apportion the effect of improvement to CLPI for each factor for examples 7 to 9. In example 7, there is a 50% increase in CLPI after re-tuning the controller and a 50% increase after the noise structure is removed and then re-tuned. Likewise, in example 8 this improvement to CLPI is 20.4% and 79.6% respectively. Similarly in example 9, the effect is 13.2% and 86.8% respectively.

6.11.4 Simulation Set 4

In this simulation set, we use the same process, controller and noise models as what is used in set 1. In addition, valve stiction is added to the system to represent a problem with the valve. The stiction is simulated using the classical stiction model (as described in chapter 3). The stiction parameters used for this study are F_s = 1750N, F_c = 0N and F_v = 612N (Choudhury et al., 2004). Table 6.11 presents the results from the tests of Gaussianity and nonlinearity.

Table 6.11: Kurtosis, BI and SDM results for simulation set 4

Example	Kurtosis	BI (f_1,f_2)	SDM (Observed Statistic)
10	-0.5128	0.1867 (-0.015,-0.015)	2.347
11	-0.6513	0.1930 (-0.015,-0.492)	2.465
12	0.2025	0.1709 (-0.046,-0.046)	2.301

Results in Table 6.11 show that the Kurtosis for all 3 examples is not close to 0 and this implies that the distribution may be non-Gaussian. Subsequently, the data are tested for nonlinearities. The BI values are in the range of 0.17 to 0.19 and these values indicate mild nonlinearity. This is confirmed by the SDM as well since the observed statistic is marginally beyond the value 2. Figures 6.13 and 6.14 show the BI and SDM plots for example 11.

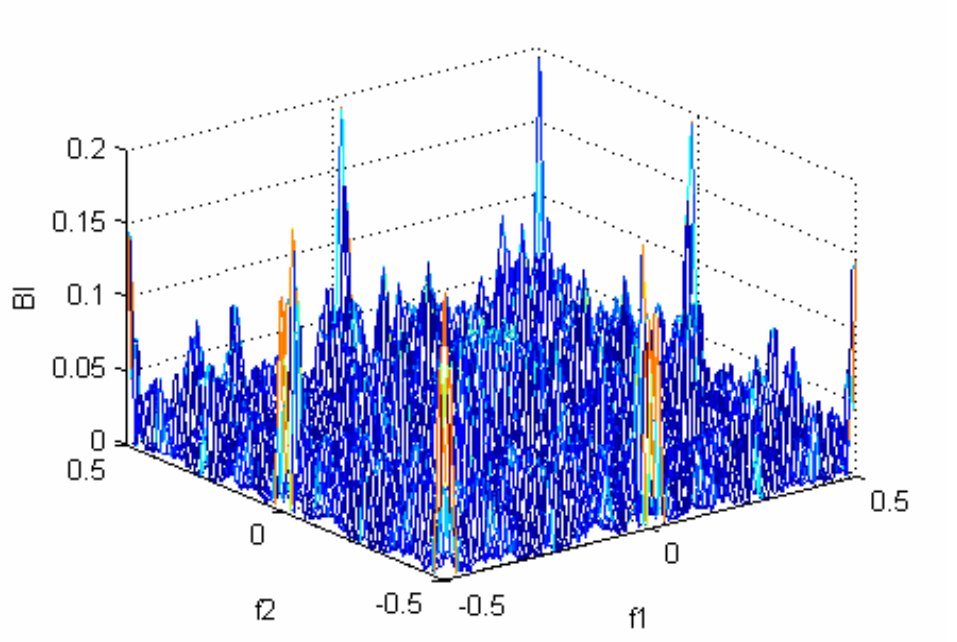

Figure 6.13: BI of process variable (y) in example 11

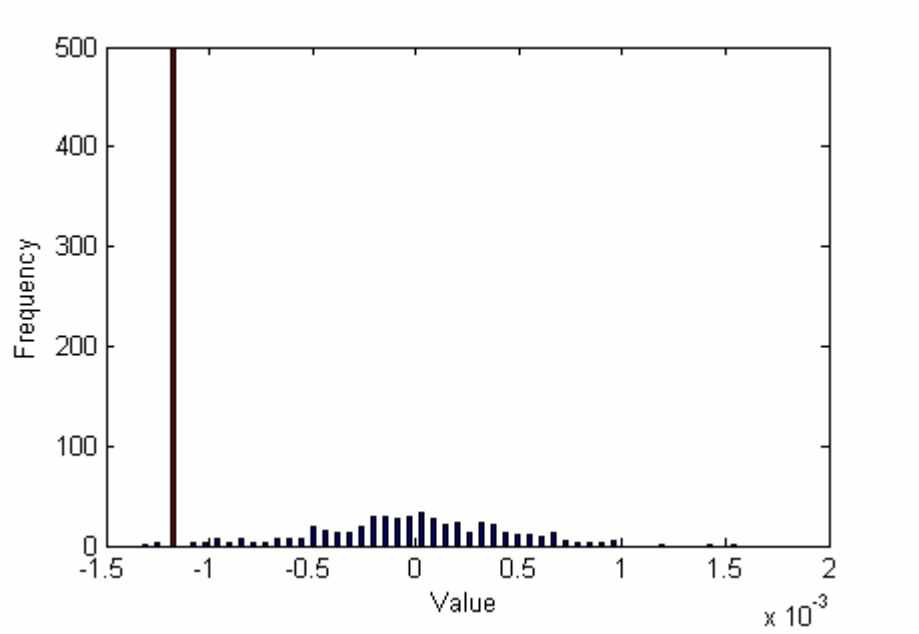

Figure 6.14: Surrogate data plot of process variable (y) in example 11

After the data is deemed to have come from a nonlinear system, the next logical step is to identify a Hammerstein model of the overall system. This is to facilitate further examination of the system. We expect the Hammerstein model to be similar for all three examples. This is because the process and valve nonlinearity are identical. However, due to the different noise models in each example and limitations in data excitation, the linear dynamic and static polynomial models might differ slightly. Figure 6.15 illustrates the process (y) and Hammerstein model (ymodel) for example 11.

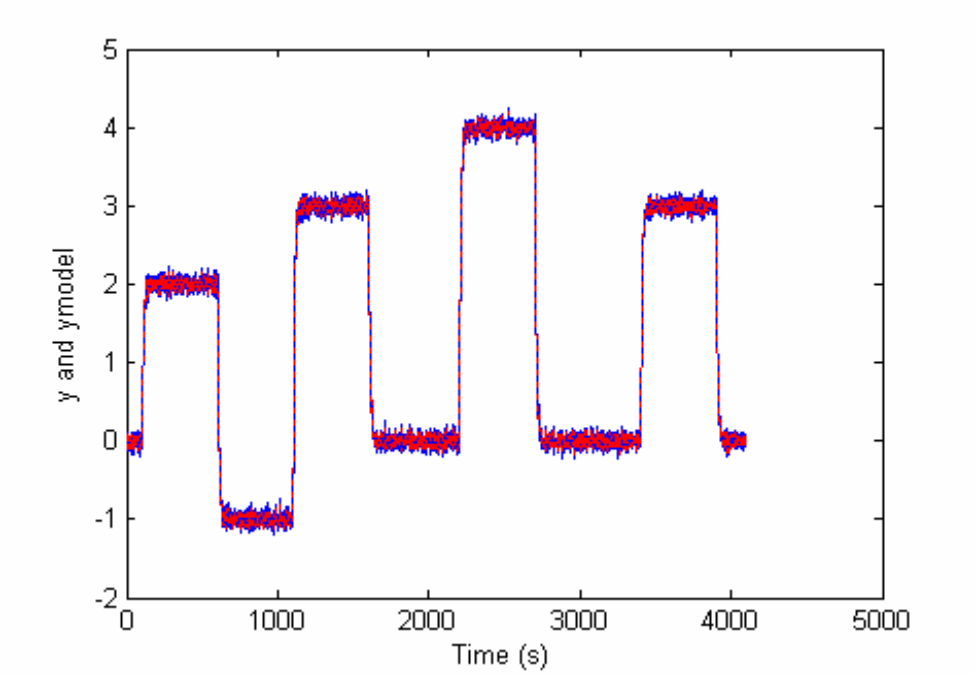

Figure 6.15 Plot of y (blue) and ymodel (red) in example 11

Models identified from the Hammerstein system identification are, $G_m = \dfrac{0.0592\,z^{-2}}{1-0.9861z^{-1}}$ and $u^* = u - 0.27u^2 + 0.067u^3$ with a SSE value of 0.0061. We note that the process model (G_m) differs slightly from that of the model in example 1. In theory, these 2 models should be exact. However, because the SSE value in this example is poorer than that of example 1, we expect that the G_m of example 1 to be more accurate than the G_m of this example. But this difference is marginal and overall results clearly show that the SSE value ensures a reasonable good fit of the model to the process and this can be seen in Figure 6.15. The polynomial u* is also able to capture the nonlinearity of the stiction model. Another way of proving that the model is an accurate depiction of the simulated process would be to ensure that various indices such as CLPI, BI and SDM (observed statistic) are similar. This would further confirm that the model is also able to capture the

dynamics of the process (refer to Table 6.12). We also treat each example as a different process and similar to example 11, we identify separate Hammerstein models for examples 10 and 12.

Table 6.12: BI, SDM and CLPI results for simulation set 4

Example	BI		SDM (Observed Statistic)		CLPI	
	Process	Model	Process	Model	Process	Model
10	0.1867	0.2039	2.347	2.5864	0.7918	0.7724
11	0.1930	0.2247	2.465	2.6021	0.2397	0.2288
12	0.1709	0.2173	2.301	2.6324	0.5759	0.5572

In Table 6.12, we see that the BI values of the model are slightly higher than that of the BI values of the process. The same trend is observed for the observed statistic. This shows that the nonlinearities in the model are slightly elevated compared to the process. However, this difference is marginal and results show that the dynamics of the model and process are similar. From the Table, we also note that the CLPIs of the model are very close to that of the process. However, the CLPIs of the model are a shade lower than that of the process and this is attributed to the higher degree of nonlinearity in the model as compared to the process. Overall, the CLPIs are close enough to indicate that the model is a realistic representation of the process. Henceforth, we use the CLPIs of the model in our analysis, as opposed to the CLPIs of the real process.

The CLPI results from Table 6.12 also show that the best performance is seen in example 10 and the worst in example 11. This shows that the integrating noise degrades the performance the most, followed by the colored noise structure and then no noise

structure. This trend is similar to what is observed in the earlier examples. Overall, the control loop performance for all three examples is poor and this is attributed to a combination of valve stiction, sub-optimal controller tuning and presence of noise structure (if any). Tables 6.13 to 6.15 present the CLPI results of our analysis.

Table 6.13: CLPI results for simulation set 4 after re-tuning

Example	CLPI(original)	CLPI(after re-tuning)
10	0.7724	0.9546
11	0.2288	0.6990
12	0.5572	0.8923

Results from Table 6.13 show the original values of the CLPI and the CLPI values after re-tuning the controller. The CLPIs calculated after re-tuning indicates the best possible control loop performance under conditions of stiction and noise structure (if any). We can see that under such conditions, CLPI for example 10 is fairly high. This seems to suggest that for a purely white noise disturbance, the effect of nonlinearities is not significant in this example. However, the CLPIs of examples 11 and 12 have room for improvement.

Table 6.14: CLPI results for simulation set 4 after stiction and noise structure removal

Example	CLPI(after stiction removal + re-tuning)	CLPI(after stiction and noise structure removal + re-tuning)
10	0.9974	0.9974
11	0.8896	0.9974
12	0.9946	0.9974

The second column in Table 6.14 presents the CLPIs after the stiction model is removed and the controller re-tuned. We note that at this juncture, the CLPIs are fairly optimal but there still might be room for improvement in the case of example 11. Hence, the noise

structure is then removed and column 3 shows the optimal values of the CLPIs. Our results show that re-tuning the controller, removing the stiction and eliminating any structure in noise are able to significantly improve the CLPI for all three examples. However, it is vital to apportion the individual effect of each control loop problem to the CLPI and Table 6.15 presents these results.

Table 6.15: Individual Improvement to CLPI

Example	Increase in CLPI after re-tuning (%)	Increase in CLPI after stiction removal (%)	Increase in CLPI after noise structure removal (%)
10	80.9	19.1	0
11	61.1	24.8	14.1
12	76.1	23.2	0.7

Results in Table 6.15 show that for all three examples, effect of re-tuning the controller is the most significant. This is followed by removing stiction and then eliminating any structure in noise. In example 10, the effect of re-tuning the controller is more than that of examples 11 and 12. This can be attributed to the fact that there is no noise structure in this process and that also that the effect of stiction may not be as predominant as it is for the other examples. We can see that for examples 11 and 12, the effect of stiction is higher and therefore, the removal of stiction would be more useful in these cases. Example 11 is of particular interest because it clearly shows that all 3 control loop problems have an impact on CLPI and our results are able to separate their individual effect. We also note that the nonlinearity introduced in this simulation set is mild (as determined by the BI and observed statistic from SDM). Therefore, we might falsely expect the effect of this nonlinearity to be insignificant. On the contrary, results show that

even with this mild nonlinearity, a fairly significant improvement to CLPI can be obtained if the nonlinearity is removed.

6.11.4.1 Parameter Estimation

Parameter estimation is an integral part of our analysis. In simulations, precise knowledge of the valve nonlinearity is known but this information is not known to control engineers in an industrial setting. Therefore, in our study we aim to use several mathematical models of valve nonlinearities to determine the type of valve nonlinearity present in the control loop. Let us consider example 11. Figure 6.16 illustrates the dynamics of the process variable (y) against time.

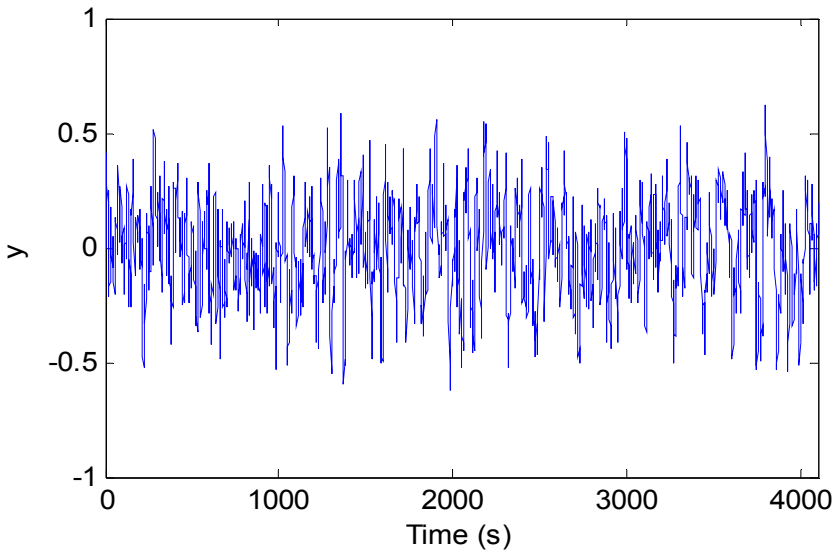

Figure 6.16: Graph of y against time

The output (y) is afflicted with valve stiction which is disguised by the random fluctuations. This shows that valve stiction is not easy to spot from a graphical analysis of the process variable (y), thereby necessitating the use of parameter estimation methods.

The valve stiction is simulated using the classical stiction model. For our purposes, we will assume that we are not privy to this information. Hence we attempt to model this output by incorporating the simple stiction, Weiss, backlash and deadzone model. If one of the models provides a good fit to the actual output, we will know the cause of the valve nonlinearity. If none of the models provide a good fit, we can conclude that either no valve nonlinearity is present (which means the process could be nonlinear instead) or that there exists another kind of valve nonlinearity aside from stiction, hysteresis, backlash and Deadzone. Figures 6.17 to 6.20 show the results from parameter estimation using the various models

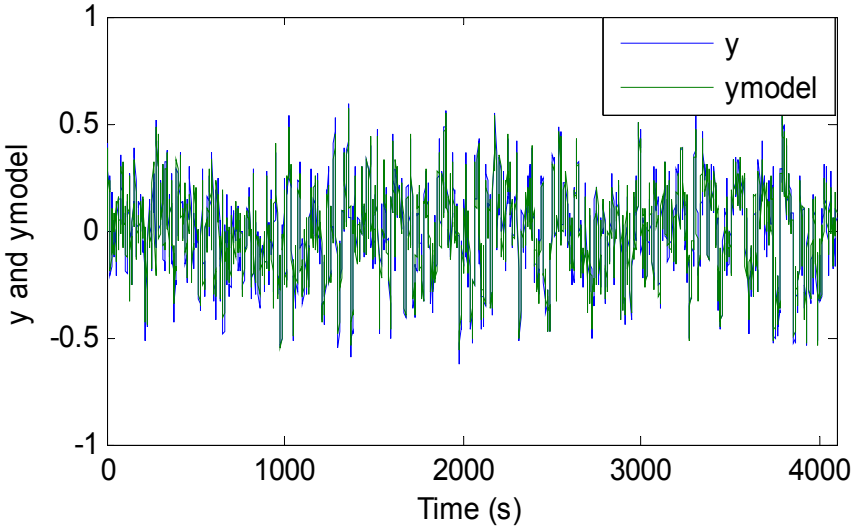

Figure 6.17: Graph of y and ymodel against time using stiction model

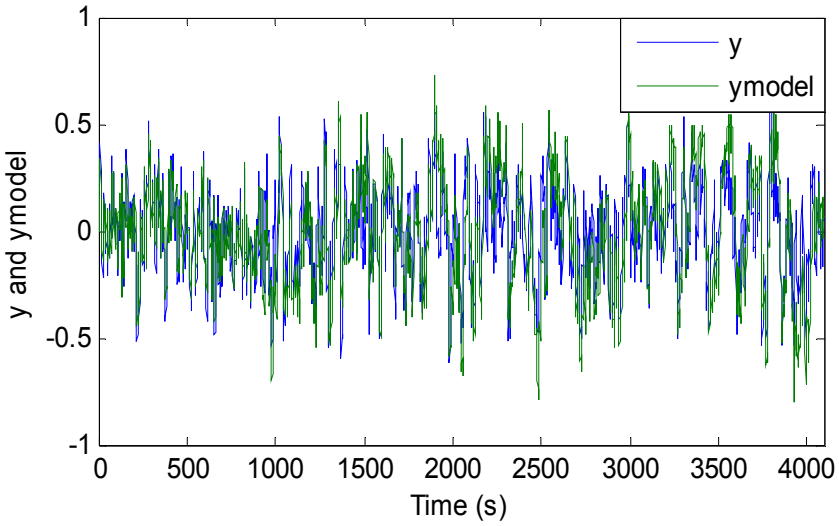

Figure 6.18: Graph of y and ymodel against time using Weiss model

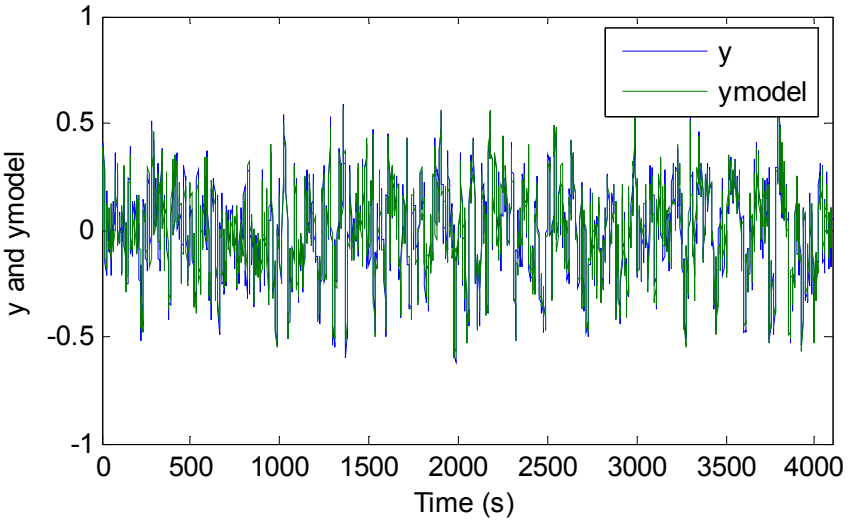

Figure 6.19 Graph of y and ymodel against time using backlash model

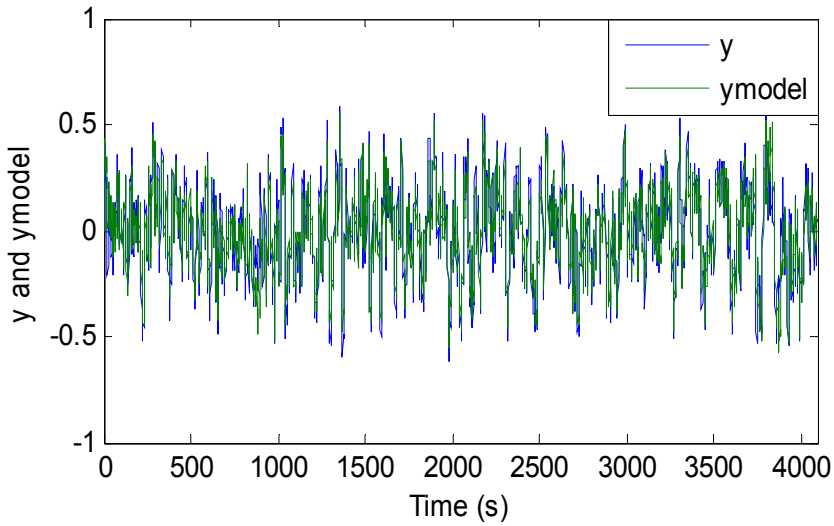

Figure 6.20: Graph of y and ymodel against time using deadzone model

From Figures 6.17 to 6.20, we can see that the output data (y) provides a better fit to the stiction and backlash valve model compared to the Weiss and deadzone model. However, for a quantitative determination of which are the best fits, we compare the SSE values calculated from the different fits. Table 6.16 presents these results.

Table 6.16: SSE results for various valve models

Index	Valve Model	SSE
1	Stiction	0.419
2	Weiss (hysteresis)	896.153
3	Backlash	1.402
4	Deadzone	12.563

Results in Table 6.16 show that the SSE value for the stiction valve model is the lowest. This shows that the valve nonlinearity present in the loop is stiction. Although, prior knowledge of stiction is already known, this goes to show that our parameter estimation

methods are effective in determining the type of valve nonlinearity afflicting the control loop.

6.11.5 Simulation Set 5

In this simulation set, we use the same process, controller and noise models as what is used in set 3. In addition, valve stiction is added to the system to represent a problem with the valve. The examples in set 5 are also similar to that in set 4, with the exception of a more severe noise model as seen by the addition of a periodic noise through a first order filter. Results so far have shown that our methods are robust and work well in linear and nonlinear cases amidst different noise models and controller tuning parameters. Prior results already provide the justification that the data are nonlinear. Similar to what was seen in set 4, we identify separate Hammerstein models for these three examples. The Hammerstein model plot for example 14 is shown in Figure 6.21. The reported SSE is 4.822E-4 which indicates the model identified is a very good fit to the process.

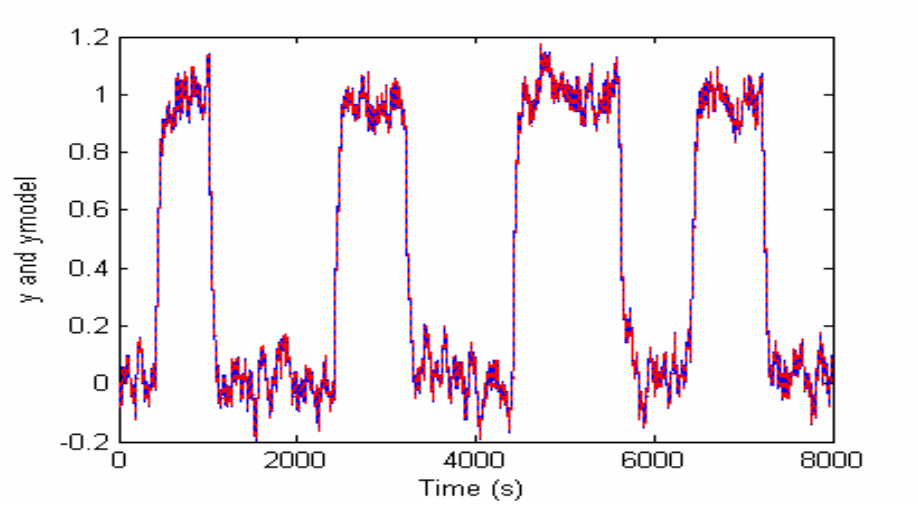

Figure 6.21 Plot y (blue) and ymodel (red) in example 14

In this sub-section, we purport only to show the effect nonlinearity, poor controller tuning and noise structure on CLPI. Tables 6.17, 6.18 and 6.19 present the CLPI results of our analysis.

Table 6.17: CLPI results for simulation set 5 after re-tuning

Example	CLPI(original)	CLPI(after re-tuning)
13	0.6732	0.9430
14	0.0108	0.0121
15	0.5036	0.5434

Table 6.18: CLPI results for simulation set 5 after stiction and noise structure removal

Example	CLPI(after stiction removal + re-tuning)	CLPI(after stiction and noise structure removal + re-tuning)
13	0.9884	0.9974
14	0.2314	0.9974
15	0.6581	0.9974

Table 6.19: Individual Improvement to CLPI

Example	Increase in CLPI after re-tuning (%)	Increase in CLPI after stiction removal (%)	Increase in CLPI after noise structure removal (%)
13	83.2	14.0	2.8
14	0.13	22.2	77.67
15	3.98	23.2	72.82

Results in Table 6.19 show that for example 13, the biggest improvement to CLPI is due to the re-tuning of the controller. This supersedes the effect of stiction and noise structure on CLPI. Examples 14 and 15 demonstrate that the effects of stiction and noise structure are more significant. Overall, results are able to categorize the effect of each factor (controller tunings, stiction and noise structure) on the CLPI. In the next section we present a summary of our findings using these fifteen simulated examples.

6.11.6 Summary

Re-tuning the controller, removal of valve stiction and elimination of noise structure all have a direct impact on the CLPI. Table 6.20 summarizes these results.

Table 6.20: Summary of individual improvement to CLPI

Example	Increase in CLPI after re-tuning (%)	Increase in CLPI after stiction removal (%)	Increase in CLPI after noise structure removal (%)
1	100	N.A	0
2	84.3	N.A	16.7
3	91.2	N.A	8.8
4	100	N.A	0
5	86.5	N.A	13.5
6	99	N.A	1
7	50	N.A	50
8	20.4	N.A	79.6
9	13.2	N.A	86.8
10	80.9	19.1	0
11	61.1	24.8	14.1
12	76.1	23.2	0.7
13	83.2	14.0	2.8
14	0.13	22.2	77.67
15	3.98	23.2	72.82

From the results presented in Table 6.20, we can perform a cross-comparison between the examples. We now group the examples that have the same noise models. Hence group 1 comprises of examples 1, 4, 7, 10 and 13, group 2 consists of examples 2, 5, 8, 11 and 14 and group 3 consists of examples 3, 6, 9, 12 and 15. We find that for group 1, the effect of controller retuning is the most predominant compared to valve nonlinearity (only for examples 10 and 13). This implies that for such loops, controller re-tuning should be the main focus in ameliorating control loop performance. In group 2, we note that now the effect of noise structure removal has significantly increased and that effect of nonlinearity

removal (only for examples 11 and 14) is also more significant. This implies that for a process afflicted with integrated white noise, the focus should also be on servicing the valves and alleviating the noise structure (by better process control upstream and / or process redesign) and not just on controller re-tuning. For group 3, the effect of noise structure is less than that of group 2 but the effect of nonlinearity is similar. Therefore, we suggest that the focus should be more on valve servicing to limit the effect of valve nonlinearities.

From the overall results in Table 6.20, we can see that for each example (which represents a different system), we are able to determine which is the most important component (controller parameters, valve nonlinearity or noise structure) that results in a poor CLPI. Such knowledge would be very useful to the control engineer who can then implement the necessary rectification action to ameliorate the control loop performance. In the next section, we will apply our methodology to two industrial case studies.

6.12 Industrial Case Studies

In the previous section, we showed that our novel framework is able to work well and yield useful results for the fifteen realistic simulations. To add an extra dimension, we purport to test our framework on two industrial case studies. This would ensure that our methods are robust in dealing with industrial data and conditions. For the purpose of this thesis, we consider 2 case studies. In case study 1, we examine a poorly performing temperature control loop from an industrial polymerization reactor in a local chemical

plant. In case study 2, we also examine a temperature control loop but in another industrial polymerization reactor from the same chemical plant. The only data available are PV, OP and SP. The data is gathered during a period of feed change which resulted in frequent changes to the set-point (SP). Therefore, we expect more excitation in the data compared to what we normally would expect under stable conditions. However, this extra data excitation would be useful for our methods as we have shown that data has to be persistently excited to identify good Hammerstein models.

6.12.1 Case Study 1

Figure 6.22 shows the error signal versus time of the process variable (y).

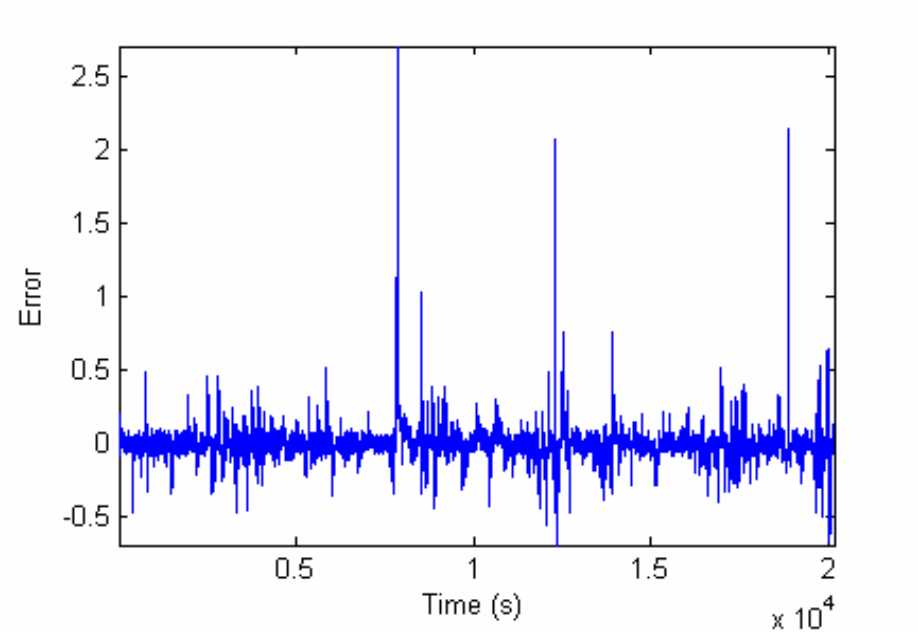

Figure 6.22: Graph of error against time.

After the poorly performing control loop is identified (from CLPI and ACF), the data are tested for Gaussianity and nonlinearity. Table 6.21 presents these results.

Table 6.21: Kurtosis, BI and SDM results for case study 1

No.	Kurtosis	BI (f_1,f_2)	SDM (Observed Statistic)
1	0.7849	0.392 (0,-0.31)	12.237

From the results in Table 6.21, we can conclude that the data are non-Gaussian. Furthermore, the BI and observed statistic from the SDM indicate that the data are nonlinear. Refer to Figures 6.23 and 6.24 for a visual depiction.

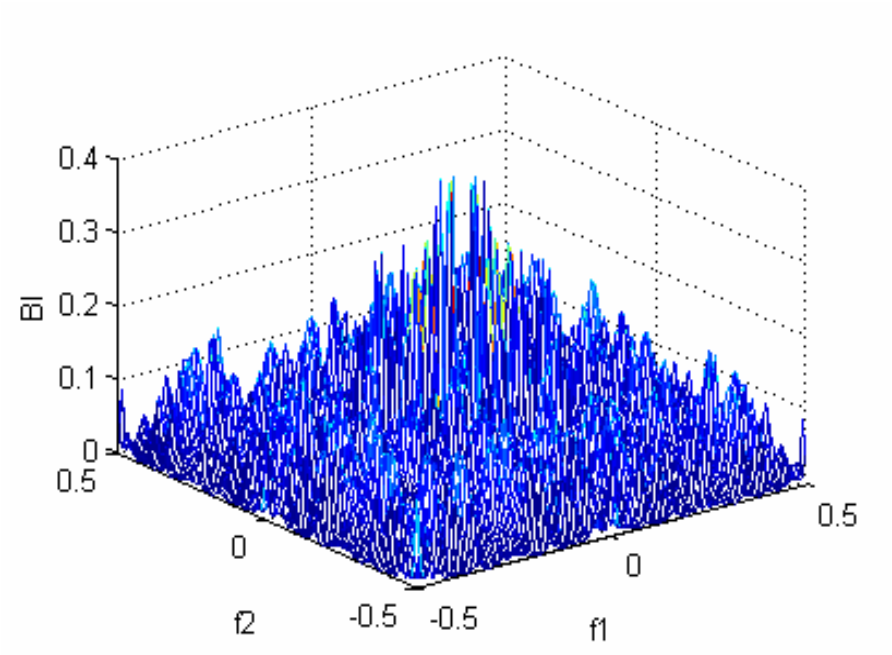

Figure 6.23: BI of error signal

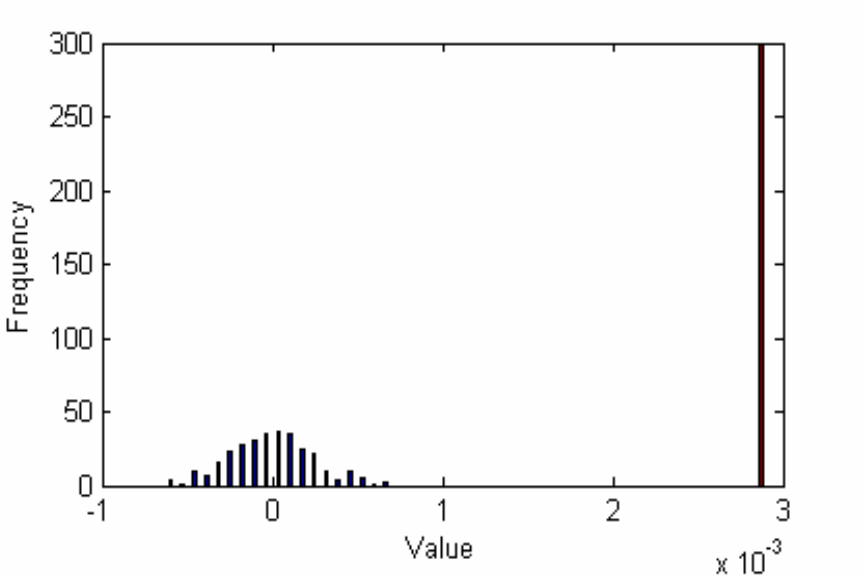

Figure 6.24: Surrogate data plot of error signal

Having quantified the degree of nonlinearity present in the data, we now evaluate the control loop performance from the error signal. Figures 6.25 and 6.26 illustrate the ACF and CLPI respectively.

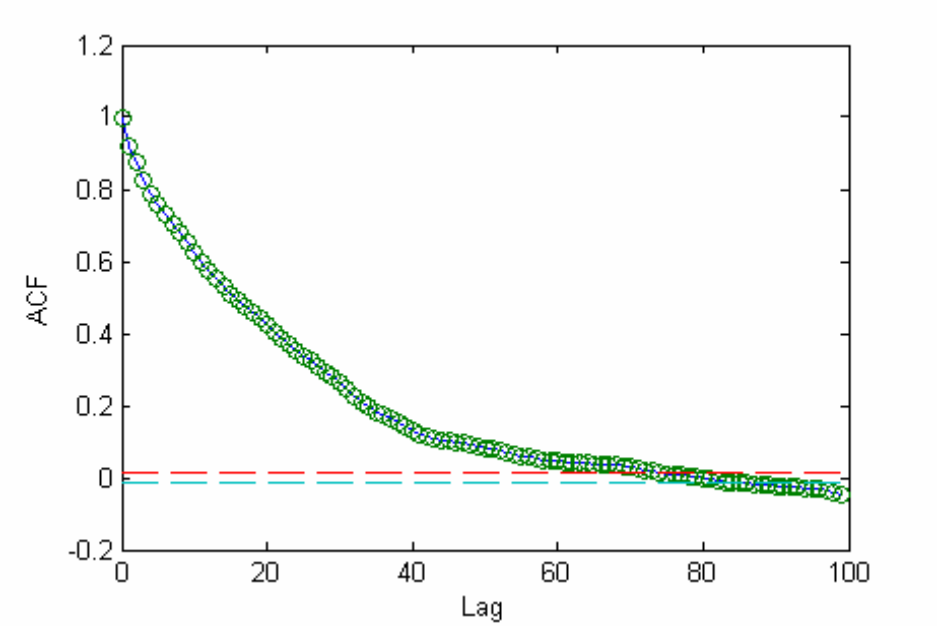

Figure 6.25: ACF of error signal

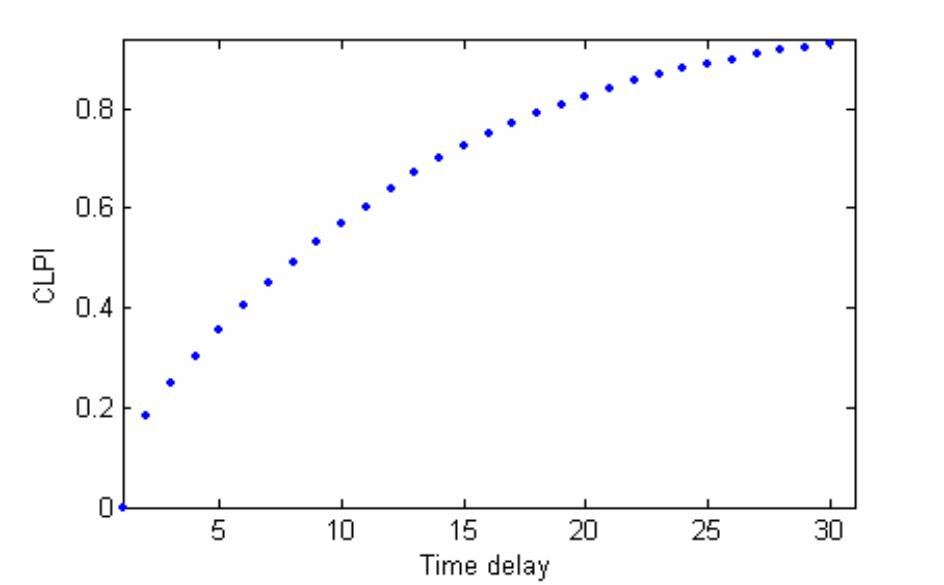

Figure 6.26: CLPI plot of error signal

From Figure 6.25, we observe that the data are extremely correlated and this signifies poor performance. In Figure 6.26 we plot the CLPI as a function of time delay. This is because the precise knowledge of time delay is not known. However, we expect the time delay to be in the range of 3 to 8 (as determined by our industry contact). Hence, based on this information the calculated CLPI is between 0.25 and 0.50 which is anything between poor and moderate. After characterizing the dynamics of the data and evaluating the control loop performance, we identify a Hammerstein model from the data. Figure 6.27 shows the Hammerstein plot.

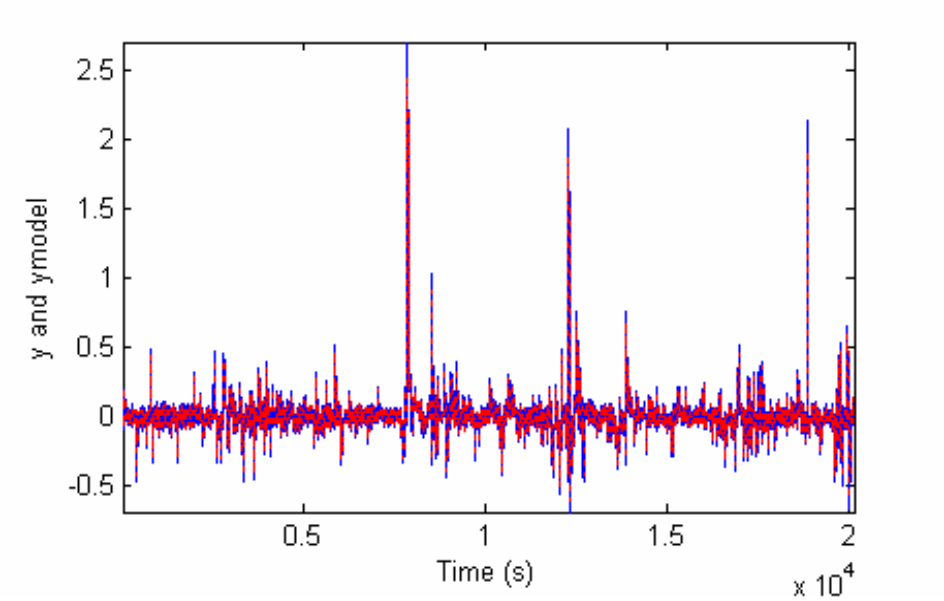

Figure 6.27: Plot of y (blue) and ymodel (red)

From Figure 6.27, we can see that the model is a fairly good fit to the process with a SSE value of 0.003. The parameters of the linear dynamic model are α = 0.8988 and β = -2.630e^{-4} and the nonlinear static model is, $u^* = u + 0.186u^2 - 0.430u^3$. The nonlinearity captured in u* also confirms that the data are nonlinear. Since we are dealing with industrial data, we further validate the model by comparing the BI, SDM and CLPI indices of the process and the model. Table 6.22 presents the results of BI and SDM.

Table 6.22: BI and SDM results for case study 1

No	BI		SDM (Observed Statistic)	
	Process	Model	Process	Model
1	0.392	0.376	12.237	11.957

Results in Table 6.22 show that the BI and observed statistic of the model are comparable to that of the process. This implies that our model is able to accurately capture the dynamics of the true process. Figure 6.28 computes the CLPI of the model.

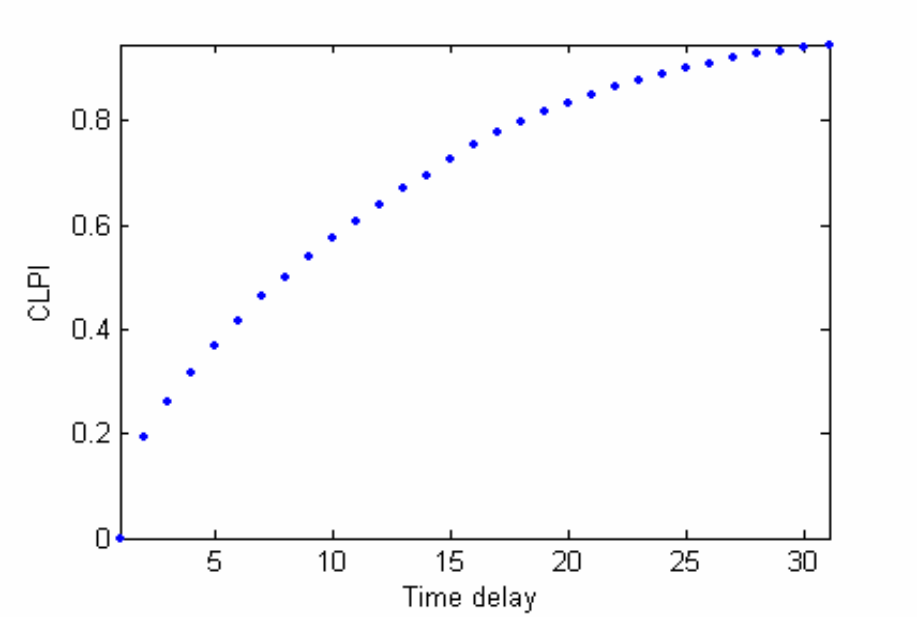

Figure 6.28: CLPI plot of ymodel

Figure 6.28 shows that the range of CLPI for the model is very similar to that of the process (Figure 6.26). Hence we can conclude that the model is an apt representation of the real process. For future analysis, we assume that the time delay of the process is 5, which is an unbiased and realistic assumption. Therefore, for a time delay of 5 the corresponding CLPI would be 0.42. At this point, it is important to highlight that because we use the direct approach in identification of Hammerstein models, information about controller tuning parameters and noise models are not needed. However, the knowledge of such information would be useful in our analysis. In the simulation examples discussed earlier, knowledge of controller and noise models are known and hence we are able to show comprehensive results. For this temperature control loop, the nature and tuning parameters of the controller are not accurately known. We know that this loop is the inner loop of a cascade control loop and hence it could be a simple PID controller. However the nature of the controller is unlikely to be standard (textbook) PID controller and most

likely is a non-standard one. For our purposes, we will assume it to be an ideal PID controller. However, the tuning parameters obtained from the industry cannot be used as they are specific for the non-standard PID controller. Therefore, it is imperative that we obtain the correct tuning parameters for our standard PID controller. Also, the noise model of the process is unknown but as discussed earlier we will assume the system to be contaminated with 1) integrated white noise and 2) colored noise passing through a first order filer. Both noise models are the same as the models used in the simulation examples. We will analyze the effect of each noise model separately. The objective in our analysis is to optimize the controller tuning parameters such that the CLPI is approximately 0.42 as that is the original CLPI of the process. For each of the noise models, we expect the tuning parameters to be different such that the resultant CLPI is 0.42. Hence, for integrated white noise, the tuning parameters are $k_c = 15$, $\tau_i = 0.07$ and $\tau_d = 0$. For colored noise, the tuning parameters are $k_c = 5$, $\tau_i = 0.09$ and $\tau_d = 0$. The tuning parameters are obtained from an optimization algorithm.

With the assumption of the noise model, controller tuning parameters, the level of nonlinearity present and the Hammerstein model of the system, we now proceed with apportioning the effect of each of the control loop problems on CLPI. Tables 6.23 to 6.25 presents these results.

Table 6.23: CLPI results for case study 1 after re-tuning

Noise Model	CLPI(original)	CLPI(after re-tuning)
Integrated Noise	0.42	0.7826
Colored Noise	0.42	0.8385

Table 6.24: CLPI results for case study 1 after nonlinearity and noise structure removal

Noise Model	CLPI(after nonlinearity removal + re-tuning)	CLPI(after nonlinearity and noise structure removal + re-tuning)
Integrated Noise	0.9436	0.9987
Colored Noise	0.9572	0.9987

Table 6.25: Individual Improvement to CLPI

Noise Model	Increase in CLPI after re-tuning (%)	Increase in CLPI after nonlinearity removal (%)	Increase in CLPI after noise structure removal (%)
Integrated Noise	62.6	27.8	9.6
Colored Noise	72.3	20.5	7.2

Results in Table 6.25 show that for both noise models, poor controller tunings are the main cause of low CLPI. It can also be seen that removing the nonlinearity (which signifies valve servicing) would account for between 20% to 28% increase in CLPI. This shows that for these two scenarios, valve nonlinearity also contributes to the poor CLPI. Removal of the noise structure by establishing better control in upstream variables, accounts for between 7% to 10% improvement in CLPI. It must be also noted that although the BI and observed statistic indicate a high degree of nonlinearity, the improvement of CLPI after removing the nonlinearity is not extremely significant. This can be attributed to the fact that given the data is substantially excited, the BI and

observed statistic tend to overestimate the degree of nonlinearity. However, this does not compromise the accuracy of these methods. Overall, results show that we are able to quantify the exact improvement to CLPI, using merely PV, OP and SP data.

6.12.2 Case Study 2

In this section, we consider the temperature control loop of the second reactor. We present a similar analysis as what is shown in case study 1. Figure 6.29 shows the error signal versus time of the process variable (y).

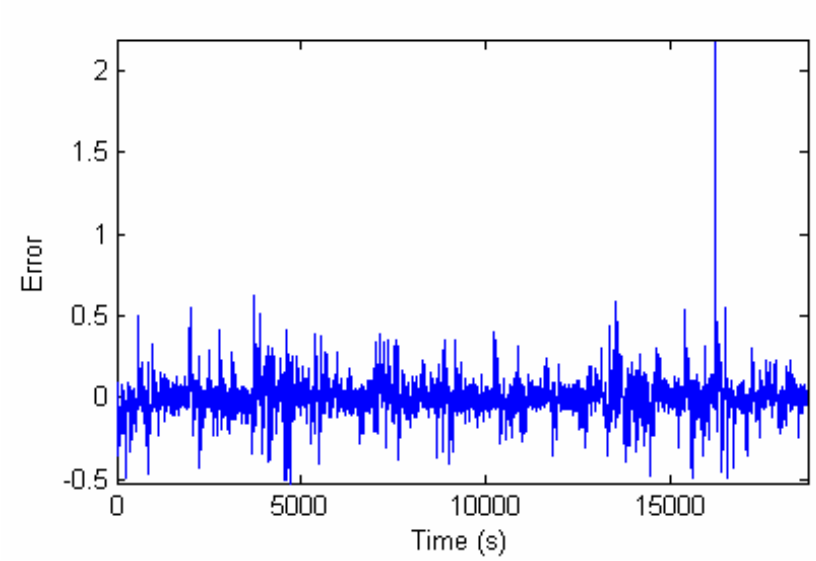

Figure 6.29: Graph of error against time.

Subsequently, we perform the tests for Gaussianity and nonlinearity on the data.

Table 6.26: Kurtosis, BI and SDM results for case study 2

No.	Kurtosis	BI (f_1,f_2)	SDM (Observed Statistic)
1	0.5930	1.2103 (0,-0.031)	33.880

Results in Table 6.26 show that the data are non-Gaussian. The seemingly high values of BI and SDM indicate that the data are more nonlinear than that of case study 1. We then quantify the poor performance of this loop by examining the ACF and CLPI plots. Figures 6.30 and 6.31 present these results.

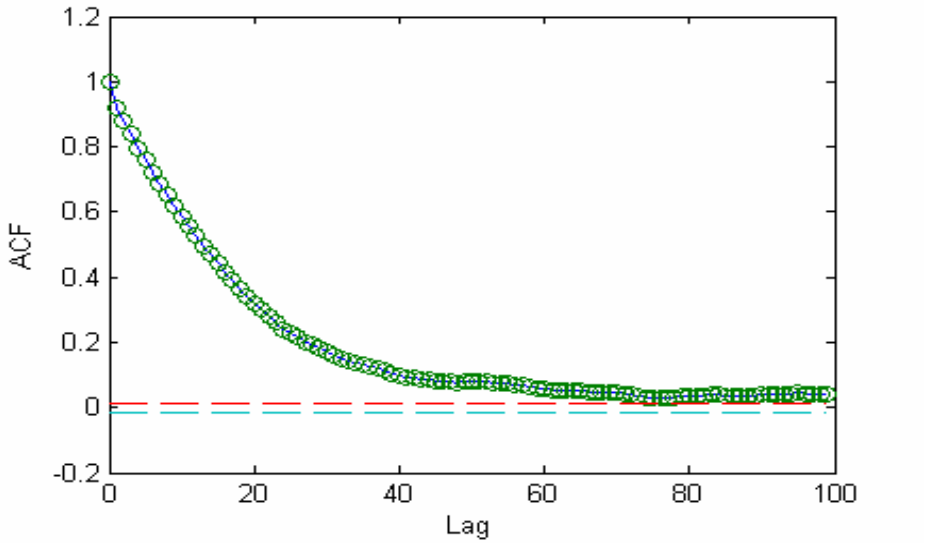

Figure 6.30: ACF of error signal

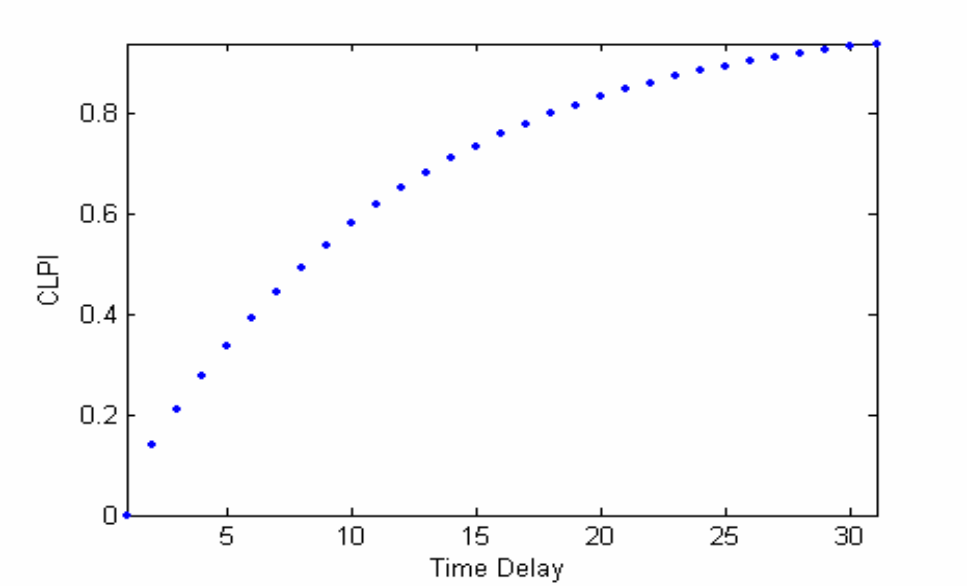

Figure 6.31: CLPI plot of error signal

Similar to our analysis in case study 1, Figure 6.30 shows that the data are correlated and hence this accounts for poor control loop performance. The CLPI plot in Figure 6.31 also shows that the performance is poor in the time delay range of 3 to 8. At a time delay of 5, the CLPI is 0.39. After characterizing the dynamics of the data and evaluating the control loop performance, we identify a Hammerstein model from the data. Figure 6.32 shows the Hammerstein plot.

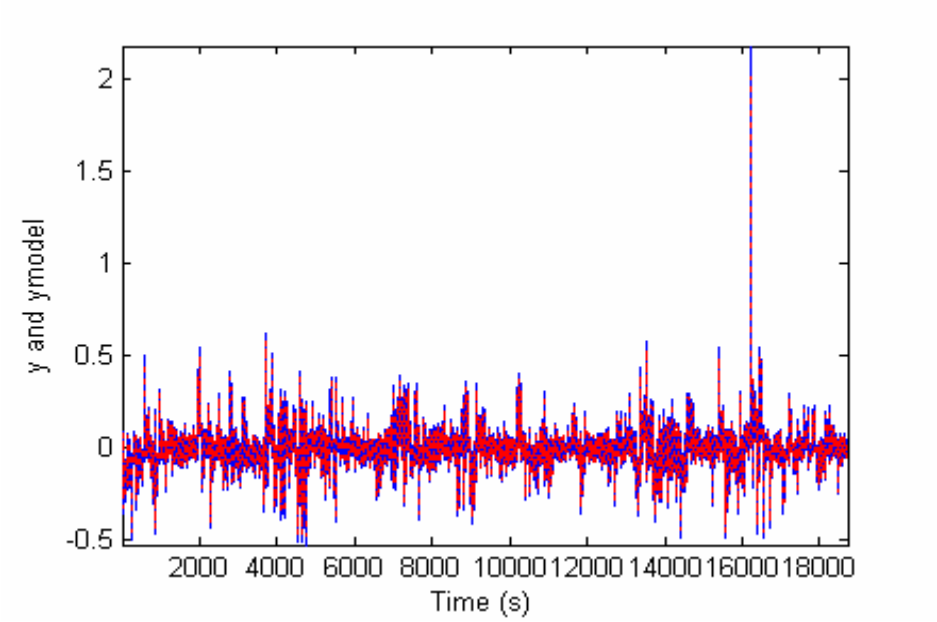

Figure 6.32: Plot of y (blue) and ymodel (red)

From Figure 6.32, we can see that the model is a fairly good fit to the process with a SSE value of 0.003. The parameters of the linear dynamic model are α = 0.9214 and β = $2.4574e^{-5}$ and the nonlinear static model is, $u^* = u - 4.5572u^2 + 2.0648u^3$. We also observe that u* captures the nonlinearity and the polynomial also confirms that the data are nonlinear. We further validate the model by comparing the BI, SDM and CLPI indices of the process and the model. Table 6.27 presents these results.

Table 6.27: BI, SDM and CLPI results for case study 2

Case Study	BI		SDM		CLPI	
	Process	Model	Process	Model	Process	Model
2	1.2103	1.2547	33.880	34.541	0.39	0.38

Results in Table 6.27 show that the BI and SDM of the model are comparable to that of the process. This implies that our model is able to accurately capture the dynamics of the true process. Similar to case study 1, we assume two different noise models and tune the PID controller to achieve an overall CLPI of 0.38. With the knowledge of the noise model, controller tuning parameters, the level of nonlinearity present and the Hammerstein model of the system we now proceed with apportioning the effect of each of the control loop problems on CLPI. Tables 6.28 to 6.30 presents these results.

Table 6.28: CLPI results for case study 2 after re-tuning

Noise Model	CLPI(original)	CLPI(after re-tuning)
Integrated Noise	0.38	0.7335
Colored Noise	0.38	0.7856

Table 6.29: CLPI results for case study 2 after nonlinearity and noise structure removal

Noise Model	CLPI(after nonlinearity removal + re-tuning)	CLPI(after nonlinearity and noise structure removal + re-tuning)
Integrated Noise	0.9646	0.9973
Colored Noise	0.9673	0.9973

Table 6.30: Individual Improvement to CLPI

Noise Model	Increase in CLPI after re-tuning (%)	Increase in CLPI after nonlinearity removal (%)	Increase in CLPI after noise structure removal (%)
Integrated Noise	57.2	37.4	5.4
Colored Noise	65.7	29.4	4.9

Results in Table 6.30 show that for both noise models, poor controller tunings are the main cause of low CLPI. It can also be seen that removing the nonlinearity (which signifies valve servicing) would account for between 29% to 38% increase in CLPI. Removal of the noise structure by establishing better control in upstream variables, accounts for between 4% to 6% improvement in CLPI. Comparing case study 1 and 2 we see that effect of nonlinearity on CLPI is more significant in the latter. This is expected as our methods previously indicated that a higher degree of nonlinearity is observed in case study 2.

6.13 Effect of Poor Data Selection

In sections 6.11 and 6.12 we presented several simulated examples and industrial case studies to show the effectiveness of our method. This is confirmed by our results and analyses as discussed in those sections. In this section, we purport to show that our method works well given the data (PV, OP and SP) used, meet a certain criteria. If not, results obtained may be inaccurate and misleading. To generate the so called ‘poor’ data, we consider example 1. We then simulate it to obtain only 1500 data points. We also do not excite the data sufficiently enough. Figures 6.33 and 6.34 illustrate the BI and SDM plots of the error (e) signal.

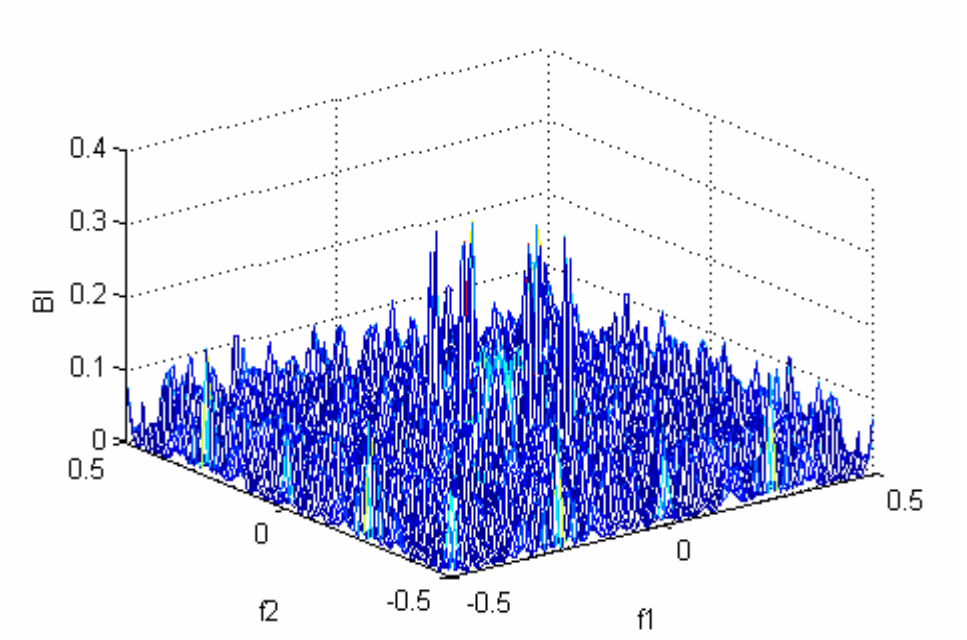

Figure 6.33: BI of error signal

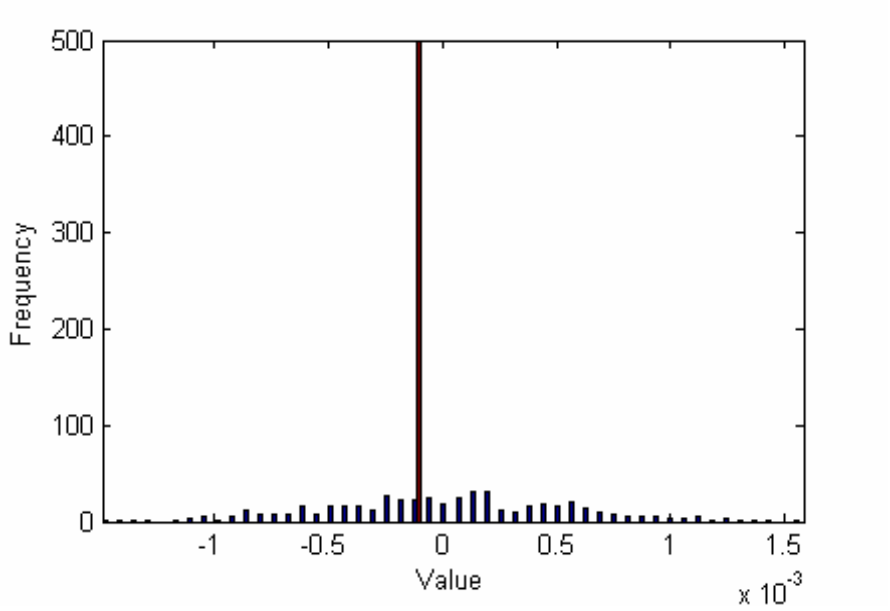

Figure 6.34: Surrogate data plot of error signal

From Figure 6.33, we note that the BI is 0.3072 at the bifrequencies of 0 and -0.02. This indicates that mild nonlinearities are present when in actual fact, the data originates from a linear system. From Figure 6.34, the observed statistic is 0.6521. This result indicates that nonlinearities are absent and this is consistent with our knowledge of the system. This dichotomy would present a conundrum as we wouldn't know which measure yields the correct result (assuming prior knowledge of the system is not known). Hence, the logical step would be to identify a Hammerstein model which would confirm if any nonlinearity is present. Figure 6.35 depicts the Hammerstein plot.

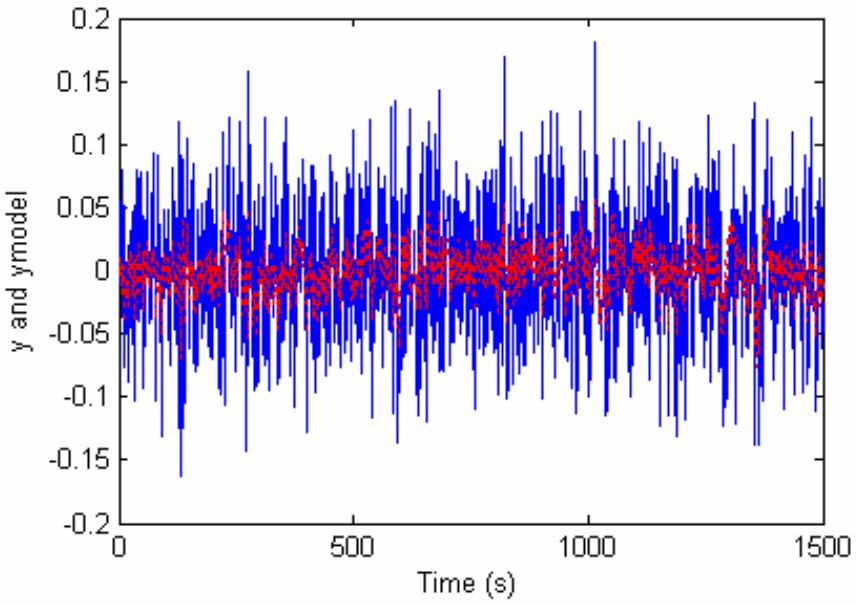

Figure 6.35: Plot of y (blue) and ymodel (red)

From Figure 6.35, we can see that the model is a very poor fit to the process. Furthermore, $u^* = u - 0.451u^2 + 6.851u^3$ and this indicates the presence of a nonlinearity. Hence, we note that the Hammerstein model identification procedure has identified a spurious model of the process. Similar to the BI, it has also identified a false nonlinearity.

Only the SDM has detected the true result. We attribute the failing of the BI to the length of the data set. We can see that 1500 samples are too few for the BI to give the correct result. Similarly, our Hammerstein model algorithm failed to identify a better model because the data is not excited sufficiently, such that the correlation between the input and noise signals is broken. Therefore, it is imperative that an appropriate length of data is analyzed and the data must be sufficiently excited to identify good Hammerstein models (as discussed in section 6.6.3). However, given significant advances in technology, ensuring that the routine operating data meets these specific characteristics is easy.

6.14 Summary

In this chapter, we present a novel framework of statistical techniques to detect, diagnose and rectify poor control loop performance. The feature of this chapter is that we make use of only the control error and controller output in the analysis. Such routine operating plant data (with a small portion of it persistently excited) is easily available from industrial control loops, and this ensures that our methods are realistic and easy to implement. From several realistic simulations, we are able to identify poor control loops and subject them to a multitude of statistical tests. From these tests, we can diagnose the plausible causes of poor performance. Subsequently, from the identification of a Hammerstein model of the system, we can then accurately go on to apportion the effect of each control loop problem to the CLPI. Such knowledge would be useful to the control engineer, who would then know which is the more important factor to rectify and a cost-

benefit analysis can then be carried out. This is to determine if the improvement to the CLPI outweighs the costs in addressing the individual problems. Furthermore, given that the control loop is often subject to valve nonlinearity, we use a combination of mathematical models and parameter estimation techniques to determine the type of valve nonlinearity. This is also useful to the control engineer who can then embark on the proper correction techniques to mitigate the particular type of valve nonlinearity identified. Thereafter, we implement our methods on two industrial case studies and perform a similar analysis. Given the higher degree of uncertainties in industrial systems, our methods are still able to yield useful results and hence this is testament to their utility and robustness. In the next chapter, we will round up this thesis with our conclusions from the present work and recommendations for future work.

CHAPTER 7

CONCLUSIONS

This chapter lists the contributions of this thesis and the directions identified for future research.

7.1 Contributions of this Thesis

This thesis deals with two important aspects of process control, namely data analysis and control loop performance assessment and enhancement. The former involves investigating dynamic data via statistical and mathematical methods to solve engineering problems. The latter deals with the detection, diagnosis and rectification of poor control loop performance.

Methods to detect poor control loop performance are ubiquitous and are widely reported in the control literature. However, the diagnosis and implementation of suitable corrective action(s) for poor control loop performance are not well researched. Therefore, this thesis considered these two challenging aspects, in the quest to attain good control loop performance. Furthermore, most studies in this area focus only on simulated examples when assessing control loop performance. In our study, we extend our analysis not only to a multitude of realistic simulated examples, but also to various industrial case studies. The inclusion of the latter increases the complexity of the problem and also

accounts for the relevance and validity of our methods. Amongst these case studies, an industrial FCC unit is chosen as the main focus of our investigation because it is difficult to model and control. Hence, such a unit would be ideally suited for us to apply our data analysis and CLPA methodologies.

The FCC process is highly complex and consists of an ensemble of interlinked units. In chapter 2, a concise description of the FCC process is presented, which introduces to the reader the main components of the FCC unit and also enables the reader to understand the fundamental idea of the FCC process. A simple schematic of the riser and regenerator in the FCC unit is also incorporated to facilitate better understanding of the FCC process. This visual depiction of the FCC process coupled with a brief description of the various key variables provides the reader with adequate information about the FCC process.

Chapter 3 presents an array of tools consisting of various statistical, mathematical and graphical techniques. These techniques comprehensively characterize the nature of the dynamic data by testing for stationarity, Gaussianity, nonlinearity and chaos. A thorough understanding of the behavior of the data would enable the control engineer in determining the root cause(s) of poor control loop performance. The underlying feature of these techniques is that they utilize routine operating data which are easily available, given major advances in sensor technology. Lastly, most of these techniques are coded into software programs (such as MATLAB / FORTRAN) that are commercially available and easy to use. These programs can be used on any routine operating data to characterize their dynamics. A list of these programs and their functions are provided in appendix A.

The application of the above mentioned techniques to the industrial FCC unit is presented in chapter 4. The riser temperature and other key variables of the FCC unit are analyzed to determine the type of dynamics exhibited (i.e., stationary, Gaussian, linear, nonlinear and / or chaotic). Results show that the riser temperature exhibits chaotic fluctuations and this could be caused by the nonlinear and linear fluctuations present in several disturbance variables. Such a detailed analysis on industrial process variables is unique to our study and the results clearly show that a good understanding of the nature of the data is the first step in ameliorating poor control loop performance.

In chapter 5, a discerning review of several FCC models is presented and an appropriate first principles FCC model is selected to represent the industrial FCC process. The model is then tuned to match the industrial FCC process by considering one set of industrial data and is subsequently validated by successfully predicting the outputs for two other sets of data. The feature in this chapter is that a realistic FCC model is implemented to depict the industrial FCC process and thereafter all pertinent analyses are carried out using the model. Results show that it is possible to reduce the fluctuations in the riser temperature by incorporating various remedies. Significant contribution is also made by separating the effect of each control loop problem (i.e., linear and nonlinear disturbances, poor controller tuning) on the CLPI. Results (based on simulations using the model) confirm that for the riser temperature loop, re-tuning the controller is of little value and better performance can be achieved if the nonlinear disturbances followed by the linear disturbances are removed.

Chapter 6 presents a consummate and novel approach to CLPA. A detailed framework is developed to systematically quantify poor control loop performance. Upon detecting a poorly performing control loop, the methodology goes on to determine the cause of the poor performance. This is followed by suggesting suitable corrective action(s). The methodology is applied to several simulated examples and two industrial case studies. Results clearly show that we are able to detect poor performance and diagnose the cause(s) of the poor performance. This is followed by quantifying the improvement to the CLPI, if each of the control loop problems (i.e., poor controller tuning, valve nonlinearities and / or linear external oscillations) is dealt with. Substantial contribution is made in this chapter by incorporating four mathematical models of valve nonlinearities and establishing a parameter estimation technique to determine the type of valve nonlinearity. Furthermore, relating CLPI to the various control loop problems and quantifying their individual effect to the CLPI are unique to this study and have not been addressed prior to this research.

7.2 Future Directions

In the course of this study, two important recommendations are made for future research. They are:

1. A global optimization tool could be implemented. This is because, optimization is a vital ingredient in our research and oftentimes, the local optimization methods

and GA toolbox in MATLAB fail to find the global optimum. To circumvent this problem, these optimization routines have to be run many times using different initial guesses, which can be time consuming. Hence a global optimization routine (based on deterministic principles) would be highly desirable.

2. Mathematical models of valve nonlinearities that consist of more than one valve problem (eg. stiction + hysteresis) could be implemented. Such models can accurately represent valves that suffer from a combination of valve nonlinearities. Hence, this would be more accurate than assuming each valve suffers from only one type of valve nonlinearity.

BIBLIOGRAPHY

1 Abasaeed, A.E. and Elnashaie, S.S.E.H. The Effects of External Disturbances on the Performance and Chaotic Behavior of Industrial Units, Chaos, Solitons & Fractals, 12, pp. 1941-1955. 1997.

2 Abasaeed, A.E. and Elnashaie, S.S.E.H. On the Chaotic Behavior of Externally Forced Industrial Fluid Catalytic Cracking Units, Chaos, Solitons & Fractals, 9, pp. 455-470. 1998.

3 Ali, H., Rohani, S. and Corriou, J.P. Modeling and Control of a Riser Type Fluid Catalytic Cracking (FCC) Unit, Trans IChemE, Part A, 75, pp. 401-411. 1997.

4 Alligood, T.A., Sauer, T.D and Yorke, J.A. Chaos: An Introduction to Dynamical Systems. pp. 200-232. New York: Springer. 1997.

5 Ansari, R.M. and Tade, M.O. Constrained Nonlinear Multivariable Control of a Fluid Catalytic Cracking Process, Journal of Process Control, 10, pp. 539-555. 2000.

6 Arbel, A., Huang, Z., Rinard, I.H. and Shinnar, R. Dynamics and Control of Fluidized Catalytic Cracking Process. Part 1: Modeling of the Current Generation of FCC's, Industrial and Engineering Chemistry Research, 34, pp. 1228-1243. 1995.

7 Astrom, K.J. Computer Control of Paper Machine – an Application of Linear Stochastic Theory, IBM Journal, 11, pp. 389-405. 1967.

8 Balchen, J.G. and Strand, S.L. State-Space Predictive Control, Chemical Engineering Science, 47, pp. 787-807. 1992.

9 Bendat, J.S. and Piersol, A.G. Random Data: Analysis and Measurement Procedures. pp. 134-163, J. Wiley. 1991.

10 Briggs, K. A New Method of Estimating Liapunov Exponents of Chaotic Time Series, Physics Letters A, 151, pp. 27-32. 1990.

11 Chang, T., Sauer, T. and Schiff, S.J. Tests for Nonlinearity in Short Stationary Time Series, Chaos V5, 1, pp. 118-126. 1995.

12 Choudhury, M.A.A.S. Detection and Diagnosis of Control Loop Nonlinearities, Valve Stiction and Data Compression. Ph.D Thesis, University of Alberta. 2004.

13 Choudhury, M.A.A.S., Shah, S.L. and Thornhill, N.F. Diagnosis of Poor Control Loop Performance using Higher Order Statistics, Automatica, 40, pp. 1719-1728. 2004.

14 Desborough, L.D. and Harris, T.J. Performance Assessment Measures for Univariate Feedback Control, Canadian Journal of Chemical Engineering, 70, pp. 1186-1197. 1992.

15 Desborough, L.D. and Harris, T.J. Performance Assessment Measures for Univariate Feedforward / Feedback Control, Canadian Journal of Chemical Engineering, 71, pp. 605-616. 1993.

16 Desborough, L.D. and Miller, R.M. Increasing Customer Value of Industrial Control Performance Monitoring, Honeywell's Experience. Proceedings of CPC VI, 2001, Tuscon, USA.

17 DeVries, W. and Wu, S. Evaluation of Process Control Effectiveness and Diagnosis of Variation in Paper Basis Weight via Multivariate Time Series Analysis, IEEE Transactions on AC, 4, 1978.

18 Diks, C., Houwelingen, J.C., Takens, F. and DeGoede, J. Reversibility as a Criterion for Discriminating Time Series, Physics Letters A, 201, pp. 221-228. 1995.

19 Eckman, J.P., Kamphorst, S.O. and Ruelle D. Recurrence Plot of Dynamical Systems, Europhysics Letter, 4, pp. 973-977. 1987.

20 Elshishini, S.S. and Elnashaie, S.S.E.H. Digital Simulation of Industrial Fluid Catalytic Cracking Units: Bifurcation and its Implications, Chemical Engineering Science, 45, pp. 553-565. 1990.

21 Eskinat, E., Johnson, S.H. and Luyben, W.L. Use of Hammerstein Models in Identification of Nonlinear Systems, AIChE Journal, 37, pp. 255-268. 1991.

22 Fan, W., Lu, H., Madnick, S.E. and Cheung, D. Discovering and Reconciling Value Conflicts for Numerical Data Integration, Information Systems, 26, pp. 635-656. 2001.

23 Forssell, U. and Ljung, L. Closed-Loop Identification Revisited, Automatica, 35, pp. 1215-1241. 1999.

24 Fraser A.M. Chaos and Detection, Portland State University. 1999.

25 Fraser, A.M. and Swinney, H.L. Independent Coordinates for Strange Attractors from Mutual Information, Physics Review A, 33, pp. 1134-1140. 1986.

26 Galka A. Topics in Nonlinear Time Series Analysis – with Implications for EEG Analysis. pp. 147-185. World Scientific Publishing. 2000.

27 Gong, X. and Lai, C.H. Detecting Chaos from Time Series, Journal of Physics and Applied Mathematics, 33, pp. 1007-1016. 2000.

28 Goradia, D.B. Analysis and Enhancement of Performance of Industrial Control Systems. M.Eng Thesis, National University of Singapore, 2004.

29 Grassberger, P. and Procaccia, I. Dimensions and Entropies of Strange Attractors from a Fluctuating Dynamics Approach, Physica D, 13, pp. 34-41. 1984.

30 Grebogi, C. and Yorke, J.A. The Impact of Chaos on Science and Society. pp. 25-51. New York: United Nation University Press. 1997.

31 Grosdidier, P., Mason, A., Aitolahti, P. and Heinonen, V. FCC Unit Reactor-Regenerator Control, Computers and Chemical Engineering, 17, pp. 165-179. 1993.

32 Hagglund, T. A Friction Compensator for Pneumatic Control Valves, Journal of Process Control, 12, pp. 897-904. 2002.

33 Han, I.S. and Chung, C.B. Dynamic Modeling and Simulation of a Fluidized Catalytic Cracking Process. Part 1: Process Modeling, Chemical Engineering Science, 56, pp. 1951-1971. 2001.

34 Harris, T.J. Assessment of Control Loop Performance, Canadian Journal of Chemical Engineering, 67, pp. 856-861. 1989.

35 Hinich, M.J. Testing for Gaussianity and Linearity of a Stationarity Time Series, Journal of Time Series Analysis 3, 3, pp. 169-176. 1982.

36 Horch, A. A Simple Method for Detection of Stiction in Control Valves, Control Engineering Practice, 10, pp. 1221-1231. 1999.

37 Hovd, M. and Skogestad, S. Procedure for Regulatory Control Structure Selection and Application to the FCC Process, AIChE Journal, 12, pp. 1938-1953. 1993.

38 Huang, B. Performance Assessment of Processes with Abrupt Changes of Disturbances, Canadian Journal of Chemical Engineering, 77, pp. 1044-1054. 1999.

39 Huang, B. and Shah, S.L. Performance Assessment of Control Loops: Theory and Applications. Springer Verlag. 1999.

40 Jia, C., Rohani, S. and Jutan, A. FCC Unit Modeling, Identification and Model Predictive Control, a Simulation Study, Chemical Engineering and Processing, 42, pp. 311-325. 2003.

41 Kano, M., Maruta, H., Kugemoto, H. And Shimzu, K. Practical Model and Detection Algorithm for Valve Stiction, DYCOPS, Boston, USA. 2004.

42 Kantz, H. and Schreiber, T. Nonlinear Time Series Analysis. Cambridge University Press. 1997.

43 Karnopp, D. Computer Simulation of Stic-Slip Friction in Mechanical Dynamical Systems, Journal of Dynamic Systems, Measurement and Control, 107, pp. 420-436. 1985.

44 Kasat, R.B. and Gupta, S.K. Multi-Objective Optimization of an Industrial Fluidized-Bed Catalytic Cracking Unit (FCCU) using Genetic Algorithm (GA) with the Jumping Genes Operator, Computers and Chemical Engineering, 27, pp. 1785-1800. 2003.

45 Kayihan, A. and Doyle, F.J. Friction Compensation for a Process Control Valve, Control Engineering Practice, 8, pp. 799-812. 2000.

46 Kennel, M.B., Brown, R. and Abarbanel, H.D.I. Determining Embedding Dimension for Phase Space Reconstruction using a Geometrical Construction, Physics Review A, 45, pp. 3403-3413. 1992.

47 Kim, Y.C. and Powers, E.J. Digital Bispectral Analysis and its Application to Nonlinear Wave Interactions, IEEE Transactions on Plasma Science, 7, pp. 120-131. 1979.

48 Lorenz, E. Deterministic Nonperiodic Flow, Journal of Atmospheric Sciences, 25, pp. 31-40. 1963.

49 Luyben, M.L. and Luyben, W.L. Essentials of Process Control. pp. 3-5, New York: McGraw-Hill. 1997.

50 Mallat, S. A Theory of Multiresolution Signal Decomposition: the Wavelet Representation, IEEE Pattern Analysis and Machine Intelligence, 11, pp. 674-693. 1989.

51 Morud, J.C. and Skogestad, S. Analysis of Instability in an Industrial Ammonia Reactor, 44, pp. 888-895. 1998.

52 Mosdorf, R. and Shoji, M. Chaos in Bubbling – Nonlinear Modeling and Analysis, Chemical Engineering Science, 58, pp. 3837-3846. 2003.

53 Nikias, C.L. and Petropulu, A.P. Higher-Order Spectral Analysis: A Nonlinear Signal Processing Framework. pp. 123-154. PTR Prentice Hall. 1993.

54 Ott, E., Grebogi, C. and Yorke, J.A. Controlling Chaos, Physical Review Letters, 64, pp. 1196-1199. 1990.

55 Packard, N.H., Cruchfield, J.P., Farmer, J.D and Shaw, R.S. Geometry from a Time Series, Physics Review Letters, 45, pp. 717-719. 1980.

56 Padmanabhan, P. Nonlinear Modeling of Electromyogram Signals. B.Eng Thesis, National University of Singapore. 2004.

57 Rao, T.S. and Gabr, M.M. A Test for Linearity and Stationarity of Time Series, Journal of Time Series Analysis 1, 1, pp. 145-158. 1980.

58 Rao, T.S. and Gabr, M.M. An Introduction to Bispectral Analysis and Bilinear Time Series Models, 24, pp. 51-87. New York: Springer – Verlag. 1984.

59 Rossi, M. and Scali, C. A Comparison of Techniques for Automatic Detection of Stiction: Simulation and Application to Industrial Data, Journal of Process Control, 15, pp. 505-514. 2004.

60 Schreiber, T. and Schmitz, A. Surrogate Time Series, Physica D, 142, pp. 346-382. 2000.

61 Schreiber, T. Interdisciplinary Application of Nonlinear Time Series Methods, Physics Reports, 308, pp. 1-64. 1999.

62 Singhal, A. and Salsbury, T.I. A Simple Method for Detecting Valve Stiction in Oscillating Control Loops, Journal of Process Control, 15, pp. 371-382. 2004.

63 Sprott, J.C. Strange Attractors: Creating Patterns in Chaos. pp. 101-134. New York: M&T Books. 1993.

64 Srinivasan, R. and Rengaswamy, R. Control Loop Performance Assessment I. A Qualitative Pattern Matching Approach to Stiction Diagnosis. Technical Report, Clarkson University. USA. 2004.

65 Stanfelj, N., Marlin, T.E. and MacGregor, J.F. Monitoring and Diagnosing Control Loop Performance: The Single Loop Case, Industrial and Engineering Chemistry Research, 32, pp. 301-314. 1993.

66 Takens, F. Detecting Strange Attractors in Turbulence, Lecture Notes in Mathematics, 898, pp. 366-381. 1981.

67 Tanake, T., Aihara, K. and Taki, M. Detecting Chaos from Time Series, Physics Review E, 54, pp. 2122-2129. 1993.

68 Theiler, J., Eubank, S., Longtin, A., Galdrikian, B. and Farmer, J.D. Testing for Nonlinearity in Time Series – the Method of Surrogate Data, Physica D, 58, pp. 77-94. 1992.

69 Tian, Y.C., Tade, M.O. and Levy, D. Constrained Control of Chaos, Physics Letters A, 296, pp. 87-90. 2002.

70 Toh, K.H. System Identification for Industrial Processes. B.Eng Thesis, National University of Singapore. 2002.

71 Vieira, W.G., Santos, V.M.L., Carvalho, F.R., Pereira, J.A.F.R. and Fileti, A.M.F. Identification and Predictive Control of a FCC Unit using a MIMO Neural Model, Chemical Engineering and Processing, 44, pp. 855-868. 2005.

72 Wilson, J.W. Fluid Catalytic Cracking Technology and Operations. pp. 13-15, PenWell Pub. Co., 1997.

73 Xia, C. and Howell, J. Loop Status Monitoring and Fault Localization, Journal of Process Control, pp. 679-691. 2003.

Internet Websites

74 http://sprott.physics.wisc.edu/ phys505/lect09.htm, accessed on 08/07/05

75 http://cecwi.fsv.cvut.cz/jiz/stehlik/det_chao.htm, accessed on 08/07/05

76 http://www.cmp.caltech.edu/~mcc/Chaos_course/lesson12/Experiment.pdf, accessed on 08/07/05

APPENDIX A: LIST OF M-FILES DEVELOPED

Index	Filename	Purpose
1	runs.m	Implements the runs test discussed in section 3.2.1
2	reverse.m	Implements the reverse arrangements test discussed in section 3.2.2
3	power_spec.m	Implements the power spectrum of a signal discussed in section 3.4.6
4	bispec.m	Implements the bispectrum of a signal discussed in section 3.4.7
5	bicoher.m	Implements the bicoherence index of a signal discussed in section 3.4.8
6	surr1.m	Implements the phase randomized surrogate data method discussed in section 3.4.9
7	surr2.m	Implements the Gaussian-scaled surrogate data method discussed in section 3.4.9
8	Trev.m	Implements the time reversal method discussed in section 3.4.11
9	hypo.m	Implements the combined methods of surrogates and time reversal along with hypothesis testing discussed in section 3.4.12
10	embed.m	Implements the delayed coordinate embedding algorithm discussed in section 3.5.3
11	mutual.m	Implements the average mutual information algorithm discussed in section 3.5.4
12	false.m	Implements the false nearest neighbours algorithm discussed in section 3.5.5
13	Lyapunov.m	Implements the Lyapunov exponents test discussed in section 3.5.9

14	correl.m	Implements the correlation dimension algorithm discussed in section 3.5.13
15	lpf.m	Implements the low pass filter algorithm discussed in section 3.6
16	hpf.m	Implements the high pass filter algorithm discussed in section 3.6
17	bpf.m	Implements the band pass filter algorithm discussed in section 3.6
18	smoothing.m	Implements the smoothing algorithm discussed in section 3.6
19	clpi.m	Implements the CLPI algorithm discussed in section 6.3
20	design.m	Implements the design of a MVC discussed in section 6.3
21	classical_stic.m	Implements the classical stiction model discussed in section 6.5.1.1
22	simple.stic.m	Implements the classical stiction model discussed in section 6.5.1.2
23	hys.m	Implements the Weiss hysteresis model discussed in section 6.5.2
24	hammer.m	Implements the algorithm for Hammerstein model identification discussed in section 6.6
25	optimal.m	Implements a generic optimization algorithm

APPENDIX B: DATA ANALYSIS FRAMEWORK

Steps:

1. Test data for stationarity. If data are non-stationary, carry out suitable transformations to ensure stationarity. If data are stationary, no transformation is required.

2. Test data for Gaussianity. If data are non-Gaussian, further testing for nonlinearity should be carried out. If data are Gaussian, no further testing is required and data are deemed to be linear.

3. Test data for nonlinearity. If data are nonlinear, further testing for chaos should be carried out. If data are linear, no further testing for chaos is required.

4. Test data for chaos. If data are chaotic, appropriate noise removal techniques may be implemented to recover the true nature of the signal. If data are not chaotic, noise removal techniques need not be implemented.